C O M M U N I C A T I O N S

FACULTY OF SCIENCES
UNIVERSITY OF ANKARA

DE LA FACULTE DES SCIENCES
DE L'UNIVERSITE D'ANKARA

Series C: Biology

VOLUME: 34 **Number: 1** **YEAR: 2025**

Faculty of Science, Ankara University
06100 Beşevler, Ankara-Türkiye
ISSN 1303-6025 e-ISSN 2651-3749
https://dergipark.org.tr/en/pub/communc

C O M M U N I C A T I O N S

FACULTY OF SCIENCES
UNIVERSITY OF ANKARA

DE LA FACULTE DES SCIENCES
DE L'UNIVERSITE D'ANKARA

S e r i e s C : B i o l o g y

Volume: 34 **Number: 1** **Year: 2025**

This Journal is published two issues in a year by the Faculty of Science, University of Ankara. Articles and any other material published in this journal represent the opinions of the author(s) and should not be construed to reflect the opinions of the Editor(s) and the Publisher(s).

Correspondence Address:
COMMUNICATIONS EDITORIAL OFFICE
Ankara University, Faculty of Sciences,
06100 Tandoğan, ANKARA – TÜRKİYE
Tel: (+90) 312 216 86 00 Fax: (+90) 312-286 89 00
e-mail: commun@science.ankara.edu.tr
https://communications.science.ankara.edu.tr/

Print:
Ankara University Press
İncitaş Sokak No:10 06510 Beşevler
ANKARA – TÜRKİYE
Tel: (+90) 312 215 90 01

Ankara University Press, Ankara 2025

C O M M U N I C A T I O N S

FACULTY OF SCIENCES
UNIVERSITY OF ANKARA

DE LA FACULTE DES SCIENCESDE
L'UNIVERSITE D'ANKARA

Series C Biology

Volume: 34 **Number: 1** **Year: 2025**

Research Articles

Ortaç ÇETİNTAŞ, Mustafa SÖZEN, Sercan IRMAK, Kürşat Kenan KALKAN, Faruk ÇOLAK, Ferhat MATUR, Phylogeography of an anatolian endemic and alpine specialist woolly dormouse (*Dryomys laniger*) with a description of a new species 1

Elif Betül KAĞIZMAN, Şeyda FİKİRDEŞİCİ ERGEN, Burcu ERTİT TAŞTAN, Evaluation of bioaccumulation and toxicity of congo red on *Pseudochloris wilhelmii* and *Daphnia magna*..... 36

İrem Betül AYDIN, Mehmet Ali KIRPIK, Mustafa Kemal ALTUNOĞLU, Bringing the quarries in the highway landscape to the ecosystem 48

Umay Merve ŞENTURAN, Ilgaz AKATA, Ergin Murat ALTUNER, Antibiofilm effects of *Fomes fomentarius* (L.) Fr. extracts on some microorganisms..... 58

Melike ERSİN, Elif GÖNÜL, Ezginur DUMAN, Gizem GÜL, Dilay TURU, Atakan BENEK, Kerem CANLI, Investigation of *Plantago lanceolata* L.: a multidimensional study on its biochemical profiling, antioxidant capacity, and biological activities 76

Review Articles

Ahmet Aşkın YILMAZ, İlker BÜYÜK, Overview of plant-derived biomaterials..... 104

Ankara University Press, Ankara 2025

http://communications.science.ankara.edu.tr

Commun.Fac.Sci.Univ.Ank.Ser. C Biology
Volume 34, Number 1, Pages 1-35 (2025)
ISSN 1303-6025 E-ISSN 2651-3749
DOI: 10.53447/communc.1532924

Research Article; Received: August 13, 2024; Accepted: December 26, 2024

PHYLOGEOGRAPHY OF AN ANATOLIAN ENDEMIC AND ALPINE SPECIALIST WOOLLY DORMOUSE (*Dryomys laniger*) WITH A DESCRIPTION OF A NEW SPECIES

Ortaç ÇETİNTAŞ[1], Mustafa SÖZEN[1], Sercan IRMAK[2], Kürşat Kenan KALKAN[1], Faruk ÇOLAK[1], Ferhat MATUR[3]

Keywords

Gliridae
Phylogeny
Dryomys anatolicus
Taurus mountains
Anatolia

To cite this article

Çetintaş, O., Sözen, M., Irmak, S., Kalkan, K. K., Çolak, F., Matur, F., Phylogeography of an anatolian endemic and alpine specialist woolly dormouse (*dryomys laniger*) with a description of a new species. *Commun.Fac.Sci.Univ.Ank.Ser.C Biology*, 34 (1) (2025), 1-35. https://doi.org/10.1111/communc.1532924

Affiliations

[1]Department of Biology, Faculty of Arts and Science, Bülent Ecevit University, Zonguldak, TÜRKİYE

[2]Science and Technology Application and Research Center, Çağış Campus, Balıkesir University, Balıkesir, TÜRKİYE

[3]Department of Biology, Faculty of Science, Dokuz Eylül University, İzmir, TÜRKİYE

Abstract

The genus Dryomys, represented by four species, spreads a variety of habitats, including forests and mountains. The Wooly Dormouse (Dryomys laniger) is a rock-dwelling alpine species endemic to South and Central Anatolian mountains. No targeted study has been conducted to explore the full distribution area of this species nor to reveal the phylogenetic structure within the species. We used CYTB and IRBP as a molecular marker to see intraspecific diversity of the species. Besides this, morphological characters are used to reveal differences between the populations. Phylogenetic trees showed that Dryomys laniger has two different mtDNA clades, each with a distinct distribution range. The representatives of the most distinct clade also have a number of shared and distinct morphological features, and we hereby describe it as a new endemic species Dryomys anatolicus sp. nov. The other clade comprises two different clades. Despite considerable molecular differences between the two clades, we could not find any difference in morphology. Two endemic species have a complex history in Anatolia starting in the late Oligocene epoch. In that era, the ancestors of Dryomys laniger and Dryomys anatolicus separated from Dryomys nitedula and started to adapt to high altitudes. Then complete divergence between the two species occurred at the beginning of the Pliocene. In this study, we suggest that geologic events and climate have a big role in speciation events between Dryomys laniger and Dryomys anatolicus.

1. INTRODUCTION

The genus *Dryomys* comprises four recognized species, each with distinct distribution ranges. *Dryomys nitedula* (Pallas, 1778) is notable for its wide distribution range. *Dryomys laniger* [1] is an endemic species found exclusively in the Taurus Mountains of Türkiye. *D. niethammeri* [2] is currently known only

ortaccetintas@gmail.com- Corresponding author; 0000-0001-7601-2540 https://ror.org/01dvabv26
spalaxtr@hotmail.com- 0000-0002-1911-605x https://ror.org/01dvabv26
sercanirmak@balikesir.edu.tr- 0000-0002-1577-8208 https://ror.org/02tv7db43
kursatkenankalkan@gmail.com- 0000-0003-3065-2256 https://ror.org/01dvabv26
farukcolak@gmail.com- 0000-0003-3985-7864 https://ror.org/01dvabv26
ferhat.matur@gmail.com- 0000-0001-9488-1408 https://ror.org/00dbd8b73

from Balochistan, Pakistan. Recently, a new species, *D. yarkandensis* [3], was described from Xinjiang, China.

The genus *Dryomys* is exclusively distributed within the Palearctic region and is characterized by a broad yet fragmented distribution pattern [4–8]. These mammals inhabit various habitats, primarily favoring mountainous regions, including forests. *Dryomys laniger*, commonly known as the Wooly dormouse, is a rock-dwelling species initially described in the western and central Taurus mountains [4]. Subsequently, additional populations were discovered in the eastern regions of Munzur and Palandöken mountains within Eastern Anatolia [9,10]. Notably, this species exhibits a patchy distribution, with all populations recorded at elevations exceeding 1600 meters. An interesting aspect of its behavior is that it undergoes a seven-month hibernation period, starting in the final week of October and lasting until the first half of April [11]. Despite this, our understanding of *D. laniger*'s biology remains limited, with the most comprehensive study conducted by Spitzenberger (1976). The most recent research regarding the species' distribution and biology was conducted by [12].

Until now, no specific studies focused on finding out the distribution area of the species. Instead, the information we have comes from general surveys of small mammals conducted by only a few researchers. No research has been conducted on the genetic diversity within this species or the structure of its populations, even though molecular studies have been carried out comparing it to other members of the genus *Dryomys* and the family *Gliridae* [13,14]. Only two studies [14,15] used mtDNA (12 rRNA and ND1) and nuclear DNA (Fib7) to compare two geographically close populations of *D. laniger* just from the central Taurus mountains.

Anatolia's geological events and climate have had a significant impact on species diversity and evolutionary history in the region. The Neogene surface uplift in Anatolia has affected the regional biota, particularly the diversity of plants and large mammals [16]. The interaction of geological and climatic changes can lead to speciation and dramatic redistribution of various group of the species across the complex landscape and the uplift of the Anatolian plateau has created new habitats and isolated populations, leading to the diversification of species [17–19]. The Late Quaternary changes have caused substantial geographic range shifts and phylogeographic breaks for various species in this region [20].

In light of the gaps in our knowledge highlighted earlier regarding the evolutionary history and geographical patterns of mammals in this region, this study aims to provide a comprehensive understanding of *D. laniger*'s phylogenetic relationships using the both mtDNA (*CYTB*) and nuclear DNA (IRBP) marker. We intend to address these limitations by clarifying the historical biogeographic processes that have shaped the species' distribution, elucidating the influence of past climatic fluctuations and geological events on population divergence, and identifying potential conservation units within *D. laniger*. Our research not only fills critical knowledge gaps but also forms a foundational basis

for future studies, aiding in the effective conservation and management of this species.

2. MATERIALS AND METHODS

2.1 Sampling

Field studies were carried out between 2015-2018. We identified and searched the high-altitude, rocky habitats previously described as characteristic of *D. laniger* [13,14,21]. A total of 31 samples were collected from 6 localities (Figure 1 and Supplementary Table S1). Animals were captured alive using Sherman traps. Since these samples were used in another zoonotic study, the animals were dissected and the liver tissues were stored in RNA-later solution. The skins, tissues and skulls of specimens examined were deposited in the Zonguldak Bülent Ecevit University. The procedure was approved by Zonguldak Bülent Ecevit University Animal Experiments Ethics Committee (permit no. 91330202-10).

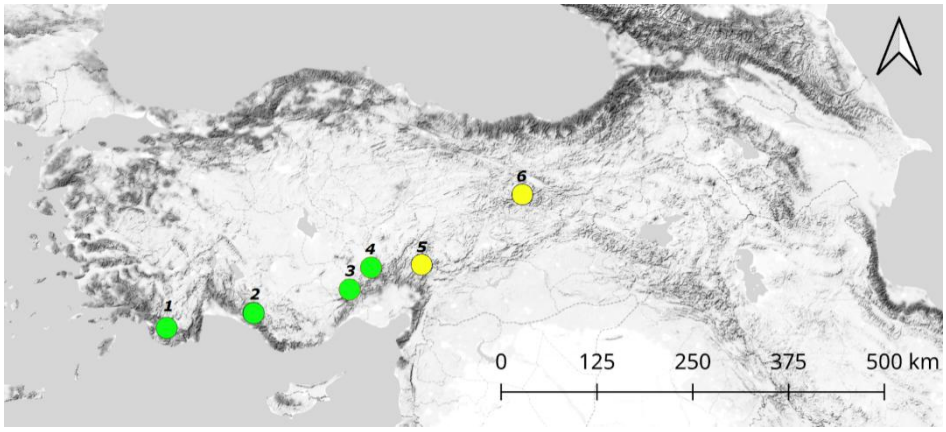

FIGURE 1. Distribution of *D. laniger* (Green) and *D. anatolicus* (Yellow). Numbers are indicate the localities of *D. laniger*; 1. Subaşı Plateau (Akdağ Mountain), 2. Salamut Plateau (Geyik Mountain), 3. Meydan Plateau Bolkar mountains, 4. Çiçekliboyun Plateau Aladağlar mountains; and *D. anatolicus*: 5. Püren Pass (Armut mountains) and 6. Eşekçayırı Plateau (Munzur mountains)

2.2 DNA isolation and amplification

Total genomic DNA was extracted from the liver using a DNAeasy extraction kit following the manufacturer's protocol (AMBRD Laboratories, Istanbul, Türkiye). The partial *CYTB* gene (1124 bp) was amplified and sequenced using the primers L7 (Forward): 5'-ACCAAT-GACAT-GAAAAATCATC GTT-3' and H6 (Reverse): 5'-TCTC-CATTTCTGGTTTACA-AGAC-3'[22]. The PCR protocol for *CYTB* included: 5 min initial denaturation of 95°C, 30 sec denaturation of 95°C, 55 sec annealing of 60°C, and 90 sec extension of 72°C,

for 35 cycles, and a final 10 min extension of 72°C. The partial IRBP gene (1172 bp) was amplified and sequenced using the primers IRBP217 (Forward): 5'-ATGGCCAAGGTCCTCTTGGATAACTACTCGTT-3' and IRBP1531 (Reverse): 5'- CGCAGGTCATCATGATGAGCTTGCTCTGTGTTCTG-3' [23]. The PCR protocol for IRBP included: 5 min initial denaturation of 95°C, 60 sec denaturation of 94°C, 60 sec annealing of 55°C, and 180 sec extension of 70°C, for 30 cycles, and a final 10 min extension of 72°C. After the PCR step, we purified the PCR products with a PCR product purification kit following the manufacturer's protocol (AMBRD Laboratories, Istanbul, Türkiye). The purified PCR products were Sanger-sequenced by the Macrogen-Europe Inc. All sequences used in this study were uploaded to GenBank (Supplementary Table S1).

2.3 Phylogenetic reconstructions

The *CYTB* and IRBP sequences were checked visually, edited, and aligned using the ClustalW algorithm in GENEIOUS software [24]. Both datasets were used to reconstruct the phylogenetic position of the samples. In total, 29 samples for *CYTB* and 12 samples for IRBP were successfully amplified. To better understand the phylogeny of the genus *Dryomys* we use all the *D. nitedula* samples uploaded in GenBank, using all available *CYTB* sequences longer than 740 bp and IRBP sequences longer than 1110 bp. We also added *Eliomys quercinus* and *Eliomys melanurus* as outgroups (Details in Supplementary Table S2).

Phylogenetic relationships were reconstructed by Maximum Likelihood (ML) and Bayesian inference (BI) algorithms. Best fit models of molecular evolution were selected by MrModelTest 2 [25]. The best model was GTR + G + I for *CYTB* dataset and HKY + G + I for IRBP dataset. ML analyses were done in RaxmlGUI [26]. ML+rapid bootstrap were selected, the number of bootstrap replicates was set to 1000, and the duplicated sequences were not included for both datasets. The Bayesian inference (BI) algorithm was performed using MrBayes 3.2 [27]. Monte Carlo Markov chain (MCMC) searches in MrBayes were run with four chains in two separate runs for 20,000,000 generations with default priors, trees sampled every 1000 generations discarding the first 25% as burn-in for both dataset. The representatives of genus *Eliomys* were used as outgroups in each tree. FigTree v1.4.3. was used to visualize the phylogenetic trees. Mitochondrial haplotypes were identified using DnaSP 6 [28]. The number of haplotypes (h), number of segregating sites (S), haplotype diversity (Hd), the average number of nucleotide differences (K), and nucleotide diversity (pi) for *CYTB* were calculated in DnaSP 6 [28]. The mean genetic distances between *D. laniger CYTB* clades and *D. nitedula* subspecies were calculated using the Kimura 2 parameter distance (K2P) model in MEGA [29]. We used the TCS method [30] to draw both *CYTB* and *IRBP* haploytpe networks. Haplotype

networks of species drawn with POPART software [31]. The datasets used in the network analyses were constructed by removing outgroups. To evaluate the demographic history pattern of the populations of *CYTB* dataset mismatch distribution analysis were run with DnaSP 6 [28]. Analysis of molecular variance (AMOVA) for *CYTB* dataset was conducted in Arlequin ver 3.5.2.2 to see variation among groups [32]. Divergence times were estimated in BEAST 2 [33] for *CYTB* dataset based on two calibration points: (1) the split between *Eliomys*/*Dryomys* which is 28.5 mya (± 2.8) and (2) divergence between two *E. quercinus* and *E. melanurus* around 7.0 mya (± 0.9) [34]. The best model chosen for the analysis was the strict clock and the calibrated Yule model tree prior. The MCMC chains were run for 50 million generations, sampled every 1000 generations. Posterior distributions of the parameter estimates were evaluated by monitoring the effective sample size (ESS >200) and trace plots in Tracer 1.6 [33]. TreeAnnotator was used to summarize the trees and the first 25% of trees were discarded as burn-in. The phylogenetic trees with divergence times were displayed in FigTree v1.4.3.

2.4 Morphometry

Skulls and mandibles were photographed for morphological evaluation. Beside our dataset we also add *D. nitedula* (n=6) museum specimens deposited in Zonguldak Bülent Ecevit University. External characters, skulls and mandibles were used for linear morphometric analyses and skulls (dorsal and ventral) and mandibles were used for the geometric morphometric analyses (Table 1). Due to possible shape changes that may arise from young individuals, these individuals were not included in the analyses.

TABLE 1. Number of samples used for both linear and geometric morphometry

	Linear morphometry		
	External characters	Skulls	Mandibles
D. laniger	n=20	n=10	n=10
D. anatolicus	n=11	n=10	n=10
D. nitedula	n=6	n=6	n=6
	Geometric morphometry		
	Skull (Dorsal)	Skull (Ventral)	Mandibles
D. laniger	n=10	n=10	n=10
D. anatolicus	n=7	n=6	n=9
D. nitedula	n=5	n=6	n=4

2.4.1 Linear morphometry

For use in morphological evaluation four external characters, head and body (HB), tail length (TaL), length of the hindfoot (HF), and length of the ear (EL), and weight (in grams) were measured following [35]. Skulls and mandibula were measured following [35]) and Krystufek and Vohralík (2005). For the analysis, a total of 33 morphological characters were measured, including 28 skulls and mandibles and 4 external characters, as well as the weights of the samples. Minimum values, maximum values, mean values and standard deviation values of a total of 32 characters and body weight obtained from *Dryomys* samples were recorded (Supplementary Table S3). All measurements were measured with Vernier caliper (to the nearest 0.1 mm) and then re-measured under a stereomicroscope to double check. The results were recorded for linear morphometric analysis. All measurements were given in millimeters and body weight in grams (0.1 grams) (as given below). **ZB**— zygomatic breadth; **RW**— rostrum width; **IC**— interorbital constriction; **OL**— occipito-nasal length; **NL**— nasal length; **NW**— nasal width; **FSL**— lenght of frontal suture; **PSL**— length of parietal suture; **OW**— occipital width; **BW**— braincase width; **CBL**— condylobasal length; **CNL**— condylonasal length; **BL**— basal length; **FRL**— length of facial region; **MB**— mastoid breadth; **BCL**— braincase lengh; **DL**— lenght of diastema; **PL**— palatal length; **FI**— lenght of foramen incisivum; **ABL**— auditory bullae length; **ABW**— auditory bullae width; **MTL**— length

of maxillary tooth row; **RH—** rostrum height; **BBL—** lenght of braincase with bullae; **BOL—** lenght of braincase without bullae; **MATL—** length of mandibular tooth row; **HL—** height of mandibula; **ML—** length of mandibula; **BW—**body weight; **EL—**length of ear; **HFL—**length of hindfoot; **TL—**length of tail; **HBL—**length of head and body.

Principal Component Analysis (PCA), Bivariate and Multivariate analysis were performed to reveal how the species were grouped and the effects of variations on the groups. IBM SPSS 26 program (IBM SPSS 26) was used for statistical analysis.

2.4.2 Geometric morphometry

The skull (dorsal, ventral) and mandible of the samples were captured with Canon R6 MII camera and the images were analyzed in accordance with the geometric morphometric procedure [36,37]. The TpsUtil software was used to edit the skull and mandible images in which landmark points were placed and to set the file formats [38]. Landmarks (LMs) were deposited on the same plane for all samples. Two-dimensional landmarks, which will enable the identification of shapes, were digitized with the tpsDig program [39]. 14 landmarks were used for the dorsal side of the skull, 19 landmarks for the ventral side and 13 landmarks for the mandible. Landmarks were placed on the right side only (Figure 2).

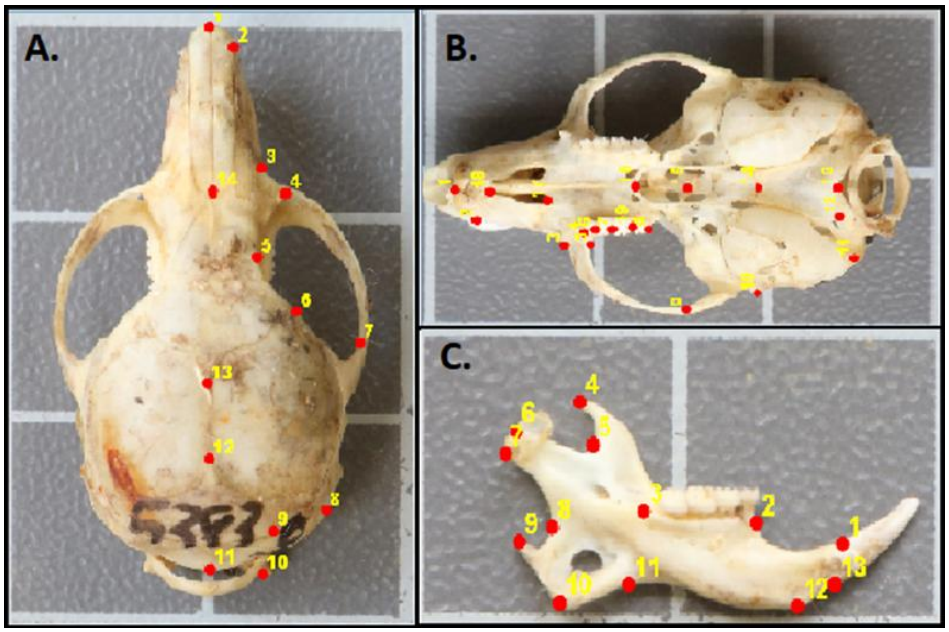

FIGURE 2. Landmark location on *Dryomys* skull. (A: Dorsal Cranium; B: Ventral Cranium; C: Mandible)

Boxplots were used to show differences between groups [40]. The significance of differences in central dimension was tested by analysis of variance. ANOVA test was performed with the help of PAST v.4.03 software [41].

Generalized Procrustease Analysis (GPA) eliminated margins of error before distributing the samples, enabling more accurate results in shape and size comparisons [36,40]. The MorphoJ software was used for the GPA [42]

Species groups were determined genetically before analyses. Principal Component Analysis (PCA) and Canonical Variate Analysis (CVA) were then performed to identify the shape diversity in the samples. Patterns of shape changes in the skull and mandible were investigated using PCAs due to variance-covariance matrices. CVAs were used to statistically distinguish groups. Discriminant Function Analysis (DFA) revealed the distinction between the two groups. The MorphoJ software used to perform the analysis [42].

3. RESULTS

3.1 Molecular analysis

All examined geographical populations of *D. laniger* split into two phylogenetic clades (Green Clade and Yellow Clade), each with strong support in *CYTB* dataset (Figure 3). The green clade comprises two clades, Clade 1; Subaşı plateau (Akdağ Mountain) and Salamut plateau (Geyik Mountain) in Western Taurus mountains. Clade 2 from the Central Taurus mountains includes populations from Meydan (Bolkar mountains) and Çiçekliboyun (Aladağlar mountains) plateaus. The yellow clade includes two populations one from Püren pass (Armut mountains) and the other one from Eşekçayırı plateau (Munzur mountains). There is a deep divergence between green clade and yellow clade, strongly supported in both BI and ML phylogenetic analyses which show the same tree topology. Regarding the phylogenetic tree constructed using the IRBP dataset, it also displays the presence of two separate clades (Green and Yellow clades). BI and ML phylogenetic analyses show the same tree topology (Figure 4).

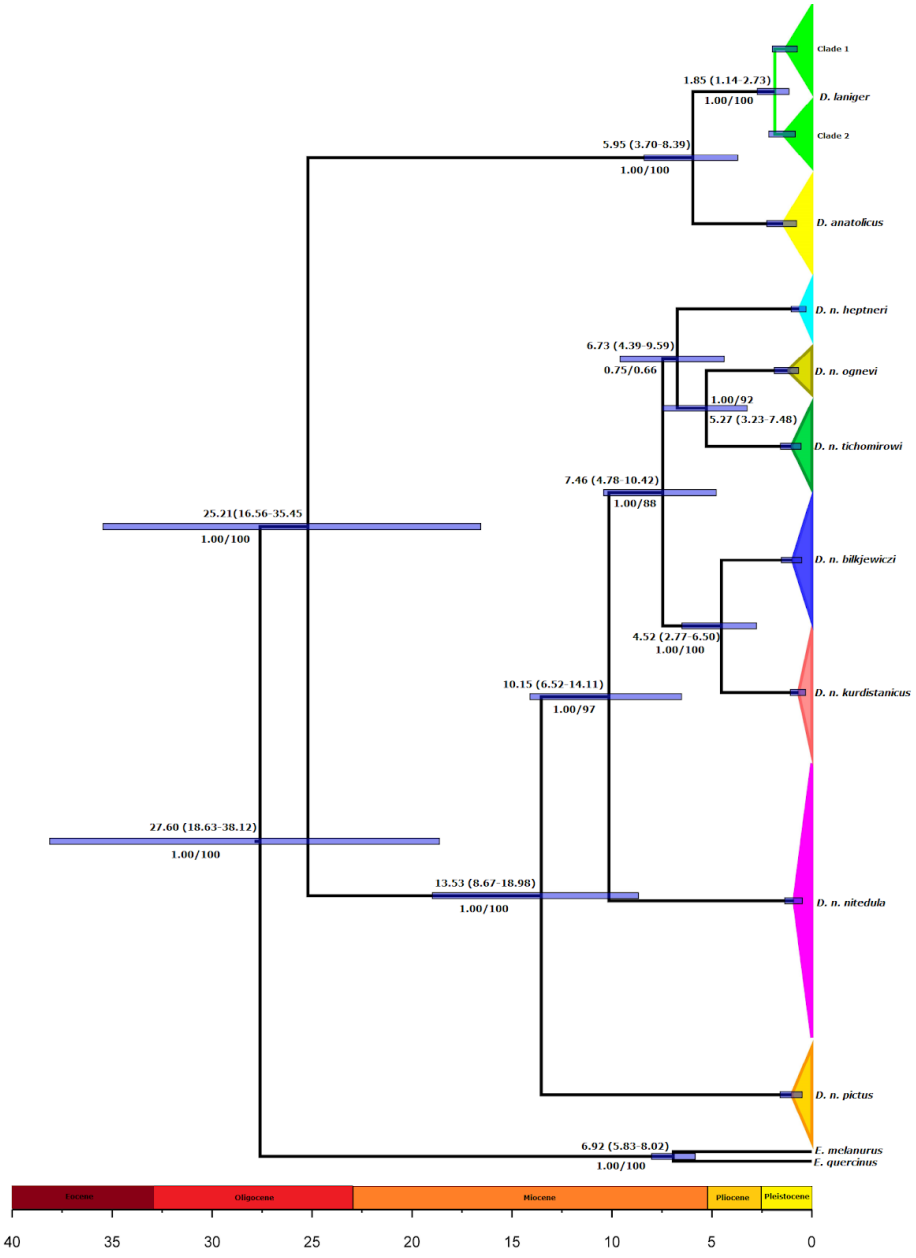

FIGURE 3. Phylogenetic relationships and divergence time based on *CYTB*. Numbers at nodes show posterior probabilities and bootstrap values for Bayesian (left) and ML inference (right), respectively. The blue bars represent the 95% HPD interval

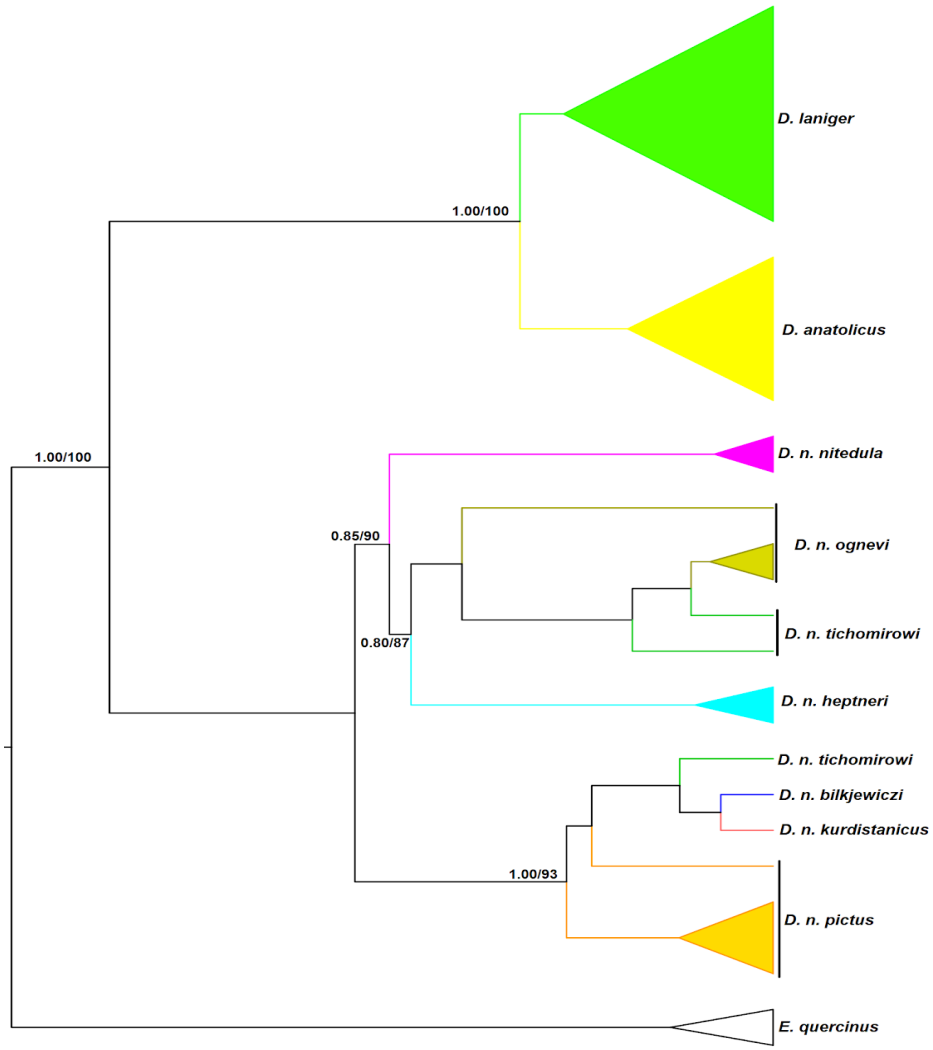

FIGURE 4. Phylogenetic relationships based on IRBP. Numbers at nodes show posterior probabilities and bootstrap values for Bayesian (left) and ML inference (right), respectively

We identified 17 unique haplotypes in *D. laniger* populations (no haplotypes were shared between clades: Supplementary Table S4). Genetic diversity analyses of two clades of green clade and yellow clade showed that the latter has low diversity compared to green clade (Table 2).

TABLE 2. Genetic differentiation of *D. laniger*'s two clades and *D. anatolicus* based on *CYTB*. Number of individuals (N), number of segregating sites (S), number of haplotypes (h), haplotype diversity (Hd), average number of differences (K) and nucleotide diversity (Pi)

	N	S	h	Hd	K	Pi
Dryomys laniger						
clade 1	10	33	8	0,956	13,33	0,012
clade 2	8	36	7	0,964	11,07	0,010
Dryomys anatolicus						
	11	19	2	0,545	10,36	0,009

The haplotype network (Figure 5) of *CYTB* reveals a substantial number of nucleotide substitution differences between two clades of *D. laniger*, clade 1 and clade 2 differ by 93 bases from *D. nitedula* clade and 27 bases from yellow clade. K2P distances between two clades of *D. laniger* and *D. nitedula* subspecies; clade 1 and clade 2 are the closest to each other (1.9%), and clade 1 and yellow clade are the most distant (7.2%). *D. n. nitedula* is the furthest (24.3% with both clade 1 and clade 2, 24.8% with yellow clade) and *D. n. kurdistanicus* is closest (19.9% with clade 1, 20.5% with clade 2, 21.1% with yellow clade). (Supplementary Table S5).

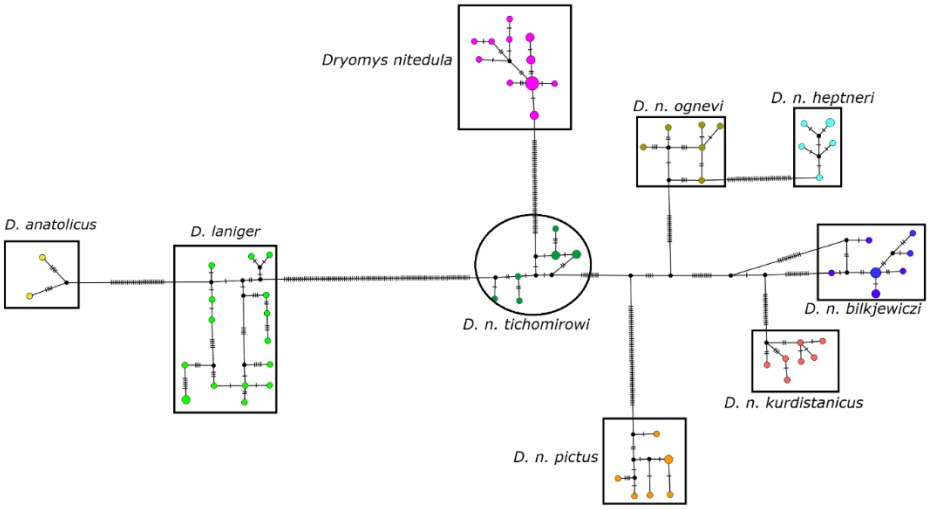

FIGURE 5. Haplotype network based on *CYTB*

The mismatch distribution of *D. laniger* is multimodal and *D. anatolicus* is bimodal (Figure 6). AMOVA shows that populations are significantly and genetically different from one another which revealed that the greatest amount of genetic variation occurred among populations (80.63%) and the p-value of the FST is p = 0.000 (P <0.05) (Figure 7).

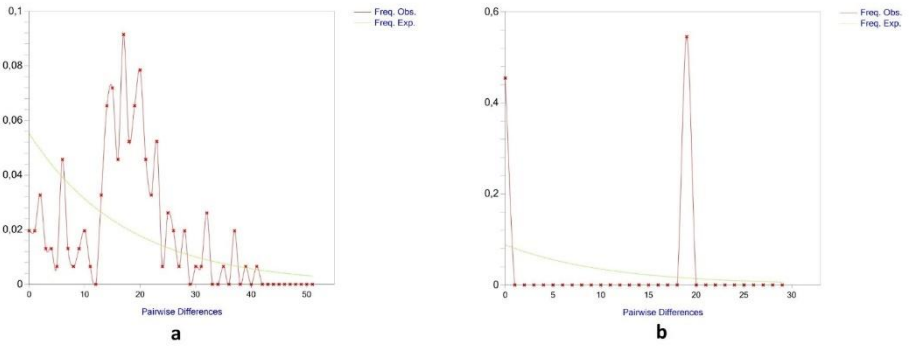

FIGURE 6. Mismatch distributions for a) *D. laniger* and b) *D. anatolicus*

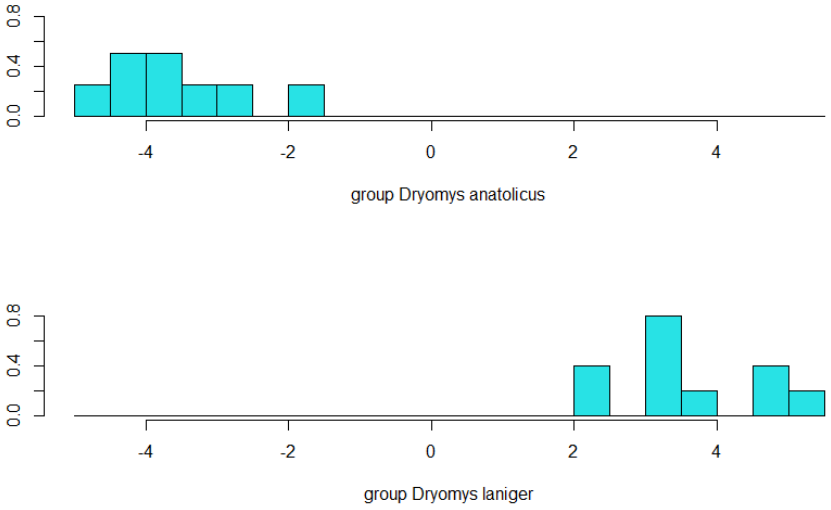

FIGURE 7. AMOVA results between *D. laniger* and *D. anatolicus*

According to our divergence time estimates, *D. nitedula* and *D. laniger* separated from each other by ~25.21 mya (HPD: 16.56 – 35.45 Mya). The split between green clade and yellow clade was dated at ~5.95 mya (HPD: 3.70 – 8.39 Mya). Within the green clade, clade 1 and clade 2 diverge 1.85 mya (HPD: 1.14 – 2.73 Mya) (Figure 3).

3.2 Morphometry

3.2.1 Linear morphometry

The genetic lineages of the *Dryomys* species samples used in morphological analysis have been previously determined and are also shown in phylogenetic analysis based on *CYTB* (Figure 3). According to the PCA analysis performed for 4 external characters and body weight data, three main components were formed and explained 81.17% of the variations. All of the variables of the main components were positively correlated (loading >0.399, loading >0.775, loading >0.573) and accounted for 32.90%, 26.11% and 22.15% of the variation, respectively (Table 3).

TABLE 3. Factor data (based on 4 external characters and body weight) variables of two main component axes of *Dryomys* species

Variables	**FAC1**	**FAC2**	**FAC3**
HBL	—	0.859	—
TL	0.890	—	—
HFL	0.680	—	0.573
EL	—	—	0.930
BW	0.399	0.775	—
Eigenvalue	1.645	1.306	1.108
Explained variance (%)	32.902	26.112	22.154

According to multivariate and bivariate analyses; HFL and TL characters were selected for the X and Y axis. Looking at the distribution graph of the species after the selected characters, it was seen that *D. nitedula* was clearly separated from the other two species, and the samples of *D. anatolicus* and *D. laniger* were clustered together, except for a few samples representing the species (Figure 8a).

According to the PCA analysis performed for 28 skull and mandible character data, two main components were formed and explained 3.80-81.51% of the variations. All variables in PC1 and PC2 were positively correlated (loading >0.409 and loading >0.345) and accounted for 81.51% and 3.80% of the variations, respectively (Table 4).

TABLE 4. Factor data of the two principal components axes (Based on 28 skull and mandible variables of *D. anatolicus*, *D. laniger* and *D. nitedula*)

Variables	**FAC1**	**FAC2**
NW	0.687	0.619
FSL	0.608	0.649
PSL	0.907	—
OW	0.817	0.534
MATL	0.780	0.560
RW	0.788	0.581
IC	0.761	0.530
NL	0.675	0.646
FRL	0.661	0.468
DL	0.627	0.632
PL	0.409	0.785
FI	0.606	0.664
MTL	0.843	0.499
ZB	0.786	0.571
RH	0.791	0.578

HL	0.791	0.590
BW	0.890	0.376
ABL	0.647	0.622
BBL	0.899	0.347
BOL	0.905	0.345
ABW	0.788	0.513
BCL	—	0.764
CNL	0.798	0.415
CBL	0.631	0.696
ML	0.680	0.577
OL	0.626	0.624
BL	0.770	0.393
MB	0.855	0.359
Eigenvalue	22.823	1.064
Explained variance (%)	81.512	3.799

According to multivariate and bivariate analyses; NW, FSL, PSL, PL were selected for the X and Y axes from the skull characters and MATL from the mandible characters. According to the distribution graphs created after the selected skull and mandible characters, it was seen that *D. nitedula* was clearly separated as in the external characters. However, it was determined that the samples belonging to *D. anatolicus* and *D. laniger* were clearly separated from each other except for a few samples representing the species. Morphological analysis shows that *Dryomys* species are distinguished based on skull and mandible variables (Figure 8b).

A.

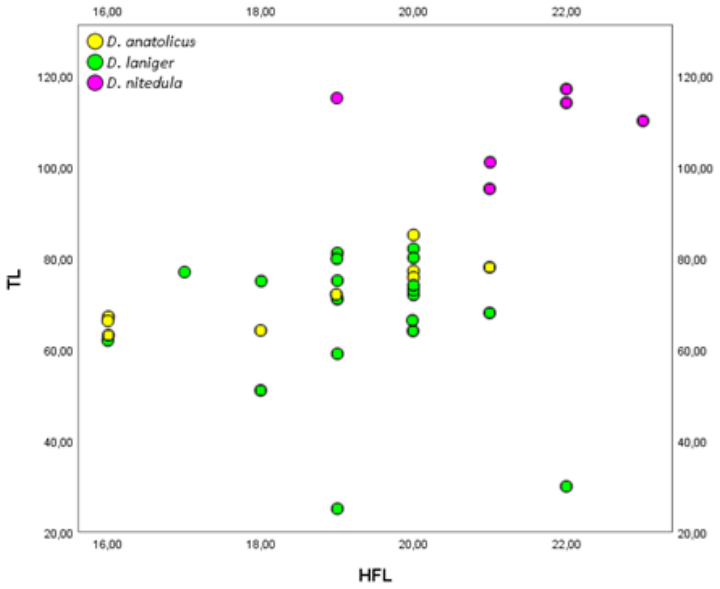

B.

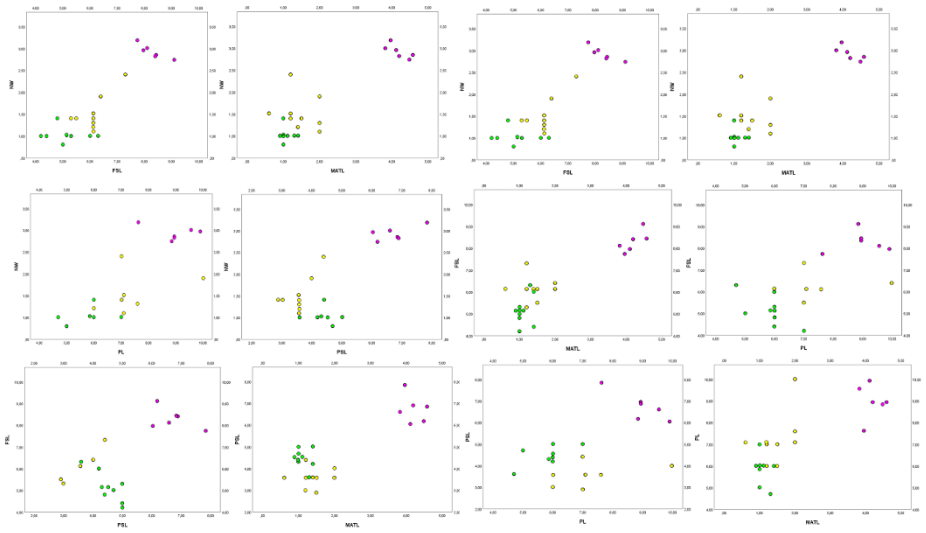

FIGURE 8. Bivariate and multivariate analyses among *D. anatolicus* (yellow circle), *D. laniger* (green circle), and *D. nitedula* (pink circle). A. Scatter plots of external variables for *D. anatolicus*, *D. laniger*, and *D. nitedula*. B. Scatter plots of skull and mandible variables (HFL, length of hindfoot; TL, length of tail; NW, nasal width; FSL, length of frontal suture; PSL, length of parietal suture; PL, palatal length; MATL, length of mandibular tooth row) for *D. anatolicus*, *D. laniger*, and *D. nitedula*

While the value ranges of external characters of 3 *Dryomys* species are as follows: (i) *D. anatolicus* TL 63.0–85.0 mm, HFL 16.0–21.0 mm (ii) D. laniger TL 25.0–82.0 mm, HFL 16.0–22.0 mm (iii) *D. nitedula* TL 95.0–117.0 mm, HFL 19.0–23.0 mm. The ranges of character values for the skull and mandible are as follows: (i) NW 1.1–2.4 mm, FSL 5.3–7.3 mm, PSL 2.9–4.4 mm, PL 6.0–10.0 mm, MATL 0.6–2.0 mm for *D. anatolicus* (ii) NW 0.8–1.4 mm, FSL 4.2–6.3 mm, PSL 3.6–5.0 mm, PL 4.7–7.0 mm, MATL 0.9–1.4 mm for *D. laniger* (iii) NW 2.7–3.2 mm, FSL 7.7–9.2 mm, PSL 6.0–7.8 mm, PL 7.6–9.9 mm, MATL 3.8–4.6 mm for *D. nitedula*.

3.2.2 Geometric morphometry

According to the centroid size analysis, it was determined that *D. anatolicus*, *D. laniger* and *D. nitedula* species were different from each other. When the average centroid size was examined, it was seen that *D. nitedula*, *D. laniger* and *D. anatolicus* had the largest skull and mandible, respectively (Figure 9). The ANOVA test results confirmed that there was a significant difference in the shape and dimensions of the dorsal, ventral and mandible of the skull among the three species groups ($p<0.0001$ and $p<0.05$) (Table 5). Differences in centroid sizes (skull and mandible) of *D. anatolicus*, *D. laniger* and *D. nitedula* were found (Table 5). It was revealed that *D. nitedula* was bigger than *D. anatolicus* and *D. laniger* on the other hand *D. anatlolicus* was found to be the smallest for both skull and mandible (Figure 9).

TABLE 5. ANOVA test results based on centroid size data of *Dryomys* species (Bold shows that Statistically Significant Difference)

	ANOVA	
	F Value	P Value
Dorsal Cranium	5.36	**0.0143**
Ventral Cranium	5.40	**0.0133**
Mandibles	30.43	**0.0001**

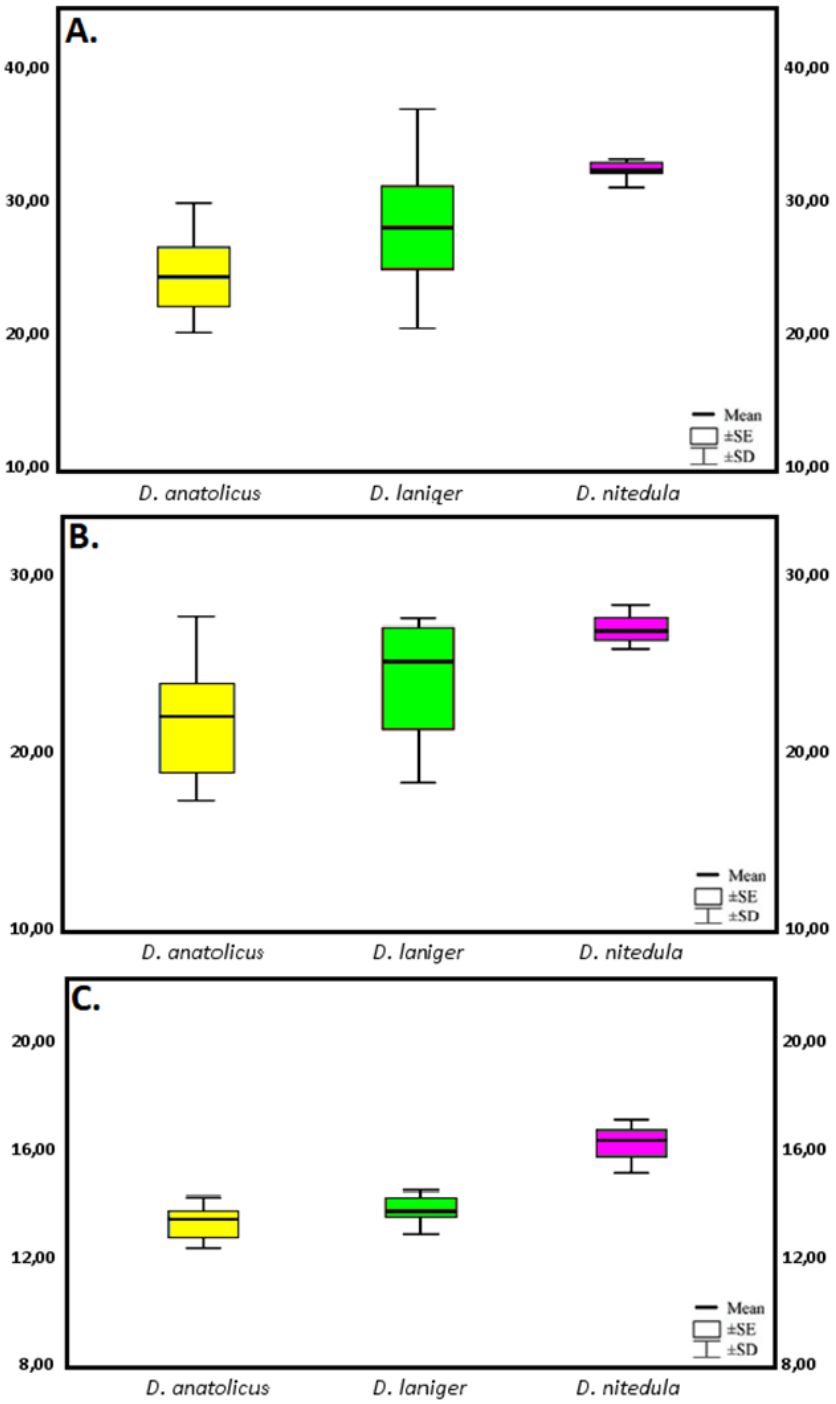

FIGURE 9. Box plot for dorsal, ventral cranium and mandible centroid sizes of *Dryomys* species (A: Dorsal Cranium; B: Ventral Cranium; C: Mandible)

According to the results of the PCA analysis, differences were observed in the shape area distributions of the dorsal, ventral and mandibular skulls of the specimens belonging to the *Dryomys* species. Accordingly, the first 6 components forming the dorsal part of the skull constituted 97% of the total variation. PC1 explained 53.69% and PC2 explained 21.24% of the total variation (Figure 10A). The first 8 components forming the ventral part of the skull constituted 97.47% of the total variation. PC1 explained 47.38% and PC2 explained 21.95% of the total variation (Figure 10B). When we look at the mandible, it was seen that the first 11 components constituted 96.65% of the total variation, while PC1 explained 38.10% and PC2 explained 19.10% of the total variation (Figure 10C).

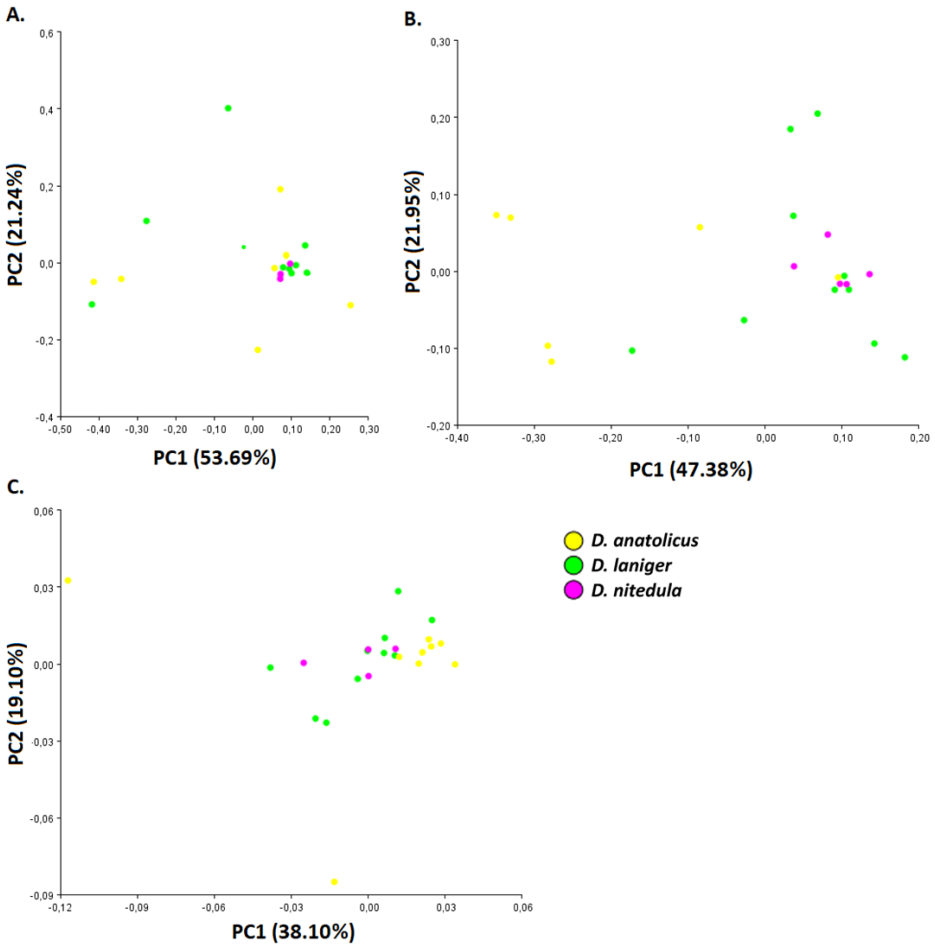

FIGURE 10. According to the Principal Component (PC), the scatter plots depict the dorsal cranium, ventral cranium, and mandibular characteristics in *Dryomys* species (A: dorsal part of the skull; B: ventral part of the skull; C: mandible)

Variations among species within the genus *Dryomys* (*D. anatolicus*, *D. laniger* and *D. nitedula*) were clearly explained by CVA analyses (Figure 11). The analysis performed for the dorsal aspect of the skull showed that *D. anatolicus* and *D. laniger* were grouped closer to each other in CV1 than *D. nitedula*, while in CV2, *D. anatolicus* and *D. nitedula* were grouped closer to each other than *D. laniger* (Figure 11A). Similarly, the analysis performed for the ventral aspect of the skull showed that *D. anatolicus* and *D. laniger* were grouped closer to each other in CV1 than *D. nitedula*, while in CV2, *D. laniger* and *D. nitedula* were grouped closer to each other than *D. anatolicus* (Figure 11B). Similarly, the analysis for the mandible showed that *D. anatolicus* and *D. nitedula* were grouped closer together in CV1 than in *D. laniger*, while in CV2, as in the ventral part of the skull, *D. laniger* and *D. nitedula* were grouped closer together than in *D. anatolicus* (Figure 11C). This analysis provides better resolution of intraspecific distinctions within the genus *Dryomys* than PCA.

The shape differences between the mentioned species were much better separated along the first axis of the scatter plot by CVA. In the analysis, CV1 for the dorsal part of the skull explained 93.16% of the total shape variation among the three species, CV1 for the ventral part of the skull explained 76.74%, and CV1 for the mandible explained 80.44%.

When the CVA results were examined, no statistically significant difference was found for Mahalanobis Distance for any of the species. According to the dorsal cranium data, the Mahalanobis and Procrustes distances between species groups and the permutation test differences based on these differences did not yield significant results. The ventral cranium data showed that *D. anatolicus* was significant in terms of Procrustes distances with *D. laniger* and *D. nitedula* and the permutation test differences based on these differences ($p<0.05$). Finally, when we examined the data belonging to the mandible, it was seen that *D. anatolicus* gave much more significant results than the ventral cranium in terms of Procrustes distances with *D. laniger* and *D. laniger* with *D. nitedula* and the permutation test differences based on these differences ($p<0.01$) (Table 6). When examined, it was shown that the CVA performed with both the data of the ventral cranium and the data of the mandible showed that all 3 species groups could be significantly and clearly separated from each other, but these 3 species groups did not show a significant difference even though they were clearly separated in the dorsal cranium (Figure 11).

TABLE 6. CVA results for dorsal, ventral cranium and mandible (Mah. Dist.: Mahalanobis Distance; Proc. Dist.: Procrustes Distance; Perm. P.: Permutation P Value), (Bold shows that Statistically Significant Difference)

Species Groups	*D. anatolicus*				*D. laniger*			
	Mah. Dist.	Perm. P.	Proc. Dist.	Perm. P.	Mah. Dist.	Perm. P.	Proc. Dist.	Perm. P.
Dorsal Cranium								
D. laniger	8.3734	0.1509	0.1407	0.3816	–	–	–	–
D. nitedula	25.6361	0.1918	0.1735	0.2820	19.9396	0.6661	0.1280	0.3437
Ventral Cranium								
D. laniger	4.9944	0.2710	0.2143	**0.0163**	–	–	–	–
D. nitedula	7.3040	0.1092	0.2551	**0.0145**	8.3879	0.2575	0.1059	0.1280
Mandible								
D. laniger	9.1697	0.4246	0.0428	**0.0044**	–	–	–	–
D. nitedula	8.8035	0.8010	0.0261	0.8452	13.9422	0.3971	0.039	0.0028

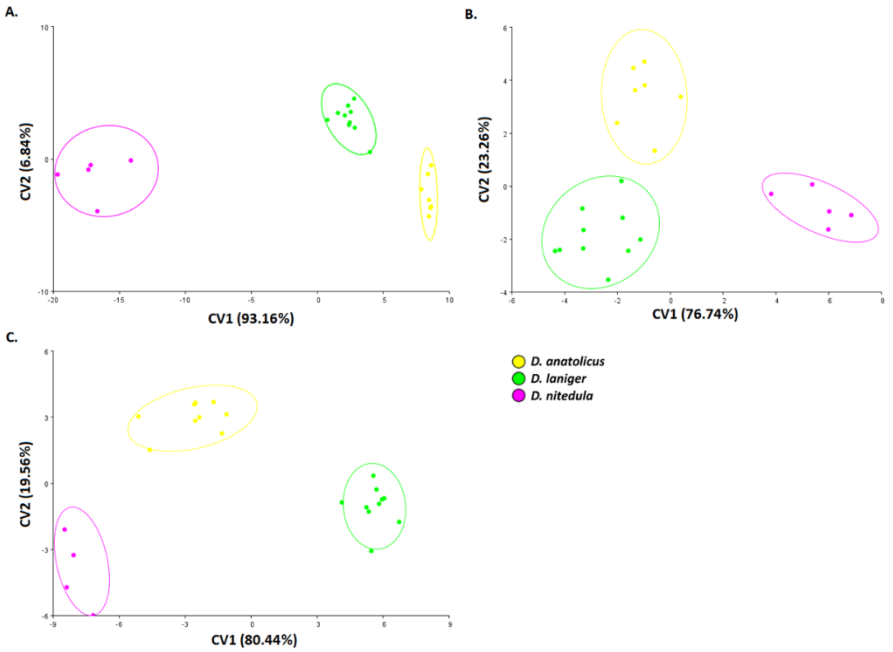

FIGURE 11. Scatter plots of results of Canonical Variate Analysis (CVA) in *Dryomys* species (A: Dorsal Cranium; B: Ventral Cranium; C: Mandible)

According to the Discriminant Function Analysis (DFA) results performed with skull and mandible data, it was observed that the correct separation of the groups from each other in the pairwise comparisons was quite high. This rate was 100% for the dorsal cranium, 100% for the ventral cranium and 97.4% for the mandible, respectively. In the pairwise grouping performed only for the mandible, 2 specimens belonging to *D. anatolicus* were grouped as *D. nitedula* (Figure 12). The average shape differences of the dorsal cranium, ventral cranium and mandible belonging to the species are shown in (Figure 13). The test results obtained during the Discriminant Function Analysis (DFA) showed that the shape differences of the dorsal cranium, ventral cranium and mandible belonging to the species groups were statistically significant (Table 7).

According to dorsal cranium data, *D. nitedula* differed from both *D. anatolicus* and *D. laniger* in terms of Permutation P Value test and this difference is statistically significant ($p<0.05$). Ventral cranium data showed that *D. anatolicus* differed from *D. laniger* and *D. nitedula* in terms of Procrustes Distance Value test and *D. nitedula* differed from *D. laniger* in terms of Permutation P Value test. These differences are $p<0.05$ and $p<0.01$ respectively and are statistically highly significant. Finally, when we examined the data belonging to the mandible, it was proven that *D. anatolicus* and *D. laniger* were different from each other in terms of the Permutation P Value test and *D. laniger* and *D. nitedula* in terms of both the Permutation P Value test and the Procrustes Distance Value test, and these differences were statistically significant ($p<0.01$, $p<0.05$) (Table 7).

TABLE 7. DFA results for dorsal, ventral cranium and mandible (T^2: T-square; Param. P.: Parametric P Values; Perm. P. (T^2): Permutation P Value; Perm. P. (Proc.): Procrustes Distance Value), (Bold shows that Statistically Significant Difference)

Species Groups	*D. anatolicus*				*D. laniger*			
	T^2	Param. P.	Perm. P. (T^2)	Perm. P. (Proc.)	T^2	Param. P.	Perm. P. (T^2)	Perm. P. (Proc.)
Dorsal Cranium								
D. laniger	147.3293	0.7645	0.0601	0.3833	–	–	–	–
D. nitedula	575.1780	0.3145	**0.0231**	0.2879	263.4833	0.5624	**0.0388**	0.3447
Ventral Cranium								
D. laniger	67.4610	0.8896	0.1069	**0.0143**	–	–	–	–
D. nitedula	35.6834	0.6710	0.5521	**0.0151**	136.2794	0.4704	**0.0088**	0.1302
Mandible								
D. laniger	238.0958	0.7141	0.1215	**0.0040**	–	–	–	–
D. nitedula	8.9454	0.9964	0.7884	0.8495	35.6136	0.9326	**0.0155**	**0.0027**

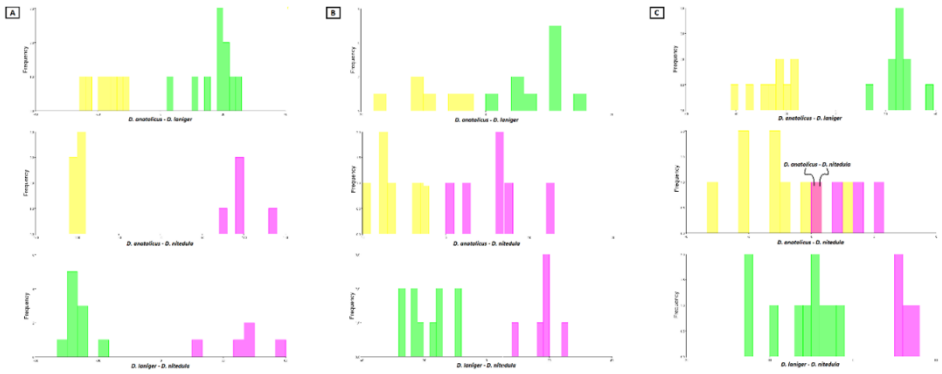

FIGURE 12. Scatter plots of result of Discriminant Function Analysis (DFA) in *Dryomys* species (A: Dorsal Cranium; B: Ventral Cranium; C: Mandible) (X-Axis: Discriminant Scores; Y-Axis: Frequency)

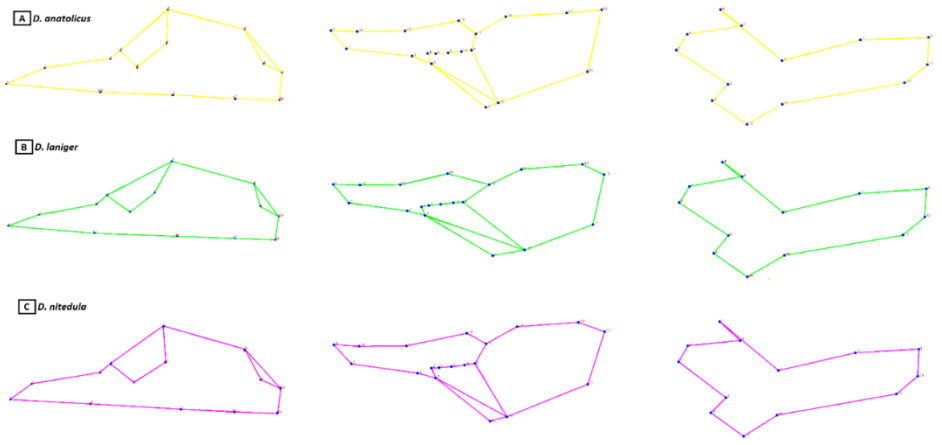

FIGURE 13. Discriminant Function Analysis (DFA) mean shape differences results for dorsal cranium, ventral cranium and mandible by respectively (A: *D. anatolicus*; B: *D. laniger*; C: *D. nitedula*)

3.3 Taxonomy

3.3.1 *Dryomys anatolicus* sp. nov.

urn:lsid:zoobank.org:pub:3AC02C5C-E8DA-47FA- 889B-73C9387EA937

3.3.2 Diagnosis and comparison

D. laniger has brownish dorsal fur on the contrary of *D. anatolicus* which has grey dorsal fur (Figure 14). According to morphological data from skull measurements (Table S3 and Figure 15) there are significant differences between two species. *D. laniger* has a larger skull than *D. anatolicus* (Figure 9). Dorsal, ventral and mandible of the skull are different (Table 5). Sexual dimorphism was not observed in our samples. Beside morphological differences there are also genetic differences between two species. Genetically distant clade in phylogenetic tree reconstructed with mtDNA (*CYTB*) and nuclear DNA (IRBP) marker. Kimura 2 parameter distance in *CYTB* between *Dryomys anatolicus* sp. nov. and *Dryomys laniger* is 7%.

3.3.3 Holotype

One adult female, the skin deposited at Zonguldak Bülent Ecevit University Molecular Systematic Laboratory (Sample no: 8715) (Figure 14). Skull, mandibular, and tissues preserved in RNA later solution.

3.3.4 Type locality and distribution

Type locality of the species is Eşekçayırı plateau, Ovacık, Tunceli, Turkey (39.420799 N, 39.240681 E, 1800 m). Another distribution record from Püren pass, Göksun, Kahramanmaraş, Turkey (37.931851 N, 36.503126 E, 1700 m).

3.3.5 Paratypes

Four females from the type locality (8712, 8713, 8714, and 8716) in addition to the type specimen (8715). One male (8682) and five females (8662, 8680, 8683, 8684, and 8685) from Püren pass, Göksun, Kahramanmaraş, Turkey.

3.3.6 Etymology

Since it is endemic to Anatolia, the name *D. anatolicus* was chosen.

3.3.7 Measurements of holotype

External characters and skull measurements (weight in g, other measurements in mm); Total length, 180; head and body, 103; Tail; 77, Hindfoot, 20; Ear; 15; Weight, 21; Zygomatic width, 12; Rostrum width, 3; Interorbital width, 2; Nasal Length, 7.3; Nasal width, 1.9; Frontal suture length, 6.4; Parietal suture length, 4; Brain capsule width, 9.7; Face area length, 12; Diestema length, 4.5; Palatal length, 10; Foramen incision length, 4.2; Upper tooth row length, 1.3; Rostrum height, 2; Lower tooth row length, 2; Mandible height, 4.4; Mandible length, 12.

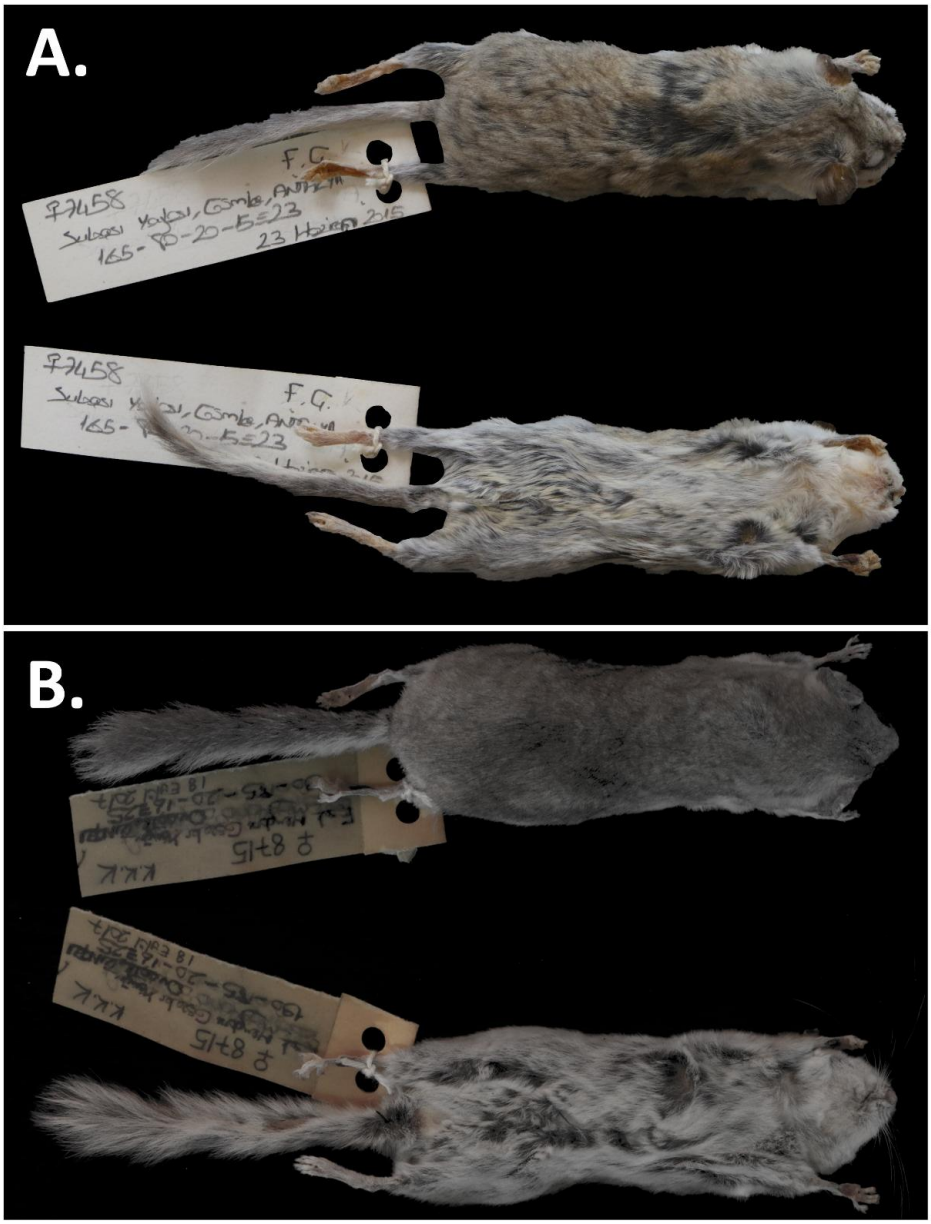

FIGURE 14. Skin of the *Dryomys laniger* (A) and *Dryomys anatolicus* sp. nov. (B)

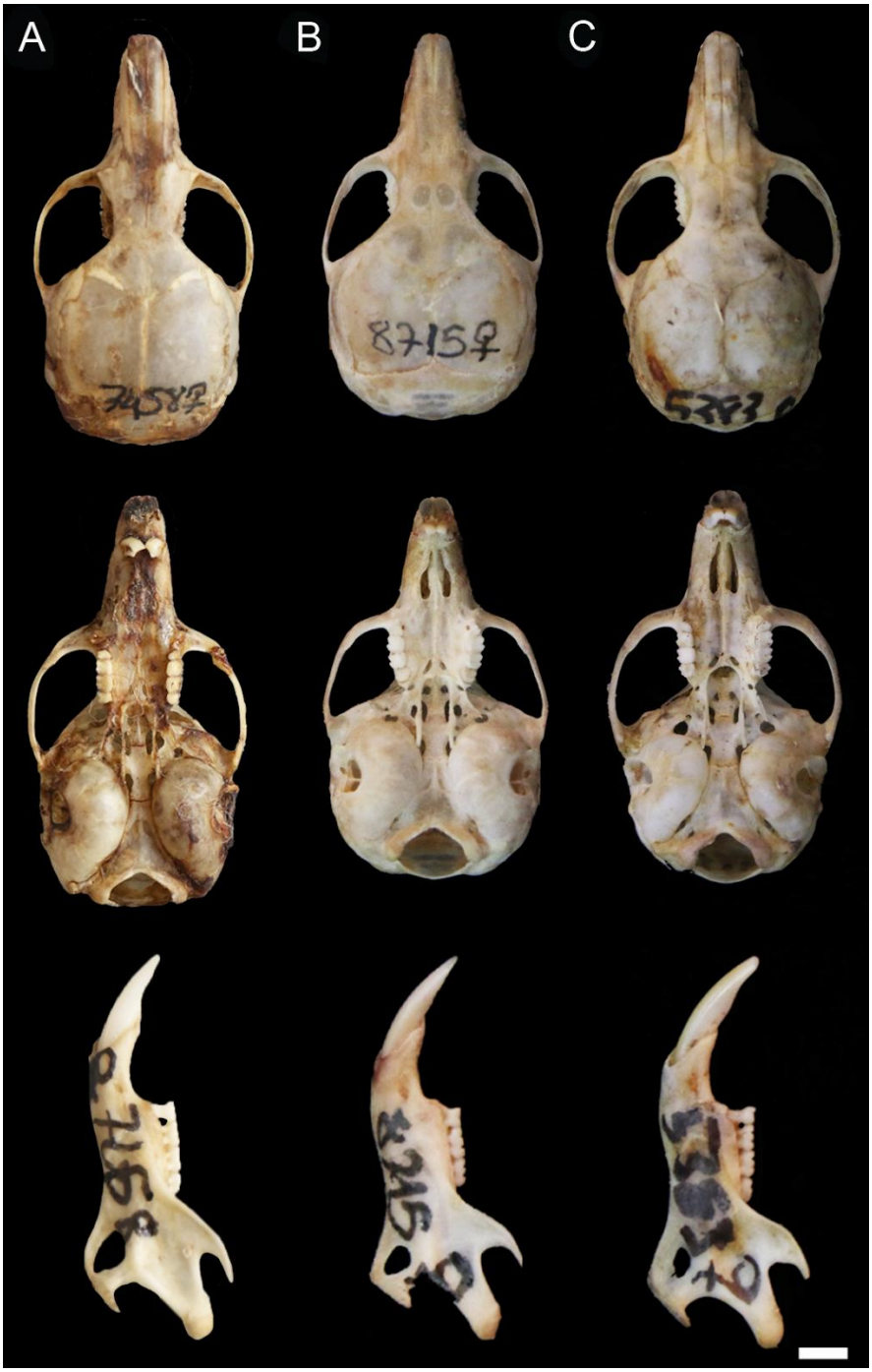

FIGURE 15. Skull and mandible of the *D. laniger* (A), type specimen (8715) of *Dryomys anatolicus* sp. nov. (B) and *D. nitedula* (C)

3.3.8 Habitat

Mountainous areas above 1700 m a.s.l. The species lives in rocky areas with sparse vegetation. The distribution area of the species is fragmented and apart from the type locality in Munzur Mountains (Figure 16), it has also been found in Püren Pass (province of Kahramanmaraş, Figure 17).

FIGURE 16. Habitat of *Dryomys anatolicus* type locality, Eşekçayırı Plateau (Munzur mountains), Ovacık, Tunceli

FIGURE 17. Habitat of *Dryomys anatolicus*, Püren pass (Armut mountains), Göksun, Kahramanmaraş

4. DISCUSSION

We presented the first results on the phylogeny, genetic diversity, and extended distribution records of *D. laniger*, a small rodent endemic to Anatolia with a highly fragmented distribution range. Besides resampling the four distribution areas that were previously identified, two new geographical locations have been recorded: the Çiçekliboyun plateau and the Subaşı plateau. Next, we found that the two populations with the easternmost distribution (Yellow clade) (Armut and Munzur mountains) possess sufficient genetic and morphological differences to warrant a new species status, *D. anatolicus sp. nov*. As alpine and montane species, *D. laniger* and *D. anatolicus sp. nov*. may have survived these areas through the Quaternary. It is likely that *D. laniger* and *D. anatolicus* had a wider distribution in the Quaternary than at present.

We can see a very deep divergence between *D. laniger* and *D. anatolicus* sp. nov. [43] The K2P distance of 7% in the full CYTB sequence is very high between these taxa, i.e. much higher than the threshold of 1,5 - 2,5% proposed by [44] for CYTB. Similar to Tobe and colleagues' work, [45] proposed a threshold of >2% to start considering the species rank. The same authors consider the genetic distance below 2% to indicate intraspecific variation: note that 2% is the level of divergence between clade 1 and clade 2 within the green clade of *D. laniger*. Beside CYTB, in the phylogenetic tree reconstructed with IRBP there is a clear seperation between *D. laniger* and *D. anatolicus* sp. nov. with a strong support (Figure 3). AMOVA also showed this deep divergence between *D. laniger* and *D. anatolicus* sp. nov. IRBP, as a nuclear gene, is particularly valuable in phylogenetic studies of mammals and other vertebrates because it provides complementary insights to mitochondrial markers like CYTB, which can sometimes reflect only maternal inheritance patterns [46–48].

According to the divergence between ancestors of *D. laniger*/*D. anatolicus* sp. nov. clade and *D. nitedula* which occurred ~25 mya, the two species separated from each other in the Oligocene. During the Eocene/Oligocene transition an extinction/immigration event occurred called “grande coupure” about 33 mya. During that time dormice survived and they were also very successful [49]. They continued to diversify throughout the Oligocene and early Miocene [50]. Our hypothesis is that during the Oligocene because of the uplift of Anatolia, ancestors of *D. laniger* and *D. anatolicus* separated from *D. nitedula* and became isolated at the high altitudes in Anatolia [51]. When the uplift event gradually occurred some populations could adapt and prevail through these topographic changes [16]. We think that the ancestors of *D. laniger* and *D. anatolicus* may have adapted to the alpine environments and speciation events occurred allopatrically between these two species. This hypothesis is consistent with the idea that Spitzenberger presented in 1976. According to their opinion, the divergence of *D. laniger* and *D. nitedula* dates back to the late Oligocene. They also proposed that these two species allopatrically diverged from each other.

Two endemic species from Anatolia, *D. laniger* and *D. anatolicus*, diverged from each other ~6 mya. Our hypothesis on the separation event of the species is that *D. anatolicus* migrated to the east first to extend its distribution range. Then when the Messinian dry climate conditions occur in the whole Mediterranean, two populations on the Anatolian Diagonal mountain system (Armut mountains and Munzur mountains) were isolated from *D. laniger* populations which are distributed in the Taurus mountains. At the end of the Messinian epoch, Taurus mountain populations and populations on the Anatolian Diagonal separated from each other at the species level. This event is a good example of peripatric speciation. Ancestral populations harbor more genetic diversity than later immigrants to the new areas [52–54]. In our case, genetic diversity also showed that *D. laniger* is the origin of the *D. anatolicus* because *D. laniger* is genetically more diverse and also even clades of *D. laniger*'s genetic diversity is greater than *D. anatolicus*. Mismatch distribution analyses also showed that both species had several population expansion events in the past.

The two clades within the green clade of *D. laniger* (clade 1 and clade 2) diverge from each other by 1.85 mya. It can be inferred that the separation of these two clades is affected by the climate. In Messinian, *D. laniger* became a separate species, and clades of these species survived on the mountaintops. As an alpine species, *D. laniger* couldn't migrate downhill from the mountaintops in Messinian dry climate. Thus two clades couldn't meet again in Quaternary although ice ages started which have better climatic conditions for an alpine species. The genetic difference between these two clades is 1,9% according to K2P distance. Tobe et al. 2010 proposed a threshold (K2P 1,5%) to separate the species. Our value is higher than this value but we didn't see any difference between morphology. Thinking about the future climate, these two clades are going to stay isolated.

Dryomys laniger currently has a DD (Data Deficient) status according to the IUCN classification, due to very few and sporadic distribution records and the lack of studies on its general biology. As a new species, obviously *D. anatolicus* has no information in the IUCN Red List of Threatened Species. Our observations of the landscapes where both species are found suggest that human impact, especially various mining activities in the Anatolian mountains, may adversely affect the extant populations. In addition, since *D. laniger* and *D. anatolicus* prefer a very specific habitat (steep rock faces), habitat destruction in these areas can have irreversible consequences. Subject to genetic bottleneck and increased chance of extinction, the current populations seem to be poorly equipped facing the threat of additional habitat destruction and the warming climate in the mountainous areas. Active conservation programs are urgently required for all known populations in the Taurus mountains and the Anatolian diagonal. Efforts to discover additional populations in the Anatolian mountains are equally important.

Finally, to better understand the evolutionary histories of two endemic dormouse species, genomic data would be best to resolve the complex taxonomy of this group. The sample sizes for future studies should be increased. We must

therefore reiterate that better genotyping is required to reconstruct the full evolutionary history of this species, beyond that of just mitochondrial lineages demonstrated in our study.

Acknowledgement This study was supported by TÜBİTAK (project no. 113R029). Field collection was done under permit no. 72784983-488.04-45764 from the Ministry of Agriculture and Forestry of the Republic of Turkey. The new species name was registered with ZooBank under urn:lsid:zoobank.org:pub:3AC02C5C-E8DA-47FA- 889B-73C9387EA937. This paper is a part of the PhD project of Ortaç ÇETİNTAŞ supervised by Mustafa SÖZEN.

Author Contribution Statements Ferhat Matur and Mustafa Sözen obtained funding and Mustafa Sözen supervised the study. Ortaç Çetintaş, Faruk Çolak, Kürşat Kenan Kalkan, Ferhat Matur and Mustafa Sözen took part in fieldwork and collected samples. Kürşat Kenan Kalkan analyzed the morphological data. Ortaç Çetintaş and Sercan Irmak performed lab work and analyzed the data. Ortaç Çetintaş designed the study and wrote the paper. All authors approved the final version of the manuscript.

Declaration of Competing Interests The authors declare no conflict of interest.

Ethical Statement The procedure was approved by Zonguldak Bülent Ecevit University Animal Experiments Ethics Committee (permit no. 91330202-10).

Use of Artificial Intelligence No artificial intelligence-based tools or applications were used in the preparation of this study. The entire content of the study was produced by the author(s) in accordance with scientific research methods and academic ethical principles.

Data availability The voucher specimens were deposited in the Molecular Systematics Laboratory in Zonguldak Bülent Ecevit University.

Appendix A. Supplementary data

Supplementary Table S1

Supplementary Table S2

Supplementary Table S3

Supplementary Table S4

Supplementary Table S5

REFERENCES

[1] Felten, H., Storch, G., Eine neue Schlafter-Art, *Dryomys laniger* n. sp. aus Kleinasien (Rodentia: Gliridae). *Senckenbergiana Biologica*, 49 (6) (1968), 429–435.

[2] Holden, M.E., Description of new species of *Dryomys* (Rodentia, Myoxidae) from Balochistan, Pakistan, including morphological comparisons with *Dryomys laniger* Felten & Storch 1968, D. nitedula (Pallas, 1778). *Bonner Zoologische Beiträge*, 46 (1996), 111–131.

[3] Liao, L., An, R., Shi, S., Xu, Y., Luo, Y., Liao, W., One new species of the genus *Dryomys* (Rodentia, Glirgae) from Xinjiang China, *Dryomys Yarkandensis* sp . nov, *BioRxiv*, (2020). https://doi.org/10.1101/2020.02.11.943381

[4] Spitzenberger, F., Beiträge zur Kenntnis von *Dryomys laniger* Felten et Storch, 1968 (Gliridae, Mammalia). *Zeitschrift Für Säugetierkunde*, 78 (1976), 485–494.

[5] Filippucci, M.G., Krystufek, B., Simson Shimon, Kurtonur, C., Özkan, B., Allozymic and biometric variation in *Dryomys nitedula* (Pallas, 1778). *Hystrix*, 6 (1–2) (1995), 127–140.

[6] Grigoryeva, O., Krivonogov, D., Balakirev, A., Stakheev, V., Andreychev, A., Orlov, V., Phylogeography of the forest dormouse *Dryomys nitedula* (Gliridae, Rodentia) in Russian Plain and the Caucasus. *Folia Zoologica*, 64 (4) (2015), 361–364. https://doi.org/10.25225/fozo.v64.i4.a12.2015

[7] Bisconti, R., Aloise, G., Siclari, A., Fava, V., Provenzano, M., Arduino, P., Chiocchio, A., Nascetti, G., Canestrelli, D., Forest dormouse (*Dryomys nitedula*) populations in southern Italy belong to a deeply divergent evolutionary lineage: Implications for taxonomy and conservation. *Hystrix*, 29 (1) (2018).

[8] Mohammadi, Z., Kami, H.G., Ghorbani, F., Khajeh, A., Olsson, U., Cryptic lineage diversity within Forest Dormice (Mammalia: *Dryomys nitedula*) revealed by deep genetic divergence among different subspecies on the Iranian Plateau and in adjacent areas. *Mammalian Biology*, 101 (2021), 21-34. https://doi.org/10.1007/s42991-020-00055-5

[9] Mursaloğlu, B., Türkiye'nin yabani memelileri, in: TÜBİTAK, Ankara, (1973), 1–10.

[10] Obuch, J., Dormice in the diet of owls in the Middle East. *Trakya University Journal of Scientific Research Series B*, 2 (2) (2001), 145–150.

[11] Kart Gür, M., Bulut, Ş., Gür, H., Refinetti, R., Body temperature patterns and use of torpor in an alpine glirid species, woolly dormouse. *Acta Theriologica*, 59 (2) (2014), 299–309. https://doi.org/10.1007/s13364-013-0154-9

[12] Krystufek, B., Vohralík, V., Mammals of Turkey and Cyprus: Rodentia I: Sciuridae, Dipodidae, Gliridae, Arvicolinae. *Koper: Zgodovinsko društvo za južno Primorsko*, 2005.

[13] Yiğit, N., Çolak, E., Çolak, R., Özkan, B., Özkurt, Ş., On the Turkish populations of *Dryomys nitedula* (Pallas, 1779) and *Dryomys laniger* Felten and Storch, 1968 (Mammalia: Rodentia). *Acta Zoologica Academiae Scientiarum Hungaricae*, 49 (SUPPL. 1) (2003), 147–158.

[14] Kankılıç, T., Şeker, P.S., Erdik, A.C., Kankılıç, T., Selvi, E., Yiğit, N., Çolak, E., Determination of genetic variations in the genus *Dryomys* Thomas, 1906 (Rodentia: Gliridae) distributed in Turkey using NADH dehydrogenase 1 (*ND1*) gene. *Mitochondrial DNA Part A*, 29 (6) (2017), 933–942. https://doi.org/10.1080/24701394.2017.1389915

[15] Kankılıç, T., Şeker, P.S., Aydın, B., Altunbaş, D., Selvi, E., Yiğit, N., Çolak, E., Nuclear and organelle genes based phylogeny of *Dryomys* (Gliridae, Rodentia, Mammalia) from Turkey. *Acta Zoologica Academiae Scientiarum Hungaricae*, 65 (4) (2019), 399–413. https://doi.org/10.17109/AZH.65.4.399.2019

[16] Huang, S., Meijers, M.J.M., Eyres, A., Mulch, A., Fritz, S.A., Unravelling the history of biodiversity in mountain ranges through integrating geology and biogeography. *Journal of Biogeography*, 46 (8) (2019), 1777–1791. https://doi.org/10.1111/jbi.13622

[17] Kafimola, S., Azimi, M., Saberi-Pirooz, R., Ilgaz, C., Mohammadi Kashani, G., Kapli, P., Ahmadzadeh, F., Diversification in the mountains: Evolutionary history and molecular phylogeny of Anatolian rock lizards. *Molecular Phylogenetics and Evolution*, (2023), 107675. https://doi.org/10.1016/j.ympev.2022.107675

[18] Gündüz, I., Jaarola, M., Tez, C., Yeniyurt, C., Polly, P.D., Searle, J.B., Multigenic and morphometric differentiation of ground squirrels (*Spermophilus*, Scuiridae, Rodentia) in Turkey, with a description of a new species. *Molecular Phylogenetics and Evolution*, 43 (3) (2007), 916–935. https://doi.org/10.1016/j.ympev.2007.02.021

[19] Kaya, S., Boztepe, Z., Çiplak, B., Phylogeography of Troglophilus (Orthoptera: Troglophilinae) based on Anatolian members of the genus: radiation of an old lineage following the Messinian, Biological Journal of the Linnean Society. *Linnean Society of London*, 108 (2) (2013), 335–348. https://doi.org/10.1111/j.1095-8312.2012.02025.x

[20] Bilgin, R., Back to the suture: the distribution of intraspecific genetic diversity in and around anatolia., *International Journal of Molecular Sciences*, 12 (6) (2011), 4080–4103. https://doi.org/10.3390/ijms12064080

[21] Kıvanç, E., Sözen, M., Çolak, E., Yiğit, N., Karyological and phallic characteristics of *Dryomys laniger* (Rodentia: Gliridae) Felten and Storch, 1968 in Turkey. *Israel Journal of Zoology*, 43 (4) (1997), 401–403.

[22] Montgelard, C., Bentz, S., Tirard, C., Verneau, O., Catzeflis, F.M., Molecular systematics of sciurognathi (rodentia): the mitochondrial cytochrome b and 12S rRNA genes support the Anomaluroidea (Pedetidae and Anomaluridae). *Molecular Phylogenetics and Evolution*, 22 (2) (2002), 220–233. https://doi.org/10.1006/mpev.2001.1056

[23] Stanhope, M.J., Czelusniak, J., Si, J.S., Nickerson, J., Goodman, M., A molecular perspective on mammalian evolution from the gene encoding interphotoreceptor retinoid binding protein, with convincing evidence for bat monophyly. *Molecular Phylogenetics and Evolution*, 1 (2) (1992), 148–160. https://doi.org/10.1016/1055-7903(92)90026-d

[24] Kearse, M., Moir, R., Wilson, A., Stones-Havas, S., Cheung, M., Sturrock, S., Buxton, S., Cooper, A., Markowitz, S., Duran, C., Thierer, T., Ashton, B., Meintjes, P., Drummond, A., Geneious Basic: an integrated and extendable desktop software platform for the organization and analysis of sequence data. *Bioinformatics*, 28 (12) (2012), 1647–1649. https://doi.org/10.1093/bioinformatics/bts199

[25] Nylander, J.A.A., MrModeltest v2, Program Distributed by the Author, (2004).

[26] Silvestro, D., Michalak, I., raxmlGUI: a graphical front-end for RAxML. *Organisms Diversity & Evolution*, 12 (4) (2012), 335–337. https://doi.org/10.1007/s13127-011-0056-0

[27] Ronquist, F., Teslenko, M., van der Mark, P., Ayres, D.L., Darling, A., Höhna, S., Larget, B., Liu, L., Suchard, M.A., Huelsenbeck, J.P., MrBayes 3.2: efficient Bayesian phylogenetic inference and model choice across a large model space, *Systematic Biology*, 61 (3) (2012), 539–542. https://doi.org/10.1093/sysbio/sys029

[28] Rozas, J., Ferrer-Mata, A., Sánchez-DelBarrio, J.C., Guirao-Rico, S., Librado, P., Ramos-Onsins, S.E., Sánchez-Gracia, A., Dnasp 6: DNA sequence polymorphism analysis of large data sets, *Molecular Biology and Evolution*, 34 (12) (2017), 3299–3302. https://doi.org/10.1093/molbev/msx248

[29] Kumar, S., Stecher, G., Li, M., Knyaz, C., Tamura, K., MEGA X: Molecular evolutionary genetics analysis across computing platforms. *Molecular Biology and Evolution*, 35 (6) (2018), 1547–1549. https://doi.org/10.1093/molbev/msy096

[30] Clement, M., Posada, D., Crandall, K.A., TCS: a computer program to estimate gene genealogies. *Molecular Ecology*, 9 (10) (2000), 1657–1659. https://doi.org/10.1046/j.1365-294x.2000.01020.x

[31] Leigh, J.W., Bryant, D., POPART: full-feature software for haplotype network construction. *Methods in Ecology and Evolution*, 6 (9) (2015), 1110–1116. https://doi.org/10.1111/2041-210X.12410

[32] Excoffier, L., Lischer, H.E.L., Arlequin suite ver 3.5: A new series of programs to perform population genetics analyses under Linux and Windows. *Molecular Ecology Resources*, 10 (3) (2010), 564–567. https://doi.org/10.1111/j.1755-0998.2010.02847.x

[33] Bouckaert, R., Heled, J., Kühnert, D., Vaughan, T., Wu, C.-H., Xie, D., Suchard, M.A., Rambaut, A., Drummond, A.J., BEAST 2: a software platform for Bayesian evolutionary analysis. *PLoS Computational Biology*, 10 (4) (2014), e1003537. https://doi.org/10.1371/journal.pcbi.1003537

[34] Montgelard, C., Matthee, C.A., Robinson, T.J., Molecular systematics of dormice (Rodentia: Gliridae) and the radiation of Graphiurus in Africa., Proceedings. Biological Sciences / the Royal Society, 270 (1527) (2003), 1947–1955. https://doi.org/10.1098/rspb.2003.2458

[35] Niethammer, J., Krapp, F., Becker, K., Handbuch der Säugetiere Europas : Bd. 1: Rodentia I: (Sciuridae, Castoridae, Gliridae, Muridae). *Akademische Verlagsgesellschaft*, 1978.

[36] Bookstein, F.L., Morphometric tools for landmark data: Geometry and biology, Cambridge University Press, Cambridge, 1992. https://doi.org/10.1017/CBO9780511573064

[37] James Rohlf, F., Marcus, L.F., A revolution morphometrics. *Trends in Ecology & Evolution*, 8 (4) (1993), 129–132. https://doi.org/10.1016/0169-5347(93)90024-J

[38] Rohlf, F.J., tps Utility program., Ecology and Evolution, SUNY at Stony Brook, (2009).

[39] Rohlf, F.J., The tps series of software. *Hystrix*, 26 (1) (2015), 9–12.

[40] Zelditch, M., Swiderski, D., Sheets, H.D., Geometric Morphometrics for Biologists: A Primer, Academic Press, (2012).

[41] Hammer, Ø., Harper, D.A.T., Past: paleontological statistics software package for educaton and data anlysis. *Palaeontologia Electronica*, 4 (1) (2001).

[42] Klingenberg, C.P., MorphoJ: an integrated software package for geometric morphometrics. *Molecular Ecology Resources*, 11 (2) (2011), 353–357. https://doi.org/10.1111/j.1755-0998.2010.02924.x

[43] Çetintaş, O., Irmak, S., Matur, F., Sözen, M., A new endemic dormouse species in Anatolia. *ARPHA Conference Abstracts*, 5 (2022). https://doi.org/10.3897/aca.5.e84506

[44] Tobe, S.S., Kitchener, A.C., Linacre, A.M.T., Reconstructing mammalian phylogenies: a detailed comparison of the cytochrome B and cytochrome oxidase subunit I mitochondrial genes. *Plos One*, 5 (11) (2010), e14156. https://doi.org/10.1371/journal.pone.0014156

[45] Bradley, R.D., Baker, R.J., A test of the Genetic Species Concept: cytochrome-b sequences and mammals. *Journal of Mammalogy*, 82 (4) (2001), 960–973. https://doi.org/10.1644/1545-1542(2001)082<0960:ATOTGS>2.0.CO;2

[46] Stanhope, M.J., Smith, M.R., Waddell, V.G., Porter, C.A., Shivji, M.S., Goodman, M., Mammalian evolution and the interphotoreceptor retinoid binding protein (IRBP) gene: convincing evidence for several superordinal clades. *Journal of Molecular Evolution*, 43 (2) (1996), 83–92. https://doi.org/10.1007/BF02337352

[47] Springer, M.S., Burk, A., Kavanagh, J.R., Waddell, V.G., Stanhope, M.J., The interphotoreceptor retinoid binding protein gene in therian mammals: implications for higher level relationships and evidence for loss of function in the marsupial mole., Proceedings of the National Academy of Sciences of the United States of America, 94 (25) (1997), 13754–13759. https://doi.org/10.1073/pnas.94.25.13754

[48] Redmond, A.K., McLysaght, A., Horizontal transfer of vertebrate vision gene IRBP into the chordate ancestor., Proceedings of the National Academy of Sciences of the United States of America, 120 (34) (2023), e2310390120. https://doi.org/10.1073/pnas.2310390120

[49] Dawson, M.R., Paleogene rodents of Eurasia. *Deinsea*, 10 (2003), 97–126.

[50] Daams, R., De Bruijn, H., A classification of the Gliridae (Rodentia) on the basis of dental morphology. *Hystrix*, 6 (1995), 3–50.

[51] Popov, S.V., Akhmetiev, M.A., Bugrova, E.M., Lopatin, A.V., Amitrov, O.V., Andreyeva-Grigorovich, A., Zaporozhets, N.I., Zherikhin, V.V., Krasheninnikov, V.A., Nikolaeva, I.A., Sytchevskaya, E.K., Shcherba, I.G., Biogeography of the Northern Peri-Tethys from the late eocene to the early miocene. Part 2. Early Oligocene. *Paleontological Journal*, 36 (Suppl. 3) (2002), 185–259.

[52] Taberlet, P., Fumagalli, L., Wust-Saucy, A.G., Cosson, J.F., Comparative phylogeography and postglacial colonization routes in Europe. *Molecular Ecology*, 7 (4) (1998), 453–464. https://doi.org/10.1046/j.1365-294x.1998.00289.x

[53] Médail, F., Diadema, K., Glacial refugia influence plant diversity patterns in the Mediterranean Basin. *Journal of Biogeography*, 36 (7) (2009), 1333–1345. https://doi.org/10.1111/j.1365-2699.2008.02051.x

[54] Hewitt, G.M., Genetic consequences of climatic oscillations in the Quaternary. *Philosophical Transactions of the Royal Society of London. Series B, Biological Sciences*, 359 (1442) (2004), 183–95. https://doi.org/10.1098/rstb.2003.1388

http://communications.science.ankara.edu.tr

Commun.Fac.Sci.Univ.Ank.Ser. C Biology
Volume 34, Number 1, Pages 36-47 (2025)
ISSN 1303-6025 E-ISSN 2651-3749
DOI: 10.53447/communc.1656451

Research Article; Received: March 12, 2025; Accepted: May 05, 2025

EVALUATION OF BIOACCUMULATION AND TOXICITY OF CONGO RED ON *Pseudochloris wilhelmii* AND *Daphnia magna*

Elif Betül KAĞIZMAN[1], Şeyda FİKİRDEŞİCİ ERGEN[1], Burcu ERTİT TAŞTAN[2,3]

Keywords

Toxicity
Dye
Algae
Water flea

To cite this article

Kağızman E. B., Fikirdeşici Ergen Ş., Ertit Taştan B., Evaluation of bioaccumulation and toxicity of congo red on *Pseudochloris wilhelmii* and *Daphnia magna*. *Commun.Fac.Sci.Univ.Ank.Ser.C Biology*, 34 (1) (2025), 36-47. https://doi.org/10.1111/communc.1656451

Affiliations

[1]Department of Biology, Faculty of Science, Ankara University, Ankara, TÜRKİYE

[2]Health Services Vocational School, Gazi University, Ankara, TÜRKİYE

[3]Life Sciences Application and Research Center, Gazi University, Ankara, TÜRKİYE

Abstract

Congo Red, which may have allergic, carcinogenic and mutagenic effects for organisms used in textiles and in biochemistry and histology for dyeing microscopic media, is an organic pollutant that causes environmental concerns. This study shows that the acute toxic effects of Congo Red on two different aquatic organisms (Pseudochloris wilhelmii and Daphnia magna). The toxic effects of increasing dye concentrations on the growth of Pseudochloris wilhelmii were demonstrated by algal inhibition test. The maximum chlorophyll (a+b) concentration was determined as 0.445 µg/mL at a dye concentration of 5.38 mg/L after 72 hours of exposure. This value decreased to 0.218 µg/mL at 28.46 mg/L dye concentration, indicating a decrease of approximately 50%. For Daphnia magna, it was also demonstrated that acute toxic effects reached their highest level with increasing concentrations and duration (72h LC50: 89.91 mg/L). This study shows that the introduction of Congo red into ecosystems could cause stress on the environment and organisms.

1. INTRODUCTION

Water is the most basic resource for all organisms and the health of the ecosystem. However, in recent years, pollution of water resources have become a growing concern. Due to rapidly increasing urbanization and globalization, the demand for industrial products is also accelerating. Increasing demand brings along industrial wastes and thus water pollution [1]. Textile industries, which are responsible for about 75% of the global dye market, cause pollution of existing waters by causing excessive application of dyes or pigments [2]. Azo dyes represent approximately 60-70% of industrial production. These xenobiotic chemicals, which are widely used due to their low cost, permanence and diversity, can be identified by the presence of the azo group (-N=N-) [3]. The

kagizman.elif@gmail.com- 0000-0002-0328-8623 https://ror.org/01wntqw50
seydafikirdesici@gmail.com- 0000-0002-4623-1256 https://ror.org/01wntqw50
burcuertit@gazi.edu.tr- Corresponding author; 0000-0003-4644-8305 https://ror.org/054xkpr46

presence of these pollutants alters photosynthetic mechanisms by reducing light transmittance, thus altering O_2 concentration [4]. Some carcinogens such as benzidine, which may be present in the structure of these chemicals used for colouring, also raise concerns. Azo dyes are very difficult to degrade, so physical and chemical processes used in wastewater removal can be quite costly and limited [5]. Congo Red is one of the azo dyes with molecular formula $C_{32}H_{22}N_6Na_2O_6S_2$ and molecular weight = 696.68 g mol-1, which is widely used in the textile industry for dyeing paper, silk and wool due to its low cost. Congo Red, discovered by Paul Bottinger in 1884, is an anionic di-azo dye consisting of a sodium salt of benzidinedithiazo-bis-1-naphthylamine-4-sulfonic acid [6] (Figure 1. Congo Red chemical structure). This study aims to determine the toxic effects of Congo red using *P. wilhelmi* and *D. magna* (Figure 2).

P. wilhelmii is a less studied species than other microalgae. It is a species with richer biomass and chlorophyll concentration than *Chlorella sorokiniana* and *Tetraselmis obliquus* [7]. In addition, this species is introduced in the literature as a species with fast growth and a wide nutrient tolerance, including wastewater [8]. In another study investigating the effects of different iron concentrations on biomass and biofuel production on *P. wilhelmii*, it was stated that increasing the iron concentration led to an increase in biomass productivity [9]. Studies on this species are limited in the literature and more research is needed.

Daphnia is a genus of small planktonic crustaceans. They are known as "water fleas". They are classified as members of the Cladocera order within the Branchiopoda class. *Daphnia* have a large head, a simple compound eye, a double shell, and are relatively transparent. *Daphnia* generally live in stagnant freshwater. They are primary consumers, filtering small suspended particles found in lakes and ponds, especially microalgae. Therefore, they are important food sources for fish [10]. *Daphnia* continue to trend as frequently studied model organisms in the fields of ecology, environmental biotechnology and ecotoxicology [11, 12, 13].

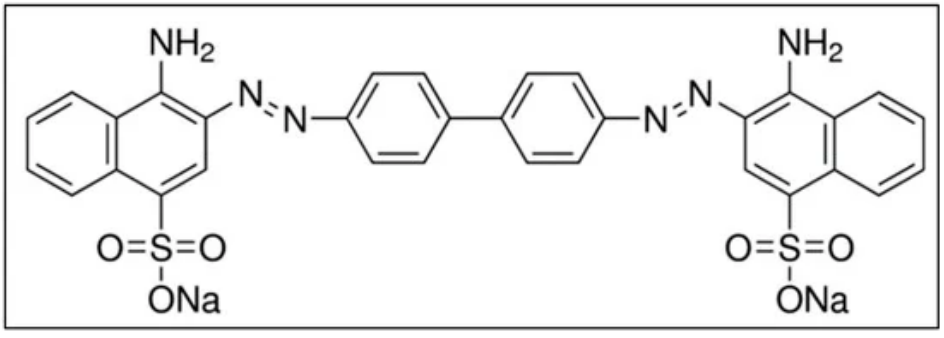

FIGURE 1. Congo Red chemical structure [14]

2. MATERIALS AND METHODS

2.1 Dye solution

Congo Red as an anionic di azo dye was obtained from Sigma (573-58-0), in pure form. Stock solution of congo red was prepared by dissolving the dye in dH_20 to obtain a concentration of 2% w/v. Stock solution of dye in relevant volumes were added in culture media.

2.2 Algal growth inhibition assay

The green algae *Pseudochloris wilhelmii* was isolataed from the spring water in Ankara, Turkey [15]. Microalgal incubation was performed in 100 mL BG11 culture medium in 250 mL Erlenmayer flasks at 25 ± 2 °C and 25 μmol/m^2s (1750 lx) under a 24:0 light:dark photoperiod. [16]. The algal growth inhibition test was performed in the BG11 culture medium according to the OECD 201 procedure [17]. Exponentially growing microalgae was inoculated in Erlenmeyer flasks containing Congo Red dye at 0, 5.38, 6.92, 10.00 and 28.46 mg/L of the BG11 media, respectively. Experimental sets without congo red were used as controls.

2.3 Acute toxicity test

Daphnia magna from Cladocera group was used for acute toxicity test trials [11]. *D. magna* culture conditions were set as 16: 8 hours light/dark cycle and constant temperature of 20 ± 1 ºC. Acute toxicity test was performed according to OECD 202 [18]. *D. magna* acute toxicity tests were carried out in the test medium specified by ISO by preparing increasing dye concentrations at 0, 5.38, 6.92, 10.00 and 28.46 mg/L. Each concentration was designed with 3 replicates and 10 *D. magna* were used for each concentration. Experimental periods were determined as 24, 48 and 72 hours and the toxic effects of Congo Red were analysed at the end of these periods. Control groups were studied simultaneously under the same conditions (Figure 2).

2.4 Bioremoval assay

Increasing concentrations of congo red dye were tested to determine algal bioremoval efficiency of *P. wilhelmii*, samples were incubated in BG11 culture media at 0, 5.38, 6.92, 10.00 and 28.46 mg/L of Congo Red dye concentrations. For analyses, 3 mL samples were taken from each experimental set at 24, 48 and 72 hours of incubation. Congo red absorbance at 498 nm was analyzed using Shimadzu UV 2001 spectrophotometer. Optical density, maximum dried cell mass and chlorophyll (a+b) concentrations are the parameters used to analyze *P. wilhelmii* growth. Optical density was determined at 600 nm, maximum dried cell mass, was determined by measuring the weights of *P. wilhelmii* pellets that were dried at 80 ºC for a night after centrifuging at 5000 rpm for 10 minutes after incubation, and chlorophyll (a + b) concentrations were determined spectrophotometrically at 646.6 nm and 663.6 nm for chlorophyll a and

chlorophyll b, respectively. Control and experimental sets were studied in 3 replicates (Figure 2).

Microalgal dye removal calculations were performed using Equation 1, which is formulated below [18]. Equation (1);

$$removal\ (\%) = \frac{(C_0 - C_t)}{C_0} \times 100 \qquad \text{Eq (1)}$$

In this equation, C_0 and C_t represent the initial and final concentrations of the Congo Red (mg/L), respectively.

Specific growth rate (μ) was calculated according to Equation (2). In this equation, X indicates the dry weight values recorded at the beginning and end of the incubation period, and t indicates the incubation period [19].

$$\mu = (\ln X_2 - \ln X_1) \div (t_2 - t_1) \qquad \text{Eq (2)}$$

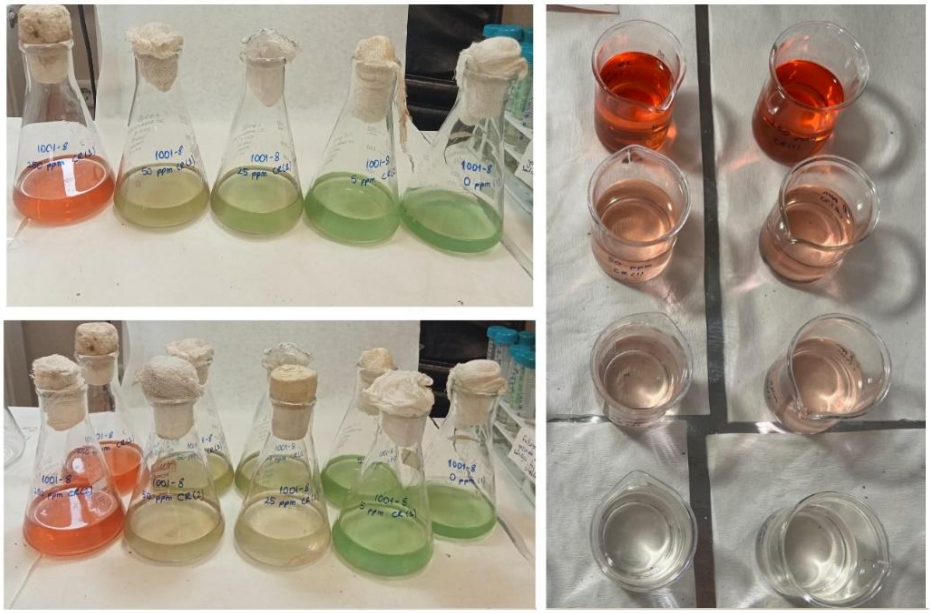

FIGURE 2. The study to determine the toxic effects of Congo red using *P. wilhelmi* and *D. magna*

3. RESULTS AND DISCUSSION

3.1 Bioremoval assay

P. wilhelmii was tested for its ability to removal of dye in BG11 culture media at increasing congo red dye concentrations. The highest bioremoval yield of congo red was 71.40 % at 5.38 mg/L dye concentration. The dry biomass concentration (X), Table 1 shows the μ value and chl(a+b) values at increasing congo red dye concentrations of 5.38-28.46 mg/L after 72 hours of incubation. It was observed that increasing congo red concentrations had a clear effect on microalgal dry weight. While the maximum biomass concentration of the control experimental set was 0.158 g/L, it decreased to 0.068 g/L in the experimental set where the dye concentration was 28.46 mg/L. Similiar results were obtained in a study that reveals the effect of dye and heavy metal ions on bioremoval effect of *A. versicolor*. Increasing remazol blue dye concentrations had a negative effect on fungal growth. As dye concentration increased, removal yield decreased [20]. In another study, *Gonium* sp. a green microalgae removed Reactive Blue 220 dye with the highest yield of 84.20% at 26.20 mg/L dye concentration at the end of 14 days of incubation period [21]. In our study *P. wilhelmii* removed 28.46 mg/L congo red dye with a yield of 29.72 % at 72 hours of incubation period. The highest chl (a+b) concentration was 0.507 μg/mL at the control group and decreased at about 12% when the dye concentration increased to 5.38 mg/L. Interestingly, the specific growth rate (μ) showed its effect up to 10 mg/L dye concentration. However, microalgal growth was not observed after 10 mg/L dye concentration. In this context, it can be considered that the dye removed after this concentration was retained by the biosorption mechanism [22].

TABLE 1. Comparison of the removal yields and X, chl (a+b) and μ values at different Congo red dye concentrations of *P. wilhelmii*

Congo red (mg/L)	**X (g/L)**	**Chl (a+b) (μg/mL)**	**μ (1/d)**	**Y (%)**
0	0.158± 0.001	0.507 ± 0.002	0.109± 0.001	0 ± 0
5.38	0.139± 0.014	0.445 ± 0.046	0.066± 0.038	71.40 ± 1.54
6.92	0.117± 0.033	0.377 ± 0.008	0.009± 0.010	55.53 ± 4.00
10.00	0.095± 0.028	0.305 ± 0.033	0	38.46 ± 4.44
28.46	0.068± 0.020	0.218 ± 0.025	0	29.72 ± 4.61

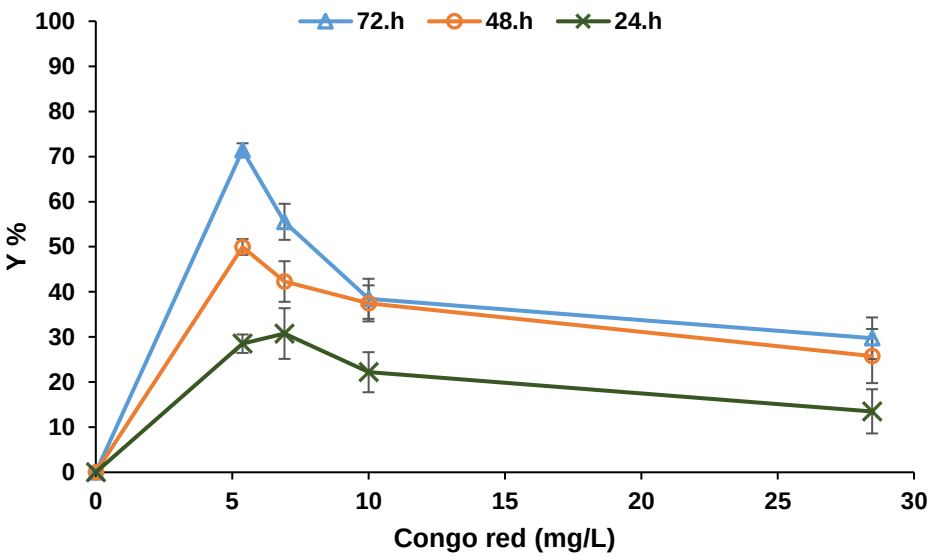

FIGURE 3. Effect of increasing Congo red dye concentrations on removal yield (Y %) of *P. wilhelmii* at 24, 48 and 72 hours

3.2 Algal growth inhibition assay

Figure 4 shows the effects of congo red dye on chl (a+b) concentrations and % dye removal of *P. wilhelmii* at the end of 72 hours. It was noted that microalgal growth decreased during the incubation period as the dye concentrations increased. The control experimental set reached the highest biomass concentration among all the sets studied (0.158 g/L at 72h). The lowest congo red concentration studied, 5.38 mg/L, had no toxic effect on *P. wilhelmii* and its biomass reached 0.139 g/L. When the concentration increased to 28.46 mg/L, *P. wilhelmii* had the lowest biomass amount (0.068 g/L) (Table 1). When the maximum specific growth rates were compared, the μ value of the control culture was recorded as 0.109 l/d, while no maximum specific growth value was recorded when the dye concentration was increased to 10 mg/L. In all experimental sets where congo red dye was applied, lower microalgal growth rates were observed than the control experimental set. When the total chlorophyll values were compared, 0.445 μg/mL was recorded at the lowest congo red concentration studied at 5.38 mg/L and approximately 50% lower chl (a+b) of 0.218 μg/ml was recorded at the highest congo red concentration studied at 28.46 mg/L (Fig. 4). As a result, it was recorded that increasing congo red concentrations had toxic effects on the growth of *P. wilhelmii* and chlorophyll (a+b) concentrations. In a study that was revealed the effect of a nanoparticle La_2O_3 on biomass of *Chlorella* sp. showed different results. The increasing La_2O_3 nanoparticle concentrations did not show an adverse effect on the biomass of *Chlorella* sp. [11]. It can be concluded from here that, Congo Red showed toxic effects of the growth of *P. wilhelmii* and the dye was more toxic than La_2O_3 nanoparticles.

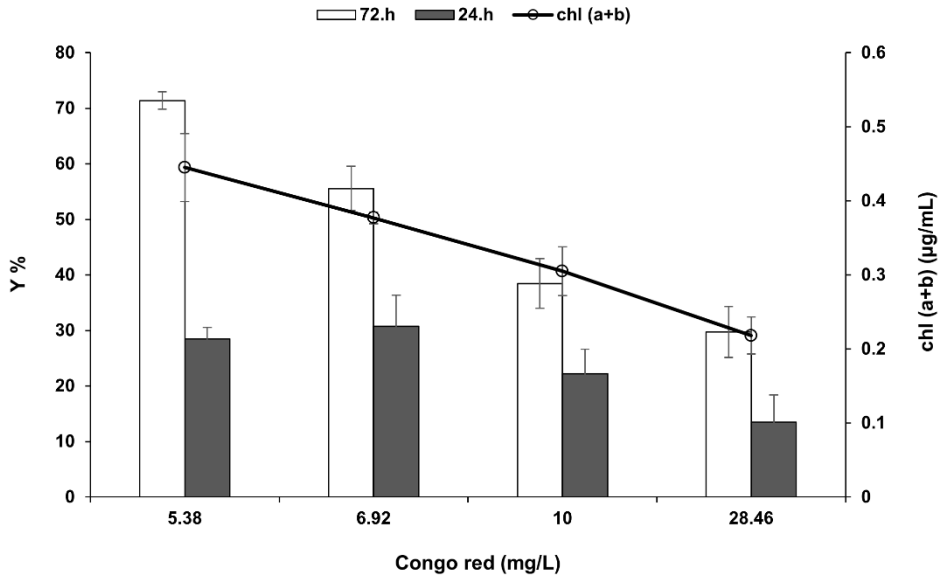

FIGURE 4. Chlorophyll (a + b) concentrations and removal yields of *P. wilhelmii* after 24 and 72h of incubation period

3.3 Acute toxicity test

Congo red, used as a colorant in the textile, dyeing, rubber, and printing industries, is an organic pollutant that raises environmental concerns. Water pollution occurs due to the input of environmental stressors at concentrations exceeding the permitted maximum levels, which restricts access to clean water [23]. *Daphnia magna* serves as a bioindicator organism for understanding the toxicity of chemicals and monitoring wastewater and contaminated waters [24,25,26]. For this reason, *Daphnia magna* was chosen in this bioassay to determine the lethal concentrations of Congo Red.

The acute toxic effects of congo red on *Daphnia magna* were studied at different time points (24, 48, and 72 hours). The highest toxic effect of Congo Red was observed at the 72 h (LC50: 89.91 mg/L) (Table 2). It was observed that the acute toxic effects of congo red on *D. magna* increased with increasing concentration and duration. Parallel to the conclusion that Congo red shows toxic effects on the growth of *P. wilhelmii* and that this dye is more toxic than La_2O_3 nanoparticles, it was also observed that Congo red had a more toxic effect on *D. magna* compared with La_2O_3 nanoparticles [17]. Congo Red is allergic, carcinogenic, and mutagenic for humans and animals and it can also cause infertility in water fleas (*Ceriodaphnia dubia*) [27,28,29,30]. Additionally, it showed phytotoxic effects on plants [31]. Due to being a di-azo dye, Congo Red appears red in basic medium and blue in acidic medium, and it can form an amine compound such as benzidine upon the cleavage of its azo groups [32]. Benzidine, a widespread carcinogen, was led to the ban on the use of Congo Red [33]. Acute toxicity studies on Congo Red were conducted on Cladocerans (*Daphnia magna*, LC_{50}:

322.9 mg/L), *Ceriodaphnia rigaudi*, LC_{50}: 62.92 mg/L) and zebra fish (*Danio rerio*, IC50: 3.11 mg/L) are found in the literature [34]. However, these studies are quite limited in number. Dose-mortality curves for Congo Red (Figure 5) were calculated using probit (Spss 22v.) analysis. Congo Red exhibited different trends characterized by an increase in daphnids mortality after the 24th hour of exposure. No deaths were observed in the control groups.

TABLE 2. Acute toxic effects of CR on *Daphnia magna* at 24, 48 and 72 hours

	LC50 (mg/L)	**Probit**	**Results**
Time	**24h**	**48h**	**72h**
Congo Red	133.096	94.921	89.913

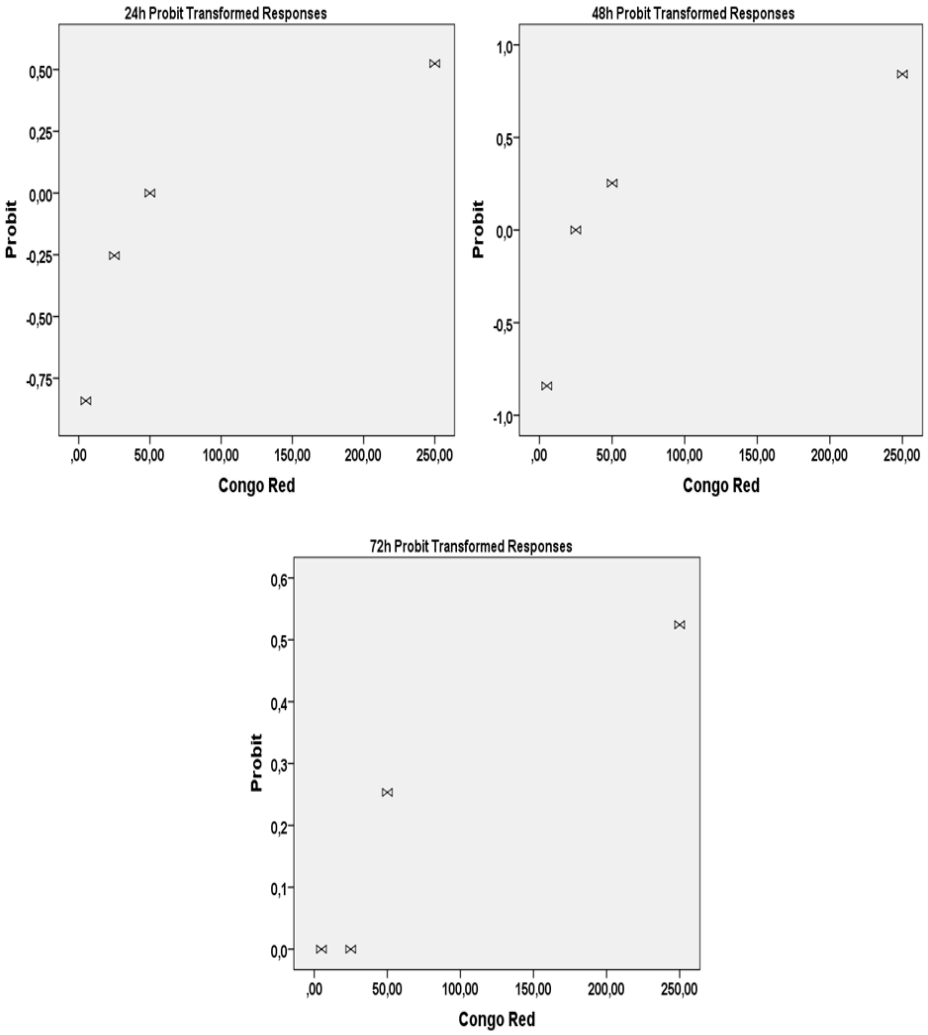

FIGURE 5. Mortality-dose curve of *D. magna* exposed to Congo Red at different durations (24, 48 and 72 hours)

4. CONCLUSIONS

The results of the study demonstrate that Congo red showed toxic effects on both the growth of *P. wilhelmii* and *D. magna*. In both test organisms, 72 hours was identified as a critical time, suggesting that an increase in exposure duration to Congo red is likely to lead to more pronounced negative effects on the organisms. There are very few studies in the literature that adequately address the stress that such dyes may impose on ecosystems. Therefore, more research is needed to elucidate the potential health risks associated with these dyes.

Acknowledgement The microorganism used in this study was isolated within the scope of TUBITAK project No 122Z742.

Author Contribution Statements All authors contributed equally to the conduct of the experiments and the writing of the article.

Declaration of Competing Interests The authors declare no conflict of interest in relation to this particular article.

Ethical Statement This research did not involve human participants or animals. Therefore, no ethical approval was required.

Use of Artificial Intelligence No artificial intelligence-based tools or applications were used in the preparation of this study. The entire content of the study was produced by the author(s) in accordance with scientific research methods and academic ethical principles.

REFERENCES

[1] Oladoye, P.O., Natural, low-cost adsorbents for toxic Pb (II) ion sequestration from (waste) water: A state-of-the-art review. *Chemosphere*, 287 (2022), 132130. https://doi.org/10.1016/j.chemosphere.2021.132130

[2] Santos, S.C., Boaventura, R.A., Adsorption modelling of textile dyes by sepiolite. *Applied Clay Science*, 42 (2008), 137-145. https://doi.org/10.1016/j.clay.2008.01.002

[3] Harja, M., Buema, G., Bucur, D., Recent advances in removal of Congo Red dye by adsorption using an industrial waste. *Scientific Reports*, 12 (2022), 6087. https://doi.org/10.1038/s41598-022-10093-3

[4] Kumar, D., Singh, H., Raj, S., Soni, V., Chlorophyll a fluorescence kinetics of mung bean (*Vigna radiata L.*) grown under artificial continuous light. *Biochemistry and Biophysics Reports*, 24 (2020), 100813. https://doi.org/10.1016/j.bbrep.2020.100813

[5] Saratale, R.G., Saratale, G.D., Chang, J.S., Govindwar, S.P., Bacterial decolorization and degradation of azo dyes: a review. *Journal of the Taiwan institute of Chemical Engineers*, 42 (2011), 138-157. https://doi.org/10.1016/j.jtice.2010.06.006

[6] Yates, E., Yates, A., Johann Peter Griess FRS (1829-88): Victorian brewer and synthetic dye chemist. *Notes and Records*, 70 (2016), 65–81. https://doi.org/10.1098/rsnr.2015.0020

[7] Polat, E., Tastan, B.E., Investigation of microalgae isolated from different water resources of Turkiye for their biotechnological utilization. *Ege Journal of Fisheries and Aquatic Sciences*, 41 (2024), 97-104. https://doi.org/10.12714/egejfas.41.2.03

[8] Blazina, M., Fafandel, M., Gecek, S., Haberle, I., Klanjscek, J., Hrustic, E., Lana H., Luka, Z., Ena, P., Klanjscek, T., Characterization of Pseudochloris wilhelmii potential for oil refinery wastewater remediation and valuable biomass cogeneration. *Frontiers in Marine Science*, 9 (2022), 983395. https://doi.org/10.3389/fmars.2022.983395

[9] Concas, A., Steriti, A., Pisu, M., Cao, G., Experimental and theoretical investigation of the effects of iron on growth and lipid synthesis of microalgae in view of their use to produce biofuels. *Journal of Environmental Chemical Engineering*, 9 (2021), 105349. https://doi.org/10.1016/j.jece.2021.105349

[10] Ebert, D., *Daphnia* as a versatile model system in ecology and evolution. *EvoDevo*, 13 (2022), 16. https://doi.org/10.1186/s13227-022-00199-0

[11] Balusamy, B., Taştan, B.E., Ergen, Ş. F., Uyar, T., Tekinay, T., Toxicity of lanthanum oxide (La_2O_3) nanoparticles in aquatic environments. *Environmental Science: Processes and Impacts*, 17 (2015), 1265. doi: 10.1039/c5em00035a

[12] Danabas, D., Ates, M., Tastan, B.E., Cimen, I.C.C., Unal, I., Aksu, O., Kutlu, B., Effects of Zn and ZnO nanoparticles on Artemia salina and *Daphnia magna* organisms: toxicity, accumulation and elimination. *Science of The Total Environment*, 711 (2020), 134869. https://doi.org/10.1016/j.scitotenv.2019.134869

[13] Ertit Taştan, B., Effective removal of fly ash by *Penicillium chrysogenum* and determination of direct fly ash toxicity with *Daphnia magna*. *Water Supply*, 21 (5) (2021), 2047-2057. https://doi.org/10.2166/ws.2020.303

[14] Clavijo, C., Osma, J.F., Functionalized leather: A novel and effective hazardous solid waste adsorbent for the removal of the diazo dye congo red from aqueous solution. *Water*, 11 (9) (2019), 1906. https://doi.org/10.3390/w11091906

[15] 122Z742 TUBITAK Project. Developing microalgae-based sustainable CO_2 reduction strategies and investigating the potential of microalgal biomass as biodiesel, biodegradant and biosorbent-based green energy source 2022-2025.

[16] Taştan, B.E., Duygu, E., İlbaş, M., Dönmez, G., Utilization of LPG and gasoline engine exhaust emissions by microalgae. *Journal of Hazardous Materials*, 246–247 (2013), 173-180. https://doi.org/10.1016/j.jhazmat.2012.11.035

[17] OECD, Freshwater Alga and Cyanobacteria, Growth Inhibition Test, OECD Guideline for the testing of chemicals, Guideline 201, 2011.

[18] OECD, *Daphnia* sp., Acute Immobilisation Test, OECD Guideline for the testing of chemicals, Guideline 202, 2004.

[19] Ip, P.F., Chen, F., Production of astaxanthin by the green microalga *Chlorella zofingiensis* in the dark. *Process Biochemistry*, 40 (2) (2005), 733–738. https://doi.org/10.1016/j.procbio.2004.01.039

[20] Tastan, B.E., Karatay, S.E., Dönmez, G., Bioremoval of textile dyes with different chemical structures by *Aspergillus versicolor* in molasses medium. *Water Science and Technology*, 66 (10) (2012), 2177-2184. https://doi.org/10.2166/wst.2012.441

[21] Boduroğlu, G., Kılıç, N.K., Dönmez, G., Bioremoval of Reactive Blue 220 by *Gonium* sp. biomass. *Environmental Technology*, 35 (19) (2014), 2410-2415. https://doi.org/10.1080/09593330.2014.908240

[22] Taştan, B.E., Ertuğrul, S., Dönmez, G., Effective bioremoval of reactive dye and heavy metals by Aspergillus versicolor. *Bioresource Technology*, 101 (3) (2010), 870-876. https://doi.org/10.1016/j.biortech.2009.08.099

[23] Oladoye, P.O., Bamigboye, M.O., Ogunbiyi, O.D., Akano, M.T., Toxicity and decontamination strategies of Congo red dye. *Groundwater for Sustainable Development*, 19 (2022), 100844. https://doi.org/10.1016/j.gsd.2022.100844

[24] Fikirdeşici, Ş., Altindağ, A., Özdemir, E., Investigation of acute toxicity of cadmium-arsenic mixtures to *Daphnia magna* with toxic units approach. *Turkish Journal of Zoology*, 36 (4) (2012), 543-550. https://doi.org/10.3906/zoo-1006-36

[25] Zhou, Q., Zhang, J., Fu, J., Shi, J., Jiang, G., Biomonitoring: an appealing tool for assessment of metal pollution in the aquatic ecosystem. *Analytica Chimica Acta*, 606 (2) (2008), 135-150. https://doi.org/10.1016/j.aca.2007.11.018

[26] Persoone, G., Baudo, R., Cotman, M., Blaise, C., Thompson, K.C., Moreira-Santos, M., Vollat, B., Törökne, A., Han, T., Review on the acute *Daphnia magna* toxicity test–Evaluation of the sensitivity and the precision of assays performed with organisms from laboratory cultures or hatched from dormant eggs. *Knowledge and Management of Aquatic Ecosystems*, 393 (2009), 01. https://doi.org/10.1051/kmae/2009012

[27] Li, H., Zhao, Y., Yin, C., Jiao, L., Ding, L., WO3 nanocrystal prepared by self-assembly of phosphotungstic acid and dopamine for photocatalytic degradation of Congo red. *Colloids and Surfaces A: Physicochemical and Engineering Aspects*, 572 (2019), 147-151. https://doi.org/10.1016/j.colsurfa.2019.03.092

[28] Litefti, K., Freire, M.S., Stitou, M., González-Álvarez, J., Adsorption of an anionic dye (Congo red) from aqueous solutions by pine bark. *Scientific Reports*, 9 (2019), 16530. https://doi.org/10.1038/s41598-019-53046-z

[29] Mandal, S., Calderon, J., Marpu, S.B., Omary, M.A., Shi, S.Q., Mesoporous activated carbon as a green adsorbent for the removal of heavy metals and Congo red: Characterization, adsorption kinetics, and isotherm studies. *Journal of Contaminant Hydrology*, 243 (2021), 103869. https://doi.org/10.1016/j.jconhyd.2021.103869

[30] Hernández-Zamora, M., Martínez-Jerónimo, F., Cristiani-Urbina, E., Cañizares-Villanueva, R.O., Congo red dye affects survival and reproduction in the cladoceran *Ceriodaphnia dubia*. Effects of direct and dietary exposure. *Ecotoxicology*, 25 (2016), 1832–1840. https://doi.org/10.1007/s10646-016-1731-x

[31] Kumar, V., Effective degradation of rhodamine B and Congo red dyes over biosynthesized silver nanoparticles-imbibed carboxymethyl cellulose hydrogel. *Polymer Bulletin*, 77 (2020), 3349–3365. https://doi.org/10.1007/s00289-019-02920-x

[32] Siddiqui, S.I., Allehyani, E.S., Al-Harbi, S.A., Hasan, Z., Abomuti, M.A., Rajor, H.K., Oh, S., Investigation of Congo red toxicity towards different living organisms: a review. *Processes*, 11 (2023), 807. https://doi.org/10.3390/pr11030807

[33] National Center for Biotechnology Information. PubChem Compound Summary for CID 11313, Congo Red. Available online: https://pubchem.ncbi.nlm.nih.gov/compound/Congo-red (accessed on 09 March 2025).

[34] Hernández-Zamora, M., Martínez-Jerónimo, F., Congo red dye diversely affects organisms of different trophic levels: a comparative study with microalgae, cladocerans, and zebrafish embryos. *Environmental Science and Pollution Research*, 26 (2019), 11743-11755. https://doi.org/10.1007/s11356-019-04589-1

http://communications.science.ankara.edu.tr

Commun.Fac.Sci.Univ.Ank.Ser. C Biology
Volume 34, Number 1, Pages 48-57 (2025)
ISSN 1303-6025 E-ISSN 2651-3749
DOI: 10.53447/communc.1616660

Research Article; Received: January 09, 2025; Accepted: May 09, 2025

BRINGING THE QUARRIES IN THE HIGHWAY LANDSCAPE TO THE ECOSYSTEM

İrem Betül AYDIN[1], Mehmet Ali KIRPIK[2], Mustafa Kemal ALTUNOĞLU[2]

Keywords

Biology
Highways
Landscape architecture
Ecology

To cite this article

Aydın İ.B., Kırpık, M.A., Altunoğlu, K., Bringing the quarries in the highway landscape to the ecosystem. *Commun.Fac.Sci.Univ.Ank.Ser.C Biology*, 34 (1) (2025), 48-57. https://doi.org/10.1111/communc.1616660

Affiliations

[1]18th Regional Directorate, Regional Directorate of Highways, Kars, TÜRKİYE

[2]Department of Biology, Faculty of Science and Letter, Kafkas University, Kars, TÜRKİYE

Abstract

The aim of this study is to reveal the current situation of 56 quarries in the provinces of Kars, Iğdır and Ardahan. In addition, after the function of supplying materials from the quarries is completed, the necessary landscaping repair works are carried out to determine what can be done to bring them into the ecosystem. In this study, a survey consisting of 16 questions was applied to a total of 150 people, 50 of whom lived where the quarries were located, 50 of whom lived in the city centre and 50 of whom were quarry technical personnel. In the study, quarries were examined on site and obtained data were analyzed statistically by SPSS programme. In addition, the environmental impacts of quarries, their damage to nature and their effects on users were determined. As a result of the study, in order to integrate quarries into the ecosystem in the highway landscape, methods of land use, planting and recreation without endangering traffic, life and property safety were suggested.

1. INTRODUCTION

Ecology, which analyses the interaction of organisms with the elements of their environment, is a branch of science that tries to provide the principles of nature conservation, the life bases of living things and the sustainability of the ecosystem [1]. The ecosystem, which consists of living and non-living elements and should be considered as a whole, creates suitable environmental conditions for living organisms to continue their lives and progeny. Factors such as ambient temperature, light, humidity, wind and edaphic factors such as soil composition determine ecosystem conditions. There are various ecosystems such as forest, lake, desert, mountain, reeds, river, ocean. The destruction of all components of the ecosystem (soil erosion, removal of the vegetative layer, reduction of water resources, increase in population, destruction or destruction of suitable habitats) causes the ecosystem to become unable to perform its basic tasks. Destruction of the natural balance of the ecosystem results in the extinction of many species.

aydinirembetul@gmail.com- Corresponding author; 0000-0001-7662-6841 https://ror.org/01rakqm07
mhmtalikrpk@gmail.com- 0000-0003-0156-8127 https://ror.org/04v302n28
mkaltun@gmail.com- 0000-0001-6906-3403 https://ror.org/04v302n28

This situation causes the amounts of the food between living in the region [2]. Among the causes of destruction in the ecosystem are erosion caused by floods due to excessive rainfall, forest fires and industrialisation. Among these, industrialisation is the most important one. Iron, steel, cement industry and industrial wastes are some of the factors that destroy nature [3].

With the increasing population in our country and the world, the construction sector is growing day by day. One of the activities of the construction sector is the construction of highways that provide intercity transport. This situation creates a great need for raw materials for the construction of new transport networks, repair or expansion of existing ones [4].

Mankind has preferred to obtain its raw material needs from nature, which is generally seen as economical in the short term. While the process of obtaining raw materials destroys nature, urbanised spaces, concrete piles, degraded landscapes have brought harm to the values of our country. The sources of raw materials obtained from nature can be forest and agricultural products as well as soil and stone. These raw materials are processed and used firstly as infrastructure material for roads and then for other structures. The material prepared for use in this way has revealed the concept of quarry. The history of the use of quarries has been observed since mankind began to shape the stone. Stones obtained from these quarries have been used in many historical monuments that still exist today and Natural Protected Areas that contain stone structures.

The use and development of quarries date back to the Seljuk and Ottoman Empire periods. It is seen that the first legal regulation on quarries was made with the "Regulation on Quarries", which entered into force in 1887 and then in 1901 [5]. Structures such as bridges, caravanserais, mosques, churches, churches, clusters, healhouses and madrasahs were built with the stones obtained from quarry works, and they were also frequently used as ornamental stones [6].

Serious damages are caused to the environment during and after the use of quarries from which road construction material is taken. In addition to the damage to the ecosystem in general, serious damage to plant and animal species in natural life can be given as an example. People are also indirectly affected by these negativities.

The importance of highway landscapes has emerged in reintroducing quarries to the ecosystem after their use. Roads and motorways, which provide intercity transportation, have a great negative impact on the environmental landscape as they cover a large area on the geography [7]. The highway landscape is a multidimensional system, both qualitative and quantitative [8]. According to Public Procurement Contracts Law of the Highways Law (4735/8), the material procurement conditions for road construction and the works to be carried out in the area afterwards are described [9]. The aim of this study is to determine the current situation of the quarries in Kars, Iğdır and Ardahan provinces, what kind and how landscape-repair works will be carried out after the material supply

function from the quarries is over, how they will be brought into the ecosystem and what can be done in this regard.

2. MATERIALS AND METHODS

In this study, the current conditions of 56 quarries located within the borders of Kars, Ardahan and Iğdır provinces between 2020-2021 were examined. In this study, a questionnaire consisting of 16 questions was applied to a total of 150 people, 50 of whom were residents of the quarries, 50 of whom were residents of the city centre and 50 of whom were quarry technical personnel. Photographs of the quarries and their surroundings were taken. According to the questionnaires, the current conditions of the quarries were determined and evaluated and the locations of the quarries were shown on the map (Figure 1).

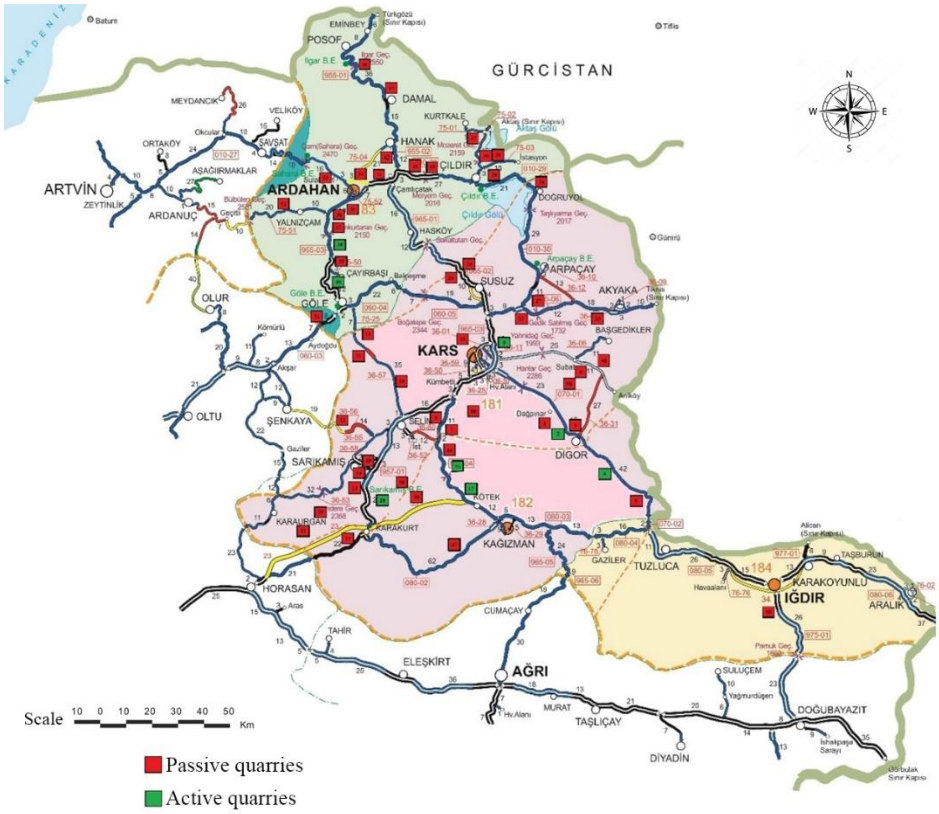

FIGURE 1. Current status of the investigated quarries on the map

3. RESULTS AND DISCUSSION

The study was conducted in 56 quarries located within the provincial borders of Kars, Ardahan and Iğdır.

FIGURE 2. Kars Subatan Quarry

The current conditions of the quarries were determined, their negative and positive effects on the ecosystem were investigated and it was tried to determine whether the quarries that are still used and used by the highways are brought back to the ecosystem. In order to determine the current status of the quarries, a questionnaire was applied to 3 different groups. These groups are:

It was applied to a group of 50 people living close to the quarries and directly experiencing the negative impacts of the quarries.

It was applied to 50 people who personally work in quarries and are directly exposed to the negative effects of quarries.

A questionnaire was applied to 50 people living in the city centre where the quarries are located. It was tried to measure the level of knowledge about the positive and negative effects of quarries on ecosystem, environment, natural life and human life. As a result of the study, 3 different results were obtained from the questionnaires applied. Depending on the data obtained about these quarries in the study area, the quarries were divided into two large groups as active and inactive and shown on the map. It has been determined that 8 quarries shown in green on the map are active and 48 quarries shown in red are inactive. Eleven of the inactive quarries were surrounded by wire fences after the animals of the

neighbouring villages perished and they reported this situation to the relevant institutions.

According to the results of the research and questionnaire surveys, it was observed that the first thing that attracts attention among the environmental impacts of quarries is the damage to the visual landscape. It has been observed that the current state of the surface shapes has deteriorated and the visual quality has decreased. As can be seen in the inventory of the quarries, the majority of the quarries are located close to the roads. It has been determined that open pit quarries are located close to roads and settlements in order to transport materials more easily. Accordingly, road users and local people are exposed to this visual pollution. Quarries are huge abysses when evaluated on a human scale.

It was determined that the quarry areas in the study area are generally in pasture status. In addition, it was observed that meadow-pasture vegetation was intermittently regenerated in passive quarries [13].

One of the features to be considered when choosing plant species to be used during the reintroduction of passive quarries to the ecosystem is their ability to with extreme conditions (frost, drought, salinity, acidity, etc.). In one of the studies, the following species are recommended [13].

- *Pinus sylvestris* L. (Pinaceae): Afforestation, erosion and landscape repair works, especially in high areas, mountains and winter landscaping, space delimitation, snow curtain;
- *Juniperus oxycedrus* L., *Juniperus foetidissima* Willd., *Juniperus communis* L. var. *saxatilis* Pall. (Cupressaceae): Highway plantings, landscape restoration, erosion, rock garden, space delimitation and orientation, snow screen, noise prevention, winter landscaping;
- *Viburnum orientale* Pall. (Caprifoliaceae): For visual purposes with its flowers, fruits and autumn leaf colouring, for wildlife habitat with its fruits, for mid-refuge plantings and noise prevention;
- *Betula nana* L. (Betulaceae): Afforestation, erosion and landscape repair works, especially in high areas, mountain and winter landscaping, highway afforestation, aesthetic areas with trunk and autumn leaf colouring;
- *Vaccinium myrtillus* L. (Ericaceae): Fruit and flower in aesthetics and wildlife, erosion, slope stabilisation, rock garden;
- *Populus tremula* L. (Salicaceae): Afforestation, erosion and landscape repair works, especially in high areas, mountain landscaping, highway afforestation, aesthetic areas with trunk and autumn leaf colouring;
- *Salix caprea* L. (Salicaceae): Landscape repair works, highway afforestation, aesthetic areas with its flowers, stream banks, parks;
- *Sorbus aucuparia* L. (Rosaceae): For visual purposes with its flower, fruit and autumn leaf colouring, for wildlife habitat with its fruits, for mid-refuge planting and noise prevention;

- *Pyrus eleognifolia* Pall. (Rosaceae): In parks and gardens for visual purposes with its flowers, fruits and autumn leaf colouring, in wildlife creation with its fruits, erosion and slope stabilisation;
- *Rosa pimpinellifolia* L., *Rosa dumalis Bechst. subsp. boissieri* (Crep.), *Rubus fruticosus* (Rosaceae), *Ribes grossuloria* L. (Grossulariaceae): Flowers, fruits and autumn leaf colouring in parks and gardens, wildlife habitat with its fruits, mid-refuge planting and noise prevention, erosion and slope stabilisation and hedge formation;
- *Euoynmus latifolius* L. Mill. (Celastraceae): It can be frequently used in parks and gardens with its beautiful flowers [10].

Active quarry operations cause irreparable damage to settlements or various agricultural areas. When deciding to open an area as a quarry, the fact that the area is a stony rocky land ensures that it causes the least damage to the environment and accordingly, the objections of the local people are prevented [13].

In a study in the International Journal of Environmental Research and Public Health;

- Of the individuals living in areas close to open pit mining, 98 per cent stated that their houses were exposed to dust, 85 per cent stated that the site was disturbed, 97 per cent stated that the leaves of plants were covered with dust, and 92 per cent stated that crops could not be grown.
- The dust released by the quarries covers the plant leaves and prevents the leaves from respiration and photosynthesis. During the flowering season, it is also observed that fruit formation decreases by preventing fertilization.
- The noise caused by the work machines used in open pit mines is at a level that can cause hearing loss to those working in the environment.
- High eye and nose allergies were observed in 22% of people in dusty environments, chest tightness in 17%, and chronic cough in 9% [13].

Published in 2010 in the official gazette, the "Regulation on the Restoration of Lands Disturbed by Mining Activities to Nature" protects these areas and determines the necessary procedures and principles [13]. Within the scope of the ecosystem restoration of the quarries located in the highway landscape, the study area was selected, and after determining the boundaries, the environment was analysed from many aspects and the environmental effects of the quarries were determined by surveys and on-site inspections. These determinations contributed to the results of the study.

4. DISCUSSION

Large funds are used for the construction and maintenance of highways, which have an important place in passenger and freight transport. For this reason, in order to prevent the deterioration of the local ecology, ecosystem and all kinds of natural balance, highway works should be in harmony with the natural environment where the construction is carried out. Technical support should be obtained from landscape architects starting from the route determination stage. Along the route, factors such as the natural flora and fauna of the area, cultural heritage, socio-economic structure should be taken into consideration. It should not be forgotten that these studies have negative effects on global warming and climate change.

The results of surveys should be utilised when making land use decisions for quarries that have been restored to the ecosystem, and the new area designed should be built in accordance with the demands of users and human ergonomics. The quarries consist of 80 to 120 meter high cliffs and artificial hills where the extracted and unused materials are accumulated. This situation should be compared with the human scale and landscape areas should be designed to tolerate this difference.

While restoring the destroyed areas to the ecosystem, planting works should be carried out by taking into account the determining features of the region such as climate, altitude, natural vegetation. Since the soil structure of passive quarries is disturbed, experiments should be carried out on the soil structure of the areas to be planted. In areas where heavy metals are detected, hyperaccumulator (species that can accumulate heavy metals and are not adversely affected by this) or phytoremediation (plants that can clean heavy metal pollution) plants should be used according to the needs of the area.

Care should be taken to ensure that the plant species to be used are species that absorb noise and pollution. *Pittosporum tobira* (Thunb.) W.T. Aiton and *Thuja orientalis* L. are some of these species [14]. In quarries located on the edge of highways, plants that do not disturb the visibility angle or endanger the safety of road traffic life and property by attracting too much attention should be selected. After the planting works, these areas should be regularly checked and the needs of the plants should be met. In areas where vegetative interventions cannot be made, economical and ergonomic non-living materials (urban furniture such as pergolas and benches) should be used and peace and security should be ensured in areas opened to public use.

In the new landscape designs to be made within the scope of ecosystemisation studies, the spaces created in the area should attract the attention of the users and the change of the created spaces over the years should be taken into consideration. It should not be forgotten that the natural resources in the area are not unlimited, and the resources should be opened to use in this direction.

Public institutions and organisations carrying out inspection duties on the subject should meticulously examine the compliance of active and inactive quarries with existing laws and regulations.

Quarry employees and supervisors should be trained on the subject, this issue should be discussed in the local and national press and the public should be informed about this issue.

This study will be a guide for the authorities who are in charge of supervising the quarries, both private and public, which have been opened and will be opened to provide material for road construction. In addition, it is thought that this study will be a determinant and source for reducing the negative contribution to global warming and climate change, preventing erosion, sustainability of natural ecosystems and less damage to biodiversity.

In Central Park, which was designed by the famous landscape architect Frederick Law OLMSTED in the 1850s and which many people visit today, it is seen that an extremely large land is used as a park. Frederick Law OLMSTED predicted that the city would spread over the whole land in the future and the area he designed would be the only landscape that the public could see. For this reason, while designing the area, he evaluated a very large area as a park [15].

If recreational use is to be made while the quarries, which are passive in our country, are being restored to the ecosystem;

- Areas for the protection of resources
- Horse riding
- Hiking trails or bird watching towers

If agricultural areas are to be designed;

- Conditions favourable for the cultivation of agricultural
- Conservation, storage or reuse of water resources

If urban areas are to be designed;

- Regularised solid waste landfill
- Passive parks
- Cycling tracks
- Areas to meet the need for rest
- Observation terraces
- Picnic areas
- Fields for children's games
- Camp sections
- Different alternatives such as artificial ponds should be considered.

Many professional disciplines such as Landscape Architects, Biologists, Lawyers, Environmental Engineers, Agricultural Engineers, Ecologists, Geologists, Landscape Architects, Biologists, Lawyers, Environmental Engineers, Agricultural Engineers, Ecologists and Geologists should come

together and try to produce solutions in order to restore the natural balance of areas such as quarries to the ecosystem. The process should be well planned and executed before the works are started. While these studies are being carried out, landscape restoration, good design of the use of the area, re-naturalisation of the resources that have lost their naturalness, improvement of the problematic areas and monitoring and maintenance of the new area should be evaluated together [16].

The purpose and objective of the final land use plans should be determined in advance in order to prevent disruptions in restoration works and to avoid economic and time loss. The final land use plans should be decided from the beginning in order to obtain compatible, economic and appropriate plans for open pit mining and landscape restoration activities [17]. There are many benefits from the reuse of defunct quarries, such as reducing steep slopes, reducing high steps, levelling gaps, creating suitable soil depth conditions for flora, as well as reducing erosion, restoring proper water regime and drainage.

The study area is located in the close vicinity of the expanding provinces and is expanding and concretising day by day. City centres are expanding towards the outskirts of the city. The need for recreation areas in the study area and its immediate surroundings has been identified through surveys and questionnaires. The main design decisions for the ecosystem of passive quarries should take into consideration the economic and social objectives of potential users.

When implementing highway landscaping applications, the vegetation around the relevant highway, historical values, use of the area, socioeconomic status, providing users with a colourful and pleasant travel opportunity, the presence of elements that attract attention in the area, hiding places with ugly appearance in the field and the harmony of the road and the surrounding appearance should be taken into consideration [18].

Acknowledgement We would like to thank the 18th Regional Directorate of Highways, which provided the data needed for this study, and Assistant Professor Gül Esma Akdoğan Karadağ, who provided technical support throughout the study.

Author Contribution Statements In this study, all authors contributed equally to the research process and the article-writing phase.

Declaration of Competing Interests The authors declare no conflict of interest.

Ethical Statement This research did not involve human participants or animals. Therefore, no ethical approval was required.

Use of Artificial Intelligence No artificial intelligence-based tools or applications were used in the preparation of this study. The entire content of the study was produced by the author(s) in accordance with scientific research methods and academic ethical principles.

REFERENCES

[1] Çepel, N., Çevre Koruma ve Ekoloji Terimleri Sözlüğü. Tema Vakfı Yayınları, Istanbul, Türkiye, 1996.

[2] Türkoğlu, M., Biodiversity and Food Chain of Iğdır. Ajans-Türk Gazetecilik Matbaacılık, Ankara, Türkiye, 2017.

[3] Tolunay, D., Türkiye'de ekosistem tahribat faktörü olarak habitat ve arazi kullanım değişiklikleri. *Memleket Siyaset Yönetim*, 16 (36) (2021), 279-304.

[4] Yılmaz, A., Sütaş, İ., Use of ferrochromium slag as highway base material. *İMO Teknik Dergi*, 19 (93) (2008), 4455-4470.

[5] Şağban, E.E., A legal history study on the stone quarries regulation. Master Thesis, Istanbul University, Istanbul, Türkiye, 2022.

[6] Özbek, Y., Anadolu mimarisinde taş süsleme. *Türkiye Araştırmaları Literatür Dergisi*, 7 (14) (2009), 141-169.

[7] Alberti, M., Advances in Urban Ecology: Integrating Humans And Ecological Process in Urban Ecosystems. Springer, New York, 2008.

[8] Masnavi, M. R., Sustainable Urban Forms Design and Planning Strategies: compact city, urban sprawl and mixed-use development in theory and practice. Academic Press: Lambert Academic Publishing, USA, 2011.

[9] Türkiye Cumhuriyeti. 2002. *Kamu İhale Sözleşmeleri Kanunu*. Resmî Gazete, no. 24648. https://www.mevzuat.gov.tr/mevzuat?MevzuatNo=4735&MevzuatTur=1&MevzuatTertip=5 (accessed May 5, 2023).

[10] Uluocak, N.. Mera ıslahında bitki türü seçimi. *Journal of the Faculty of Forestry Istanbul University*, 31 (2) (1981), 95-109.

[11] Özer, S., Yılmaz, H., Kaya, Y., Determination of the diversity of grassy and woody plant species in Sarıkamış/Turkey district and evaluation of their usability in planning and design attempts. *Biological Diversity and Conservation*, 2 (3) (2009), 75-81.

[12] Cındık Y., Acar C., Rehabilitation of quarries to finished re-gaining activity and the nature. *Artvin Çoruh University Faculty of Forestry Journal*, 11 (1) (2010), 11-18.

[13] Türkiye Cumhuriyeti. 2010. *Madencilik Faaliyetleri ile Bozulan Arazilerin Doğaya Yeniden Kazandırılması Yönetmeliği*. Resmî Gazete, no. 27471. https://www.resmigazete.gov.tr/eskiler/2010/01/20100123-1.htm (accessed May 6, 2023).

[14] Doygun, N., Doygun, H. A research on the use of vegetation barriers in traffic noise control. *KSÜ Journal Of Agriculture and Nature*, 21 (4) (2018), 599 - 606. https://doi.org/10.18016/ksudobil.369519

[15] Euronews. 2021. "Taş Ocaklarının İnsan Sağlığı ve Çevre Üzerindeki Etkileri Neler?" *Euronews*, May 7, 2021. https://tr.euronews.com/2021/05/07/tas-ocaklar-n-n-insan-sagl-g-ve-cevre-uzerindeki-etkileri-neler (accessed May 6, 2023).

[16] Akpınar, N. Environmental impact assesment for strip coal mining and land reclamation case study: Milas-Sekköy strip coal mine. PhD Thesis, Ankara University, Ankara, Türkiye, 1994.

[17] Özcan A., A study on landscape reclamation on Ankara-Hasanoğlan quarries its evaluation in terms of urban utilization. PhD Thesis, Ankara University, Ankara, Türkiye, 2009.

[18] Sezen, I., Highway landscape and scenic roads. *Journal of Architectural Sciences and Applications*, (2018), 3 (1) (2018), 54-65. https://doi.org/10.30785/mbud.356523

http://communications.science.ankara.edu.tr

Commun.Fac.Sci.Univ.Ank.Ser. C Biology
Volume 34, Number 1, Pages 58-75 (2025)
ISSN 1303-6025 E-ISSN 2651-3749
DOI: 10.53447/communc.1667669

Research Article; Received: March 28, 2025; Accepted: May 16, 2025

ANTIBIOFILM EFFECTS OF *Fomes fomentarius* (L.) FR. EXTRACTS ON SOME MICROORGANISMS

Umay Merve ŞENTURAN[1], Ilgaz AKATA[2], Ergin Murat ALTUNER[3]

Keywords

Fomes fomentarius
Antibiofilm activity
Antimicrobial activity
GC/MS

To cite this article

Şenturan, U.M., Akata., I., Altuner, E.M., Antibiofilm effects of *Fomes fomentarius* (L.) fr. extracts on some microorganisms. *Commun.Fac.Sci.Univ.Ank.Ser.C Biology*, 34 (1) (2025), 58-75. https://doi.org/10.1111/communc.1667669

Affiliations

[1]Department of Biology, Institute of Science, Kastamonu University, Kastamonu, TÜRKİYE

[2]Department of Biology, Faculty of Science, Ankara University, Ankara, TÜRKİYE

[3]Department of Biology, Faculty of Science, Kastamonu University, Kastamonu, TÜRKİYE

Abstract

Biofilms, structured microbial communities, are a significant focus of research due to their nature as they provide protection against environmental stressors but also cause substantial medical and industrial problems. These communities, embedded in an extracellular matrix, are implicated in persistent infections, corrosion in infrastructure, and food spoilage, while also holding potential in beneficial applications like biofuel production and wastewater treatment. Consequently, there is growing interest in modulating biofilm formation, with natural products emerging as promising candidates. This study assessed the impact of Fomes fomentarius (L.) Fr. extracts on some microorganisms. The impact of ethanol (EtOH) and chloroform extracts on biofilm formation was evaluated using crystal violet staining, with SEM and AFM imaging used for confirmation. A comprehensive chemical analysis of the extracts was performed via gas chromatography-mass spectrometry (GC/MS). The EtOH extract was found to contain compounds such as stearic acid and oleic acid, while the chloroform extract contained compounds like methyl stearate and octadecadienoic acid. The key finding was that the F. fomentarius-EtOH extract significantly inhibited biofilm formation in S. aureus MRSA between 30.90-47.06%. The chloroform extract, however, showed no discernible effect on biofilm development. The effectiveness of the EtOH extract was compared using Halamid® as a positive control. Inhibition was observed for the S. aureus MRSA strain, as 54.21% with 125 µg/mL of the Halamid® concentration. This suggests that F. fomentarius extracts may offer a natural source of compounds with the potential to control and manage biofilm formation.

1. INTRODUCTION

Biofilms are structured microbial communities embedded within a self-produced extracellular polymeric substance (EPS) matrix. This matrix acts as a protective shield, enhancing microbial resistance to environmental stressors and antimicrobial agents [1-8]. The advantages and disadvantages of biofilm structure vary depending on the microorganism's species, its pathogenic potential, the environment in which it forms, and the intended application. The controlled modulation of biofilm formation, encompassing both its stimulation and inhibition, holds significant scientific and practical value across a wide range

msenturan@gmail.com-
akata@science.ankara.edu.tr-
ergin.murat.altuner@gmail.com-
Corresponding author; 0000-0003-2700-7088 https://ror.org/015scty35
0000-0002-1731-1302 https://ror.org/01wntqw50
0000-0001-5351-8071 https://ror.org/015scty35

of fields, from scientific research to industrial applications. Therefore, the ability to control biofilm formation is a critical tool for various disciplines. For example, it is possible to reduce the risk of infection by inhibiting biofilm formation on the surfaces of medical devices, ensure product safety in the food industry by preventing unwanted biofilm formation, or remediate environmental pollution by promoting the formation of specific biofilms in bioremediation applications [9,10]. Biofilms offer numerous advantages, including their applications in biodegradable packaging, nutraceutical supplements, biofertilizer and biofuel production, enhancing the energy efficiency of high-energy batteries, and wastewater treatment systems. This diverse range of uses highlights the importance of identifying compounds that stimulate biofilm formation and introducing novel biofilm inducers into the scientific literature [11-13]. However, in environments where hygiene is vital, such as hospitals and food production facilities, the formation of biofilms by pathogenic microorganisms poses a serious risk to human and public health. Moreover, biofilms contribute to the development of antimicrobial resistance, thereby exacerbating a global public health crisis. Therefore, preventing biofilm formation is crucial for safeguarding public health. In this regard, the identification of biofilm-inhibiting compounds and the development of novel antibiofilm agents are essential [14,15].

Nature offers a vast and valuable reservoir of resources for the discovery of such compounds, providing researchers with a diverse array of natural materials, including macrofungi. Macrofungi contribute significantly to ecosystem stability by actively participating in biogeochemical cycles [16-21]. While some species are edible and consumed as food, others contain pharmacologically active components and are used in traditional medicine. Recent studies on fungi have revealed the presence of a multitude of bioactive molecules. Research has shown that various compounds isolated from species belonging to the phylum Basidiomycota, in particular, exhibit antibacterial, antifungal, phytotoxic, cytotoxic, antiviral, and other pharmacological activities [20,22,23].

The discovery of bioactive compounds in macrofungi with potential therapeutic applications has made them an increasingly valuable resource for developing new pharmaceutical, therapeutic, industrial, and biotechnological products. Despite the existence of numerous studies on the antimicrobial activities of macrofungi, studies specifically evaluating their effects on microbial biofilm formation remain limited. To address this literature gap and to discover novel bioactive molecules, more comprehensive research on macrofungi is required [20,24,25].

Fomes fomentarius (L.) Fr., a fungus within the Basidiomycota division, is a medicinal mushroom species with a long history of use in traditional medicine owing to its diverse array of bioactive compounds. Research into the antimicrobial and antibiofilm properties of this fungus offers potential avenues for alternative therapeutic strategies. Bioactive constituents present in *F. fomentarius,* including triterpenes, polysaccharides, and phenolic compounds,

have demonstrated both antimicrobial activity and the ability to inhibit biofilm formation or disrupt pre-existing biofilms. Recent investigations corroborate the antimicrobial effects of *F. fomentarius* extracts against a range of pathogenic microorganisms. These studies underscore the potential of macrofungi to exhibit activity against both Gram-positive and Gram-negative bacteria, yeasts, and certain viruses. The capacity of *Fomes fomentarius* extracts to impede biofilm development and eradicate established biofilms positions this fungus as a compelling candidate, particularly in the context of biofilm-associated infections such as those related to catheters and implants [14,15,24,26].

This study was designed to evaluate the *in vitro* effects of chloroform and ethanol (EtOH) extracts derived from *Fomes fomentarius*on biofilms formed by a methicillin-resistant *Staphylococcus aureus* (MRSA) strain, renowned for its robust biofilm production. The impact of these extracts on biofilm formation was quantitatively assessed via crystal violet staining and qualitatively corroborated through scanning electron microscopy (SEM) and atomic force microscopy (AFM) imaging. The findings were benchmarked against those obtained with Halamid®, a recognized biofilm inhibitor. Furthermore, the chemical constituents of the extracts were characterized utilizing gas chromatography-mass spectrometry (GC-MS).

2. MATERIALS AND METHODS

2.1 Macrofungus sample

Fomes fomentarius (L.) Fr. sample was obtained from the personal collection of Prof. Dr. Ilgaz AKATA. The fungi were collected from the Istanbul Belgrad Forest and identified by Prof. Dr. Ilgaz AKATA.

2.2 Extraction procedure

This study aimed to extract and quantify the active components present in *Fomes fomentarius* samples. The mushroom samples were pulverised using a blender. The ground sample was extracted separately in ethanol (EtOH) and chloroform solvents for three days at 140 rpm to release the active components. After the extraction process, the obtained extracts were filtered using 125 mm diameter filter paper (Sigma-Aldrich, USA). The filtrates were concentrated using a rotary evaporator at a temperature range of 40-50°C, ensuring the complete removal of solvents. The residues obtained after evaporation were dissolved in a mixture of sterile distilled water (sdH_2O) and dimethyl sulfoxide (DMSO) in varying proportions based on their solubility properties. The *F. fomentarius*-EtOH extract stock was prepared at a ratio of 50:50 (sdH_2O:DMSO) and a concentration of 0.419 g/4 mL and the *F. fomentarius*-Chloroform extract stock was prepared at a ratio of 40:60 (sdH_2O:DMSO) and a concentration of 0.537 g/5 mL. The DMSO concentration in the obtained extracts was reduced to 2% to minimise the cytotoxic effect on microorganisms. Finally, the extract concentrations applied to the initial wells were calculated as 2095 µg/mL (*F. fomentarius*-EtOH) and 1790 µg/mL (*F. fomentarius*-Chloroform), respectively.

2.3 Microorganisms used

A total of twenty microorganisms were tested, including *Escherichia coli* isolates (2, 3, 4, 5, 6, 7, 8, 9, 10, 11) and the *E. coli* ATCC 25922 (1) standard strain, *P. mirabilis*, *S. pneumoniae*, *S. flexneri*, *A. baumannii*, two strains of *S. aureus*, one of which is MRSA, and three yeast strains (*Candida albicans* DSMZ1386, *Candida glabrata*, and *Candida tropicalis*). Six microorganisms exhibiting high biofilm formation (*E. coli* 7, 9, 11, *S. aureus*, *S. aureus* MRSA, and *C. albicans* DSMZ1386) were selected for further study.

2.4 Inoculum preparation

Bacterial strains were cultured at 37°C for 24 h, whereas *Candida albicans* was incubated at 27°C for 48 h. Inocula were prepared by suspending morphologically similar colonies of each microorganism in a sterile 0.9% saline solution, and the cell density was adjusted to approximately 1×10^8 CFU/mL, corresponding to a 0.5 McFarland standard. Mueller-Hinton agar (Merck, Germany) served as the culture medium for bacterial strains, while Sabouraud dextrose agar (Merck, Germany) was utilized for *C. albicans* [27,28].

2.5 MIC method

To ascertain the sub-lethal concentrations of extracts exhibiting antibiofilm activity against the target microorganisms, the Minimum Inhibitory Concentration (MIC) was determined via a two-fold serial microdilution assay, following the methodology outlined by [29]. The MIC was defined as the lowest concentration of the extract at which no visible microbial growth was observed. All experiments were conducted in triplicate.

2.6 Minimum Bactericidal Concentration (MBC)/Minimum Fungicidal Concentration (MFC) method

Although the MIC test results were higher than the initial well concentration, as previously described by Norrby and Jonsson [30], samples from the initial wells were transferred to Nutrient Agar (NA) for bacterial cultures to perform the MBC test. Similarly, the *Candida* strain was transferred to Sabouraud Dextrose Agar (SDA) for the MFC test and incubated under optimal growth conditions, considering the appropriate time and temperature for each microorganism.

2.7 Biofilm detection method with Congo Red Agar (CRA)

Following the protocol described by Freeman et al. [31], a specialized medium was prepared utilizing Congo Red (CR), an azo dye. Bacterial strains were incubated at 37°C, whereas *Candida* strains were incubated at 27°C for 24 h on Congo Red Agar (CRA). Biofilm-producing microorganisms were phenotypically identified using the CRA method.

2.8 Antibiofilm activity

Consistent with the findings of Ozturk et al. [32], the crystal violet assay was employed to quantify biofilm production in microorganisms previously identified via the CRA method.

The antibiofilm activity assay, adapted from the method originally described by Karaca et al. [33], comprised two primary stages: first, optimization of biofilm formation conditions and second, evaluation of the antibiofilm activity of the prepared extracts.

To establish optimal biofilm formation conditions, all microorganisms were standardized to a 0.5 McFarland turbidity. Each strain was inoculated into culture media supplemented with varying glucose concentrations (0%, 0.5%, 1.5%, 2%, and 2.5%) and incubated at 37°C for 24 h and 48 h. Following incubation, 200 µL of crystal violet solution was added to each well and allowed to incubate for 30 min. The wells were then rinsed with distilled water and air-dried. Subsequently, 200 µL of a 70:30 ethanol/acetone solution was added to each well and incubated for 15 min. The contents of each well were then carefully transferred to a new microplate, and the absorbance was measured at 550 nm using a microplate reader.

Based on these results, the optimal biofilm formation conditions were determined to be 48 h of incubation in a medium supplemented with 0.5% glucose for *E. coli* 7, *E. coli* 9, *E. coli* 11, *E. coli* 12, *S. aureus*, *S. aureus* MRSA, and *C. albicans* DSMZ 1386 strains. Consequently, subsequent biofilm activity assays were performed under these optimized conditions.

During the biofilm activity assays, 100 µL of each extract was added to the wells in row A of a microplate, followed by two-fold serial dilutions down to row H. Inocula, standardized to a 0.5 McFarland turbidity in physiological saline, were then transferred into the wells. Halamid® served as a positive control, and all cultures were incubated at 37°C for 48 h. Following incubation, the crystal violet staining, washing, and ethanol/acetone elution steps were repeated, and absorbance measurements were obtained at 550 nm [32,34,35].

2.9 Biofilm SEM and AFM analysis

Based on the results obtained from the crystal violet biofilm detection method, the microorganism for which biofilm inhibitory effects were observed was selected for SEM and AFM analysis.

To perform these analyses, cell suspensions, culture medium, and extracts were prepared in 24-well microplates containing sterile metal coupons and incubated for 5 days, considering the optimum growth temperatures of the microorganisms. Imaging was performed with SEM and AFM at the end of the incubation period [36,37].

2.10 Statistical analysis

All experiments in this study were performed in triplicate, and statistical significance was assessed using one-way analysis of variance (ANOVA) in R Studio (v3.3.2). A *p*-value of < 0.05 was considered statistically significant. Furthermore, Pearson's correlation coefficient was calculated to evaluate the relationship between extract concentration and observed effect [38].

3. RESULTS AND DISCUSSION

3.1 Extraction yield

The preparation of ethanol and chloroform extracts of *F. fomentarius* used in the study has been described in detail previously. The extract yield obtained according to the amount of extract was calculated as 20.160% and 26.25%, respectively. When the extraction yield was examined, it was observed that the ethanol extract had a lower yield than the chloroform extract.

3.2 MIC and MBC tests

To mitigate potential concentration-dependent loss of microbial viability in subsequent antibiofilm experiments, the antimicrobial activity of *F. fomentarius* ethanol and chloroform extracts was assessed against all tested microorganisms via Minimum Inhibitory Concentration (MIC) and Minimum Bactericidal/Fungicidal Concentration (MBC/MFC) assays. At the end of the conducted research, it was found that the MIC result was >1790 µg/mL for *F. fomentarius*-EtOH, >2095 µg/mL for *F. fomentarius*-Chloroform due to the application of extracts at low doses. MBC/MFC tests could not be applied due to the MIC test results being higher than the initial well concentration. Given that the primary objective of this study was to identify sub-lethal extract concentrations for subsequent use in antibiofilm assays, rather than to conduct a comprehensive assessment of antimicrobial activity, the absence of a quantifiable MIC value is not considered particularly consequential. It is plausible that a MIC result could be obtained through the utilization of higher initial concentrations of the macrofungal extract.

3.3 Biofilm experiments

3.3.1 Congo Red Agar (CRA) method

In this study, the microorganisms were first phenotypically determined to produce biofilms by applying the CRA method. The results obtained using this method are shown in the photographs given below. Biofilm production was observed in the microorganisms that appeared black, whereas it was not detected in the strains lacking the black pigmentation.

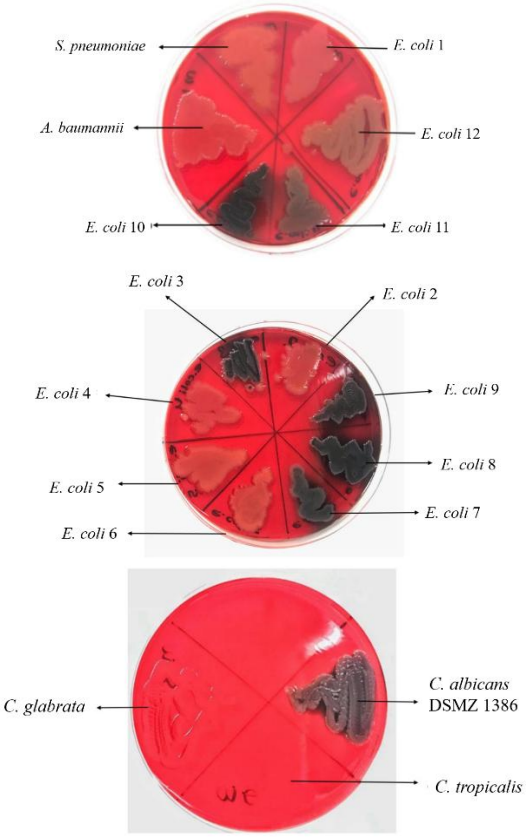

FIGURE 1. CRA results

3.3.2 Determination of optimum biofilm formation parameters

In this study, six different glucose concentrations (0.0%, 0.5%, 1.0%, 1.5%, 2.0%, and 2.5%) and two different incubation times (24 and 48 hours) were tested. The results indicated that the optimum conditions for all microorganisms were a 48-hour incubation in a medium containing 0.5% glucose ($p < 0.05$). The statistical analysis revealed no significant differences between the parallel studies conducted ($p > 0.05$).

3.3.3 Antibiofilm activity

The antibiofilm activities of the microorganisms, for which optimum biofilm formation parameters were determined, were assessed using the crystal violet method, as previously described. The antibiofilm activity assays demonstrated that the *F. fomentarius*-EtOH extract significantly inhibited biofilm formation by *S. aureus* MRSA (Figure 2). No statistically significant inhibitory or activating effects were observed for the *F. fomentarius*-Chloroform extract against the tested strains. Halamid®, used as a positive control, also demonstrated an inhibitory effect.

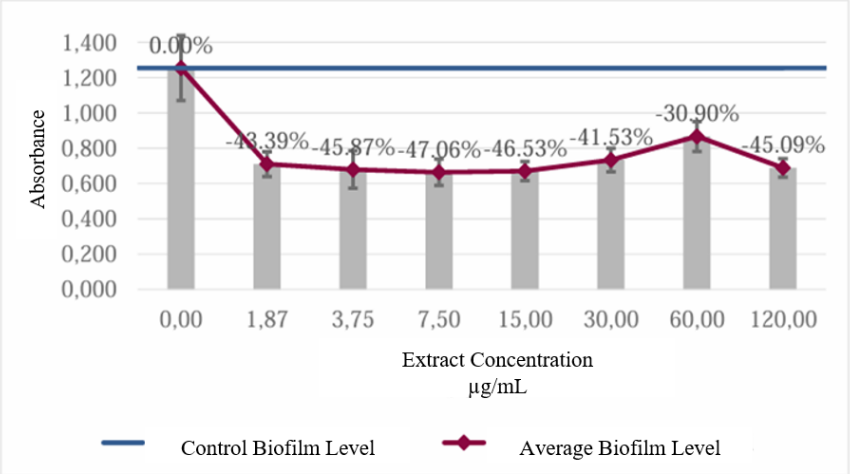

FIGURE 2. Effects of the *F. fomentarius*-EtOH extract *on S. aureus* MRSA biofilm formation (bars indicated extract concentration (µg/mL))

3.3.4 SEM images

Examination of the SEM images revealed a clear reduction in biofilm production when *F. fomentarius*-EtOH extract was applied to the *S. aureus* MRSA strain (Figure 3b). Comparison of the *F. fomentarius*-EtOH extract images (Figure 3b) and negative control (Figure 3a) demonstrated that the environment with the most biofilm formation was the one lacking the *F. fomentarius*-EtOH extract. It was observed that the Halamid® also reduced biofilm formation (Figure 3c), which was consistent with the spectrophotometric results.

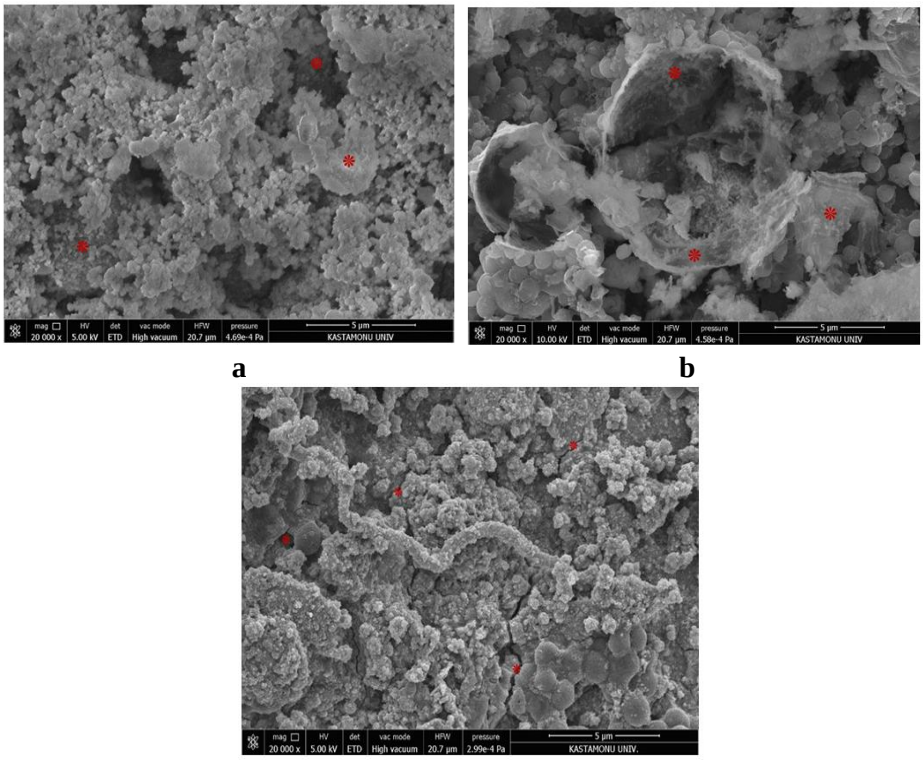

FIGURE 3. **a)** presents SEM images of control sample of *S. aureus* MRSA (20.000x) **b)** *F. fomentarius*-EtOH-treated/*S. aureus* MRSA (20.000x) **c)** Halamid-treated /*S. aureus* MRSA (20.000x)

3.3.5 AFM images

Analysis of the AFM images revealed that the *S. aureus* MRSA strain treated with the *F. fomentarius*-EtOH extract exhibited significantly reduced biofilm production (Figure 4a). A comparison between the extract-treated sample (Figure 4a) and the negative control without the extract (Figure 4b) clearly indicated that the extract application resulted in lower biofilm formation, thereby inhibiting biofilm development. These findings are consistent with the SEM results and spectrophotometric data.

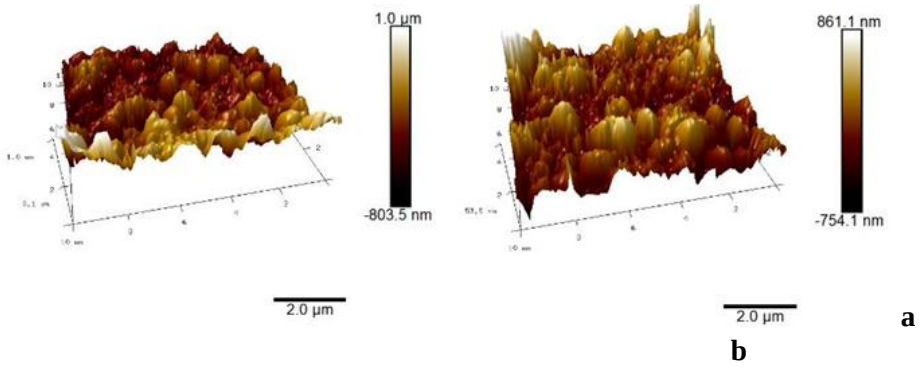

FIGURE 4. **a)** *F. fomentarius*-EtOH-treated/*S. aureus* MRSA, **b)** Negative control/*S. aureus* MRSA

3.3.6 GC/MS

Content analysis of both extracts obtained from the *F. fomentarius* mushroom was performed using GC/MS. The chromatograms for *F. fomentarius*-EtOH and *F. fomentarius*-Chloroform are given in Figure 5a and 5b, respectively.

In addition, the major components of *F. fomentarius*-EtOH and *F. fomentarius*-Chloroform are given in Table 1.

GC/MS analysis revealed that the *F. fomentarius*-EtOH extract contained 15.86% stearic acid, 14.28% palmitic acid, 11.28% alpha-linoleic acid, 9.64% Oleic acid, 6.99 % linocaine hydrochloride, 6.95% methyl tetracosanoate, 4.58% anethole, 2.29% benzoic acid, and 2.15% D-allose, along with other minor components. Stearic acid is a recognized anti-inflammatory lipid with significant and multifaceted effects on hepatic metabolism [39,40]. Numerous fatty acids are known to exhibit antibacterial, antifungal, antioxidant, and antibiofilm properties to varying degrees across different microbial strains, including palmitic acid and stearic acid [41–44].

The GC/MS analysis revealed that the *F. fomentarius*-Chloroform extract contained 21.44% methyl stearate, 18.71% 9,12-octadecadienoic acid, and 18.70% methyl palmitate, along with other minor components. Methyl palmitate is used in the production of detergents, plastics, and animal feed. It possesses anti-inflammatory, antimicrobial, and antifungal properties [45-49].

a)

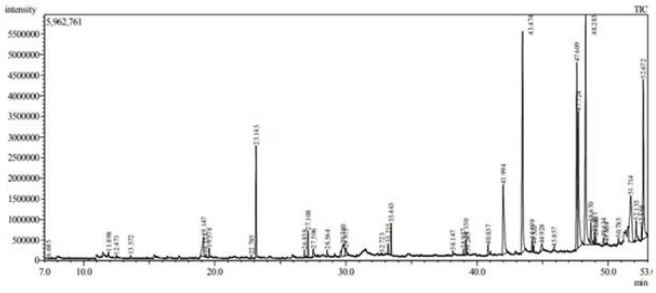

b)

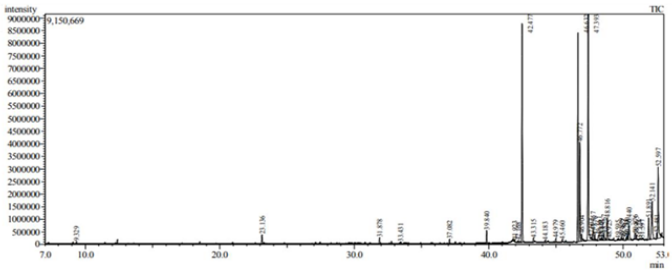

FIGURE 5. **a)** presents chromatogram illustrating the GC/MS results of *F. fomentarius*-EtOH **b)** presents chromatogram illustrating the GC/MS results of *F. fomentarius*-Chloroform

TABLE 1. Major Components of *F. fomentarius*-Chloroform and *F. fomentarius*-EtOH Extracts

***F. fomentarius*-Chloroform**		***F. fomentarius*-EtOH**	
Major Components	**Percentage (%)**	**Major Components**	**Percentage (%)**
Methyl stearate	21.44	Stearic acid	15.86
9,12-Octadecadienoic acid	18.71	Palmitic acid	14.28
Methyl palmitate	18.70	Alpha-linoleic acid	11.28
9-Octadecenamide	7.79	9-Octadecenamide	10.54
Ethyl stearate	5.23	Oleic acid	9.64
9,12-Octadecadienoic acid, methyl ester	2.39	Linocaine hydrochloride	6.99
Methyl 18-methylnonadecanoate	2.07	Methyl tetracosanoate	6.95
Tricyclo[20.8.0.0(7,16)]triacontane, 1(22),7(16)-diepoxy-	3.49	Anethole	4.58
Methyl pentadecanoate	1.06	Benzoic acid	2.29
		D-Allose	2.15
		Tetradecylcyclohexane	1.29
		Octadecanamide	1.29
		Hexadecane	1.26
		Tetradecane	1.09

Irez et al. [50] investigated the antibiofilm activity of various extracts derived from *F. fomentarius*. Their findings indicated that the *F. fomentarius*-EtOH extract significantly inhibited biofilm formation in the tested strains, with observed reductions exceeding 80% for *E. coli* and *S. aureus*, and approaching 80% for *C. albicans*. The *F. fomentarius*-Chloroform extract showed an inhibitory effect against the tested strains, but this effect was lower compared to the *F. fomentarius*-EtOH extract, with values below 20% for *E. coli* and *S. aureus*, and approximately 40% for *C. albicans*.

The *F. fomentarius*-EtOH extract exhibited an inhibitory effect on the *S. aureus* MRSA strain. In contrast, the *F. fomentarius*-chloroform extract showed neither inhibitory nor activator effects. This result may be associated with variations in extraction concentrations and the resistance profile of the tested microorganisms.

In a previous study, Halamid® was used as a positive control during the antibiofilm experiments. This study investigated the effects of Halamid® on *E. coli* 9, *S. aureus* MRSA, and *C. albicans*. The results obtained in that study were calculated as 62.91% (3.90 μg/mL) for *S. aureus* MRSA, 45.66% (0.41 μg/mL) for *E. coli* 9, and 68.70% (1.95 μg/mL) for *C. albicans* [13].

In this study, Halamid® was also used as a positive control in all biofilm analyses, demonstrating an inhibition of 54.21% for 125 μg/mL of Halamid® concentration against the *S. aureus* MRSA strain. Furthermore, the scanning electron microscopy (SEM) and atomic force microscopy (AFM) images corroborate the biofilm inhibition findings of this study. While these results align with the existing literature regarding Halamid®'s efficacy, discrepancies exist between the specific inhibition percentages and active concentrations reported herein and the data presented by Zurnaci et al. [13]. Therefore, in light of these differences, it is advisable to support any biofilm study conducted with spectroscopic methods with imaging techniques such as SEM and/or AFM for enhanced validation.

In addition to the discrepancies in biofilm inhibition percentages in this study and the studies in the literature, there are also some inconstancies in terms of the antimicrobial activity of *F. fomentarius* extracts compared to the previous studies. Such as Dokhaharani et al. [51], who reported a Minimum Inhibitory Concentration (MIC) of 0.7 mg/mL and a Minimum Bactericidal Concentration (MBC) of 12.5 mg/mL for a *F. fomentarius* methanol extract against *S. aureus* ATCC 25923 using a microdilution assay, the present study observed MIC values for *F. fomentarius* ethanol and chloroform extracts that exceeded the highest concentration tested (*F. fomentarius*-EtOH >1790 μg/mL, *F. fomentarius*-Chloroform >2095 μg/mL). This inconstancy may be attributed to differences in extraction solvents or *S. aureus* strains used.

Pavić et al. [26] synthesized silver nanoparticles (AgNPs) using a *F. fomentarius* methanol extract and subsequently evaluated the antibacterial activity of both the AgNPs and the extract against *Bacillus subtilis*, *S. aureus*, *E. coli*, and *P. aeruginosa* using a Minimum Inhibitory Concentration (MIC) assay. The MIC

values for the *F. fomentarius* methanol extract were determined to be 20.83 μg/mL, 10.41 μg/mL, 2.63 μg/mL, and 20.83 μg/mL, respectively, against the aforementioned bacterial species. The corresponding MIC values for the AgNPs were 12.69 μg/mL, 6.34 μg/mL, 12.69 μg/mL, and 12.69 μg/mL. In the present study, extracts of the same macrofungus were prepared using different solvents, and the MIC assay was performed. The discrepancies between the findings of these two studies are attributed primarily to the use of different extraction solvents.

4. CONCLUSIONS

In this study, the Congo Red Agar (CRA) assay was initially employed to screen twelve *E. coli* isolates, two *S. aureus* strains, *P. mirabilis*, *S. pneumoniae*, *S. flexneri*, *A. baumannii*, *C. tropicalis*, *C. glabrata*, and *C. albicans* strains for biofilm production. This screening revealed that *E. coli* 7, *E. coli* 9, *E. coli* 11, *E. coli* 12, *S. aureus*, and *S. aureus* MRSA were capable of producing biofilms.

The *F. fomentarius*-EtOH extract exhibited an inhibitory effect on biofilm production against the *S. aureus* MRSA strain.

Biofilms are recognized as significant contributors to infections associated with vascular catheters, Foley catheters, and cerebrospinal shunts, as well as various tissue-related infections affecting the skin and teeth. Furthermore, biofilms enhance the resistance of biofilm-forming microorganisms to both antibiotics and antifungal agents. Consequently, preventing biofilm formation is of paramount importance for public health and in industrial settings [1,3,24].

Based on the biofilm data obtained in this study, it is evident that spectrophotometric assays alone may not always provide conclusive results and require corroboration from scanning electron microscopy (SEM), atomic force microscopy (AFM), and/or other complementary techniques. Therefore, for future biofilm investigations, it is recommended that spectrophotometric assays be combined with SEM and/or AFM to obtain more robust and reliable data. Given the importance of biofilm inhibition, further investigation of the *F. fomentarius*-EtOH extract, which demonstrated significant biofilm inhibitory effects in this study, is critically warranted.

In addition to the analyses performed herein, future research should focus on the purification of major constituents identified through compositional analysis or the acquisition of commercially available compounds to elucidate whether these components are responsible for the biofilm inhibitory effects of the extracts. Such studies would provide valuable insights.

Data Availability The data used in this study are available from the corresponding author upon reasonable request.

Acknowledgement This work was supported by the Kastamonu University Scientific Research Coordination Unit, with project number KU-HIZDES/ 2021-32.

Author Contribution Statements Conceptualisation, E.M.A.; data curation, U.M.S. and E.M.A.; methodology, U.M.S. and E.M.A.; supply and identification of the macrofungi, I.A.; writing, U.M.S. and E.M.A.; supervision, E.M.A.; project administration, E.M.A.; funding acquisition, E.M.A. All authors have read and agreed to the manuscript.

Declaration of Competing Interests The authors declare no conflict of interest.

Ethical Statement This research did not involve human participants or animals. Therefore, no ethical approval was required.

Use of Artificial Intelligence No artificial intelligence-based tools or applications were used in the preparation of this study. The entire content of the study was produced by the author(s) in accordance with scientific research methods and academic ethical principles.

Impact Statement This study demonstrates the potential of *Fomes fomentarius* extracts for targeted modulation of biofilms, offering a foundation for developing novel strategies to combat biofilm-related challenges in both clinical and industrial settings.

REFERENCES

[1] Achinas, S., Charalampogiannis, N., Euverink, G.J.W., A brief recap of microbial adhesion and biofilms. *Applied Sciences*, 9 (2019), 2801. doi.org/10.3390/app9142801

[2] Donlan, R.M., Biofilms: microbial life on surfaces. *Emerging Infectious Diseases*, 8 (2002), 881-890. doi.org/10.3201/eid0809.020063

[3] Du Toit, A., Bacterial architects build the biofilm structures. *Nature Reviews Microbiology* (2024), 187. doi.org/10.1038/s41579-024-01020-6

[4] Dufrêne, Y.F., Viljoen, A., Binding strength of gram-positive bacterial adhesins. *Frontiers in Microbiology*, 11 (2020), 554551. doi.org/10.3389/fmicb.2020.01457

[5] Feng, X., Wu, Q., Che, L., Ren, N., Analyzing the inhibitory effect of metabolic uncoupler on bacterial initial attachment and biofilm development and the underlying mechanism. *Environmental Research*, 185 (2020), 109390. doi.org/10.1016/j.envres.2020.109390

[6] Joseph, R.L., Prosthetic joint infections: Bane of orthopaedists. *Clinical Infectious Diseases*, 36 (2004), 1157-1161. doi.org/10.1086/374554

[7] Roy, R., Tiwari, M., Donelli, G., Tiwari, V., Strategies for combating bacterial biofilms: A focus on anti-biofilm agents and their mechanisms of action. *Virulence*, 9 (2018), 522-554. doi.org/10.1080/21505594.2017.1313372

[8] Samrot, A. V., Abubakar Mohamed, A., Faradjeva, E., Si Jie, L., Hooi Sze, C., Arif, A., ... & Kumar, S. S., Mechanisms and impact of biofilms and targeting of biofilms using bioactive compounds: A review. *Medicina*, 57 (2021), 839. doi.org/10.3390/medicina57080839

[9] Markou, G., Georgakakis, D., Cultivation of filamentous cyanobacteria (blue-green algae) in agro-industrial wastes and wastewaters: a review. *Applied Energy*, 88 (2011), 3389-3401. doi.org/10.1016/j.apenergy.2010.12.042

[10] Pan, M., Lyu, T., Zhang, M., Zhang, H., Bi, L., Wang, L., Chen, J., Yao, C., Ali, J., Best, S., Ray, N., Pan, G., Synergistic recapturing of external and internal phosphorus for *in situ* eutrophication mitigation. *Water*, 12 (2019), 1-9. doi.org/10.3390/w12010002

[11] Nie, L., Li, Y., Chen, S., Li, K., Huang, Y., Zhu, Y., Sun, Z., Zhank, J., He, Y., Wei, S., Biofilm nanofiber-coated separators for dendrite-free lithium metal anode and ultrahigh-rate lithium batteries. *ACS Applied Materials & Interfaces*, 11 (2019), 32373-32380. doi.org/10.1021/acsami.9b08656

[12] Singh, R., Puri, A., Panda, B.P., Development of menaquinone-7 enriched nutraceutical: insights into medium engineering and process modeling. *Journal of Food Science and Technology*, 52 (2015), 5212-5219. doi.org/10.1007/s13197-014-1600-7

[13] Zurnaci, M., Senturan, U. M., Sener, N., Gur, M., Altinoz, E., Sener, I., Altuner, E. M., Studies on antimicrobial, antibiofilm, efflux pump inhibiting, and ADMET properties of newly synthesised 1, 3, 4-Thiadiazole derivatives. *ChemistrySelect*, 6 (2021), 12571-12581. doi.org/10.1002/slct.202103214

[14] Mukherjee, S., Bassler, B.L., Bacterial quorum sensing in complex and dynamically changing environments. *Nature Reviews Microbiology*, 17 (2019), 371-382. doi.org/10.1038/s41579-019-0186-5

[15] Shome, S., Talukdar, A.D., Nath, R., Tewari, S., Curcumin-ZnO nanocomposite mediated inhibition of *Pseudomonas aeruginosa* biofilm and its mechanism of action. *Journal of Drug Delivery Science and Technology*, 81 (2023), 104301. doi.org/10.1016/j.jddst.2023.104301

[16] Altuner, E.M., Akata, I., Antimicrobial activity of some macrofungi extracts. *SAU Fen Bilimleri Dergisi*, 14 (2010), 45-49. https://doi.org/10.16984/saufbed.31339

[17] Fendoglu, B., Kuruuzum-Uz, A., Sohretoglu, D., Alkaloids obtained from fungi. *Journal of Fungi*, 9 (2018), 117-125. https://doi.org/10.30708/mantar.415589

[18] Forland, D.T., Johnson, E., Tryggestad, A.M.A., Lyberg, T., Hetland, G., An extract based on the medicinal mushroom *Agaricus blazei Murill* stimulates monocyte-derived dendritic cells to cytokine and chemokine production *in vitro*. *Cytokine*, 49 (2010), 245-250. doi.org/10.1016/j.cyto.2009.09.002

[19] Homer, J.A., Sperry, J., Mushroom-derived indole alkaloids. *Journal of Natural Products*, 80 (2017), 2178-2187. doi.org/10.1021/acs.jnatprod.7b00390

[20] Ozturk, M., Tel-Cayan, G., Muhammad, A., Terzioglu, P., Duru, M.E., Mushrooms: A source of exciting bioactive compounds. *Studies in Natural Products Chemistry*, 45 (2015), 363−456. doi.org/10.1016/b978-0-444-63473-3.00010-1

[21] Pommerville, J.C., Fundamentals of Microbiology. Burlington, Mass: Jones and Bartlett Publishers, 2014. ISBN: 9781284039652

[22] Barros, L., Cruz, T., Baptista, P., Estevinho, L.M., Ferreira, I.C.F.R., Wild and commercial mushrooms as sources of nutrients and nutraceuticals. *Food Chem Toxicol*, 46 (2008), 2742-2747. doi.org/10.1016/j.fct.2008.04.030

[23] Sohretoglu, D., Huang, S., *Ganoderma lucidum* polysaccharides as an anti-cancer agent. *Anticancer Agents in Medicinal Chemistry*, 18 (2018), 667-674. doi.org/10.2174/1871520617666171113121246

[24] Alves, M.J., Ferreira, I.C., Lourenco, I., Costa, E., Martins, A., Pintado, M., Wild mushroom extracts as inhibitors of bacterial biofilm formation. *Pathogens*, 3 (2014), 667-679. doi.org/10.3390/pathogens3030667

[25] Papetti, A., Signoreto, C., Spratt, D.A., Pratten, J., Lingström, P., Zaura, E., Ofek, I., Wilson, M., Pruzzog, C., Gazzania, G., Components in *Lentinus edodes* mushroom with anti-biofilm activity directed against bacteria involved in caries and gingivitis. *Food & Function*, 9 (2018), 3489-3499. doi.org/10.1039/c7fo01727h

[26] Pavić, V., Kovač-Andrić, E., Ćorić, I., Rebić, S., Užarević, Z., Gvozdić, V., Antibacterial efficacy and characterization of silver nanoparticles synthesized via methanolic extract of *Fomes fomentarius* L. Fr. *Molecules*, 29 (2024), 3961. doi.org/10.3390/molecules29163961

[27] Baldas, B., Altuner, E.M., The antimicrobial activity of apple cider vinegar and grape vinegar, which are used as a traditional surface disinfectant for fruits and vegetables. *Communications Faculty of Sciences University of Ankara Series C Biology*, 27 (2018), 1-10. doi.org/10.1501/commuc_0000000187

[28] Hammer, K.A., Carson, C.F., Riley, T.V., Antimicrobial activity of essential oils and other plant extracts. *Journal of Applied Microbiology*, 86 (1999), 985-990. doi.org/10.1046/j.1365-2672.1999.00780.x

[29] Salmon, S.A., Watts, J.L., Aarestrup, F.M., Pankey, J.W., Yancey Jr, R.J., Minimum inhibitory concentrations for selected antimicrobial agents against organisms isolated from the mammary glands of dairy heifers in New Zealand and Denmark. *Journal of Dairy Science*, 81 (1998), 570-578. doi.org/10.3168/jds.s0022-0302(98)75610-3

[30] Norrby, S.R., Jonsson, M., Antibacterial activity of norfloxacin. *Antimicrobial Agents and Chemotherapy*, 23 (1983), 15-18. doi.org/10.1128/aac.23.1.15

[31] Freeman, D.J., Falkiner, F.R., Keane, C.T., New method for detecting slime production by coagulase-negative staphylococci. *Journal of Clinical Pathology*, 42 (1989), 872-874. doi.org/10.1136/jcp.42.8.872

[32] Ozturk, I., Yurtman, A.N., Erac, B., Gul-Yurtsever, S., Ermertcan, S., Hosgor Limoncu, M., *In vitro* effect of moxifloxacin and rifampicin on biofilm formation by clinical MRSA isolates. *Bratislava Medical Journal*, 115 (2014), 483-486. doi.org/10.4149/bll_2014_093

[33] Karaca, B., Coleri Cihan, A., Akata, I., Altuner, E.M., Anti-biofilm and antimicrobial activities of five edible and medicinal macrofungi samples on some biofilm-producing multi-drug resistant *Enterococcus* strains. *Turkish Journal of Agriculture-Food Science and Technology*, 8 (2020), 69-80. doi:10.24925/turjaf.v8i1.69-80.2723

[34] Stepanović, S., Vuković, D., Hola, V., Bonaventura, G. D., Djukic, S., Cirkovic, I., Ruzicka, F., Quantification of biofilm in microtiter plates: Overview of testing conditions and practical recommendations for assessment of biofilm production by *staphylococci*. *APMIS*, 115 (2007), 891-899. doi: 10.1111/1600-0463.2007

[35] Temel, A., Erac, B., Bacterial biofilms: detection methods and their role in antibiotic resistance. *Turkish Journal of Microbiology*, 48 (2018), 1-13. doi.org/10.5222/tmcd.2018.001

[36] Beech, I.B., Smith, J.R., Steele, A.A., Penegar, I., Campbell, S.A., The use of atomic force microscopy for studying interactions of bacterial biofilms with surfaces. *Colloids and Surfaces B: Biointerfaces*, 23 (2002), 231-247. doi.org/10.1016/s0927-7765(01)00233-8

[37] Gomes, L.C., Mergulhão, F.J., SEM analysis of surface impact on biofilm antibiotic treatment. *Scanning*, (2017), 2960194. doi: 10.1155/2017/2960194

[38] R Core Team., R: A language and environment for statistical computing. R Foundation for Statistical Computing, Vienna, Austria. https://www.R-project.org/. (accessed 2025).

[39] Goradel, N.H., Eghbal, M.A., Darabi, M., Roshangar, L., Asadi, M., Zarghami, N., Nouri, M., Improvement of liver cell therapy in rats by dietary stearic acid. *Iranian Biomedical Journal*, 20 (2016), 217-222. http://dx.doi.org/10.7508/ibj.2016.04.005

[40] Khalil, M.H., Marcelletti, J.F., Katz, L.R., Katz, D.H., Pope, L.E., Topical application of docosanol-or stearic acid-containing creams reduces severity of phenol burn wounds in mice. *Contact dermatitis*, 43 (2000), 79-81. doi.org/10.1034/j.1600-0536.2000.043002079.x

[41] Bentrad, N., Gaceb-Terrak, R., Rahmania, F., Identification and evaluation of antibacterial agents present in lipophilic fractions isolated from sub-products of *Phoenix dactilyfera*. *Natural product research*, 31 (2017), 2544-2548. doi.org/10.1080/14786419.2017.1314282

[42] Kumar, P., Lee, J.H., Beyenal, H., Lee, J., Fatty acids as antibiofilm and antivirulence agents. *Trends in microbiology*, 28 (2020), 753-768 doi.org/10.1016/j.tim.2020.03.014

[43] Prasath, K.G., Tharani, H., Kumar, M.S., Pandian, S.K., Palmitic acid inhibits the virulence factors of *Candida tropicalis*: Biofilms, cell surface hydrophobicity, ergosterol biosynthesis, and enzymatic activity. *Frontiers in Microbiology*, 11 (2020), 864. doi.org/10.3389/fmicb.2020.00864

[44] Xie, Y., Peng, Q., Ji, Y., Xie, A., Yang, L., Mu, S., Li, Z., He, T., Xiao, Y., Zhao, J., Zhang, Q. Isolation and identification of antibacterial bioactive compounds from *Bacillus megaterium* L2. *Frontiers in microbiology*, 12 (2021), 645484. doi.org/10.3389/fmicb.2021.645484

[45] El Demerdash, E., Anti-inflammatory and antifibrotic effects of methyl palmitate. *Toxicology and applied pharmacology*, 254 (2011), 238-244. doi.org/10.1016/j.taap.2011.04.016

[46] Janani S.R., Singaravadivel, K., Screening of phytochemical and GC-MS analysis of some bioactive constituents of *Asparagus racemosus*. *International Journal of PharmTech Research*, 6 (2014), 428-432.

[47] Mantawy, E.M., Tadros, M.G., Awad, A.S., Hassan, D.A., El-Demerdash, E., Insights antifibrotic mechanism of methyl palmitate: impact on nuclear factor kappa B and proinflammatory cytokines. *Toxicology and applied pharmacology*, 258 (2012), 134-144. doi.org/10.1016/j.taap.2011.10.016

[48] Roopa, M.S., Shubharani, R., Rhetso, T., Sivaram, V., Comparative analysis of phytochemical constituents, free radical scavenging activity and GC-MS analysis of leaf and flower extract of *Tithonia diversifolia* (Hemsl.) A. Gray. *International Journal of Pharmaceutical Sciences & Research*, 11 (2020), 5081-5090. doi.org/10.1186/s43094-020-00100-7

[49] Wang, Y.N., Wang, H.X., Shen, Z.J., Zhao, L.L., Clarke, S.R., Sun, J.H., Du, Y.Y., Shi, G.L., Methyl palmitate, an acaricidal compound occurring in green walnut husks. *Journal of Economic Entomology*, 102 (2009), 196-202. doi.org/10.1603/029.102.0128

[50] Irez, E.I., Hacıoğlu Doğru, N., Demir N., *Fomes fomentarius* (L.) Fr. extracts as sources of an antioxidant, antimicrobial and antibiofilm agents. *Biologica Nyssana*, 12 (2021), 55-62. doi.org/10.5281/zenodo.5523017

[51] Dokhaharani, S.C., Ghobad-Nejad, M., Farazmand, A., Moghimi, H., Rahmani, H., Evaluation of antibacterial activity of methanolic extract of the polypore fungus *Fomes fomentarius* (Polyporaceae) against *Staphylococcus aureus*. *Current Medical Mycology*, 4 (2018), 152-153. doi.org/10.1007/s12223-021-00884-y

http://communications.science.ankara.edu.tr

Commun.Fac.Sci.Univ.Ank.Ser. C Biology
Volume 34, Number 1, Pages 76-103 (2025)
ISSN 1303-6025 E-ISSN 2651-3749
DOI: 10.53447/communc.1656646

Research Article; Received: March 12, 2025; Accepted: May 15, 2025

INVESTIGATION OF *Plantago lanceolata* L.: A MULTIDIMENSIONAL STUDY ON ITS BIOCHEMICAL PROFILING, ANTIOXIDANT CAPACITY, AND BIOLOGICAL ACTIVITIES

Melike ERSİN[1], Elif GÖNÜL[1], Ezginur DUMAN[1], Gizem GÜL[2], Dilay TURU[2], Atakan BENEK[3], Kerem CANLI[1,3]

Keywords

Plantago lanceolata L.
Anti-biofilm activity
Antimicrobial activity
Antioxidant activity

To cite this article

Ersin, M., Gönül, E., Duman, E., Gül, G., Turu, D., Benek, A., Canlı, K., Investigation of *Plantago lanceolata* L.: A multidimensional study on its biochemical profiling, antioxidant capacity, and biological activities. *Commun.Fac.Sci.Univ.Ank.Ser.C Biology*, 34 (1) (2025), 76-103. https://doi.org/10.1111/communc.1656646

Affiliations

[1]Department of Biology, Faculty of Science, Dokuz Eylül University, Izmir, TÜRKİYE

[2]Department of Biology, Graduate School of Natural and Applied Science, Dokuz Eylül University, Izmir, TÜRKİYE

[3]Fauna and Flora Research and Application Center Dokuz Eylül University, Izmir, TÜRKİYE

Abstract

Plantago lanceolata L. is a medicinal and aromatic plant recognized for its antimicrobial and antioxidant effects. This research focused on evaluating its biological activity, antioxidant capacity, and volatile compound composition through Gas Chromatography-Mass Spectrometry (GC-MS) analysis. The extract's effects on biofilms formed by pathogenic bacteria were evaluated, showing significant biofilm inhibition and disruption. The antimicrobial activity was assessed based on minimum inhibitory concentration (MIC) and minimum bactericidal concentration (MBC) values. The extract exhibited strong effects against Staphylococcus aureus MRSA, Streptococcus mutans, and S. aureus MRSA+MDR strains. The antioxidant potential was assessed through the 1,1-Diphenyl-2-picrylhydrazyl (DPPH) radical assay, demonstrating a notable ability to scavenge free radicals. These findings suggest that P. lanceolata could serve as a protective or supportive agent against diseases associated with oxidative stress. GC-MS analysis identified the volatile components, with high concentrations of fatty acid derivatives such as linolenic acid and hexadecenoic acid. The study demonstrated that P. lanceolata possesses notable antibiofilm, antimicrobial, and antioxidant properties, making it a valuable natural resource. Owing to its bioactive compounds, this species exhibits significant potential for applications in the pharmaceutical, food, and cosmetic industries. It may also function as an important phytochemical in the drug developers' search for resources. Further research is required to expand its potential applications and prove its clinical efficacy.

1. INTRODUCTION

Microorganisms constitute a significant portion of global biodiversity, encompassing the domains *Archaea* and *Bacteria*, which represent two of the three fundamental domains of life [1]. The majority of microorganisms consist

ersinnmelike@gmail.com- Corresponding author; 0009-0002-2234-822X https://ror.org/00dbd8b73
elliifgnl@gmail.com- 0009-0008-6978-8058 https://ror.org/00dbd8b73
ezginrduman@gmail.com- 0009-0005-4561-2152 https://ror.org/00dbd8b73
gizeemmgull@gmail.com- 0000-0003-3928-2917 https://ror.org/00dbd8b73
dilayturu@gmail.com- 0000-0002-8485-0488 https://ror.org/00dbd8b73
atakan.benek@hotmail.com- 0000-0001-6726-5968 https://ror.org/00dbd8b73
kerem.canli@deu.edu.tr- 0000-0001-6061-6948 https://ror.org/00dbd8b73

of bacteria [2] and this group of organisms is critically important for human life [3]. Indeed, while many bacterial species contribute positively to vital processes, opportunistic pathogens can cause severe infections, particularly in cases of a weakened immune system [4]. Bacteria can employ both phenotypic and genetic strategies to develop resistance against environmental stressors, such as antibiotics, that threaten their survival [5]. These strategic adaptations enhance the ability of microorganisms to adapt and acquire resistance [6].

As reported by the World Health Organization [7], the major challenge of the modern era is the increasing antimicrobial resistance. To prevent this rising resistance, the discovery of new antimicrobial compounds is essential [8]. The discovery of antibiotics is regarded as one of the greatest achievements in the field of medicine in the modern era. The clinical use of antibiotics has provided an effective treatment for bacterial infections, significantly reducing morbidity and, consequently, mortality rates [9]. Since the 1990s, the discovery of new antibiotics has declined, and newly introduced antibiotics are merely optimized and modified versions of existing ones, without changes in their antibacterial mechanisms [6]. According to data from the Centers for Disease Control and Prevention (CDC), antibiotic-resistant bacteria cause infections in approximately 2 million people annually in the United States alone [10]. Inappropriate treatment practices and the misuse of antibiotics have contributed to the emergence of antibiotic-resistant bacteria, presenting serious challenges for future public health [11]. Resistant bacteria complicate treatment processes and gradually diminish the effectiveness of existing drugs [12]. This situation encourages scientists to develop new drugs and treatment methods; however, the number and effectiveness of current research efforts remain insufficient. The rapid ability of bacteria to develop resistance mechanisms makes the exploration of alternative treatments even more urgent and crucial [13]. Alongside advancements in synthetic technologies, plant-derived compounds play a crucial role in the development of antimicrobial agents [14]. In traditional medical practices, plant-derived substances have been widely used throughout history and have gained prominence due to their pharmacological effects [15].

Throughout history, many civilizations have used various plant extracts for wound healing, infection treatment, and even the management of numerous chronic diseases [16] Medicinally important plants continue to be key sources of bioactive compounds in pharmaceutical research and development [17]. In the study of antibiotic resistance, a major issue of our time, scientists worldwide and in Turkey are increasingly focusing on plants, which are the foundation of traditional medicine [18,19]. Plants synthesize a wide variety of secondary metabolites for environmental adaptation, competitive advantage, and defense [20]. Recent studies reveal that some of these metabolites possess antimicrobial potential and can be considered in alternative treatment strategies, particularly against global health issues such as antibiotic resistance [18, 21].

The genus *Plantago* belongs to the *Plantaginaceae* family and consists of seed-bearing plants [22]. This family, which includes approximately 275 species, is represented in Turkey by 22 species, two of which are endemic [23, 24]. It is a perennial herbaceous plant that can be found in grasslands and along roadsides [25]. It is used worldwide as a functional food and in certain diets for the treatment of various diseases [26]. It has extensive pharmaceutical applications, with *P. lanceolata* L. standing out particularly due to its phytochemical effects [27]. This plant has traditionally been utilized for treating various health conditions, including wound healing and inflammation [28]. This plant has traditionally been utilized for treating various health conditions, including wound healing and inflammation [29]. The high concentrations of flavonoids and phenolic compounds in its leaves constitute the primary biochemical basis for its pharmacological activities [30]. Recent studies have demonstrated that extracts of *Plantago lanceolata* exhibit antibacterial and biofilm-inhibitory activities against pathogenic bacteria such as *Borrelia burgdorferi* [31] The extract of the plant has also been reported to exhibit antifungal activity against certain dermatophytic fungi, suggesting the potential of *Plantago lanceolata* for dermatological applications [30].

This study was carried out primarily on P. lanceolata L., which is widespread in the Anatolian region. The biological activity of *P. lanceolata*, which has ethnobotanical importance and grows in our geography, was evaluated with 48 microorganisms. The bioactive compounds it contains were examined by GC-MS and its antioxidant capacity was evaluated accordingly. The data obtained contribute significantly to the accumulation of knowledge in the literature on the biological properties of the species in question.

2. MATERIALS AND METHODS

2.1 Chemicals

1,1-Diphenyl-2-picrylhydrazyl (DPPH, Sigma-Aldrich): Used as a stable free radical in the antioxidant capacity assay. Ethanol (Sigma-Aldrich): Absolute ethanol was used during the extraction process. Dimethyl Sulfoxide (DMSO, Sigma-Aldrich): Utilized at a 2% concentration in combination with distilled water for the preparation of extracts in antimicrobial tests. LB Broth (Merck): Employed as a liquid growth medium in antimicrobial assays. Mueller-Hinton Agar (MHA, Oxoid): Used as a solid culture medium for antimicrobial testing. Saline Solution (0.9% NaCl): Used for bacterial suspension preparation according to the McFarland standard. Ascorbic Acid (Carlo Erba): Served as the positive control in the antioxidant assay.

2.2 Preparation of *Plantago lanceolata* extract

P. lanceolata samples were collected from local markets. To extract its secondary metabolites, the plant material was finely pulverized using an IKA

grinder. A precisely measured 15-gram portion of the powdered sample was placed into an Erlenmeyer flask, and 200 milliliters of 99.8% ethanol was added. The mixture was then subjected to continuous agitation at 160 rpm for 72 hours using an orbital shaker to enhance the extraction process [32]. Following the shaking process, the mixture was filtered using Whatman No.1 filter paper to remove solid residues. The extract was then concentrated using a rotary evaporator (Buchi Labortechnik AG) at 35°C [33]. The remaining substance in the flask was weighed, yielding 0.686 grams. Finally, it was dissolved in ethanol to obtain a 15 mL extract. The extract was made into DMSO-water (2% DMSO) extract for the antimicrobial activity tests performed in the study (for MIC, MBC and Anti-biofilm tests). For bioactive content analysis, the extract was prepared with 99.8% absolute ethanol.

The ethanol extracted *P. lanceolata* solution was adjusted to a concentration of 1 mg/mL for antioxidant activity assay. Similarly, ascorbic acid solution used as a positive control was prepared at the same concentration of 1 mg/mL. Ascorbic acid (vitamin C) was used as a positive control due to its well-established antioxidant activity. It reacts with DPPH radicals, leading to a measurable color change, and thus serves as a reliable reference for comparing the antioxidant potential of samples. In the negative control group, only the DPPH solution was used to establish the baseline absorbance of the system.

2.3 Inoculum preparation

The inoculum of microorganisms used in the experiment were selected from exponentially growing colonies on nutrient media that exhibited similar morphological characteristics. The isolated colonies were transferred into tubes containing a 0.9% sterile sodium chloride (NaCl) solution, and the turbidity of the cell suspensions was adjusted to match the 0.5 McFarland standard. This standard corresponds to approximately 1.5×10^8 CFU/mL for bacteria and 1.5×10^7 CFU/mL for yeasts. Maintaining this standard is essential for ensuring a consistent cell concentration under experimental conditions, thereby enabling reproducible and reliable results. During the inoculum preparation, the optical density of the suspensions was assessed using a densitometer [33].

2.3.1 Microorganisms

The microbial strains used in this study were obtained from the Microbiology Laboratory of the Faculty of Science, Dokuz Eylül University.

The tested microorganisms consisted of a total of 48 strains, including 45 bacterial strains and 3 yeast strains. Standard isolation microorganisms, *Bacillus subtilis DSMZ 1971, Enterobacter aerogenes ATCC 13048, Enterococcus faecalis ATCC 29212, Escherichia coli ATCC 25922, Listeria monocytogenes ATCC 7644, Pseudomonas aeruginosa DSMZ 50071, Pseudomonas fluorescens P1, Salmonella enteritidis ATCC 13076, Salmonella typhimurium SL1344,*

Staphylococcus aureus ATCC 25923, Staphylococcus epidermidis DSMZ 20044, Staphylococcus hominis ATCC 27844, Staphylococcus warneri ATCC 27836, Bacillus cereus RSKK 863, Shigella flexneri RSKK 184, Acinetobacter baumannii CECT 9111, Food isolated microorganisms, Enterococcus durans, Enterococcus faecium, Klebsiella pneumoniae, Listeria innocua, Salmonella infantis, Salmonella kentucky, Escherichia coli, Clinical isolated microorganisms, Staphylococcus aureus, Streptococcus mutans, Staphylococcus hominis, Staphylococcus haemolyticus, Staphylococcus lugdunensis, Shigella boydi, Acinetobacter baumannii, Shigella flexneri, Staphylococcus aureus, Enterococcus faecalis, Klebsiella pneumoniae, multi-drug resistance microorganisms, Escherichia coli, Klebsiella pneumoniae, Acinetobacter baumannii, Enterobacter aerogenes, Serratia odorifera, Proteus vulgaris, Streptococcus pneumonia, Staphylococcus aureus MRSA, Staphylococcus aureus MRSA+MDR, Providencia rustigianii, Achromobacter sp. The yeasts are Candida albicans DSMZ 1386, Candida tropicalis, Candida glabrata.

2.4 Antimicrobial activity test

2.4.1 Disc diffusion test

In the disk diffusion assay used to assess antimicrobial activity [34], blank antibiotic susceptibility disks (Oxoid, 6 mm diameter) were impregnated with the extract at three different volumes (50, 100, and 150 µL). The corresponding extract concentrations on the disks were calculated as follows: 50 µL – 2.28 mg, 100 µL – 4.57 mg, and 150 µL – 6.86 mg. The extract-loaded disks were then allowed to dry at 30°C to facilitate ethanol evaporation. Following this, 40 mL of Mueller-Hinton Agar (BD Difco) was dispensed into sterilized 90 mm Petri dishes and left to solidify [35]. Inside a biosafety cabinet, pre-inoculated microorganism suspensions were evenly spread over the agar surface. After complete evaporation of ethanol, disks containing only the active compound were appropriately placed in each Petri dish. The plates were subsequently incubated at 37°C for 24 hours for bacterial cultures, while yeast cultures were incubated at 27°C for 48 hours. Gentamicin and Tobramycin antibiotics were used as positive controls in the study. At the end of the experiment, the sizes of the inhibition zones were determined in millimeters with a ruler and noted.

2.4.2 Minimum Inhibitory Concentration (MIC) test

The Minimum Inhibitory Concentration (MIC) assay is a crucial antimicrobial evaluation method that identifies the minimal extract concentration required to prevent bacterial proliferation. In this study, the extract obtained from *P. lanceolata* was prepared as a 2% Dimethyl Sulfoxide (DMSO)-water solution. To maintain sterility, the extract was passed through a 0.45 micrometer membrane filter. The broth microdilution method was performed in 96-well microplates to evaluate antimicrobial activity [36]. The bacterial strains used in the experiments were adjusted to the 0.5 McFarland standard. Subsequently, an

appropriate amount of culture medium was added to each well of a 96-well microplate, and the extract was serially diluted to achieve decreasing concentrations. A predetermined amount of inoculum was then added to each well. For the positive control, only the culture medium and microbial suspension were used, whereas for the negative control, wells containing only the extract and culture medium, without the microbial inoculum, were prepared. To ensure the repeatability and reliability of the experiments, all procedures were performed in three independent replicates. Following the incubation period, the wells were inspected, and the minimum extract concentration that showed no detectable bacterial proliferation was identified. This value was documented as the Minimum Inhibitory Concentration (MIC). Bacteria and culture medium without plant extract were used as positive control. As negative control, only culture medium and plant extract were selected.

2.4.3 Minimum Bactericidal Concentration (MBC) test / Minimum Fungicidal Concentration (MFC) test

The Minimum Bactericidal Concentration (MBC) is defined as the smallest amount of an antimicrobial agent necessary to effectively eliminate the bacterial population. In this study, after determining the Minimum Inhibitory Concentration (MIC) value of *P. lanceolata*, 10 µL samples were taken from all wells where bacterial growth was either inhibited or absent. These samples were then transferred onto MHA plates. The inoculated plates were incubated at 37°C for 24 hours. The MBC value was determined by observing bacterial growth before and after incubation. Based on these findings, the minimum antimicrobial concentration that completely inhibited bacterial presence on the plates was determined as the MBC value [37]. Positive and negative controls included in the MIC test were used.

The Minimum Fungicidal Concentration (MFC) is the minimum concentration of an antimicrobial agent needed to completely eradicate the yeast population. In this study, following the determination of the MIC of *P. lanceolata*, 10 µL samples were collected from all wells where yeast growth was either inhibited or absent. These samples were subsequently inoculated onto MHA plates. The plates were under controlled condition 27°C for 48 hours, after which yeast growth was assessed. The MFC value was determined as the lowest antimicrobial concentration at which no yeast colonies were observed. Positive and negative controls included in the MIC test were used.

2.4.4 Anti-biofilm test

To determine the anti-biofilm potential of *P. lanceolata* ethanol extract in different microbial strains, concentrations below the MIC values were first identified. Bacterial cell suspensions were standardized to the 0.5 McFarland turbidity level and dispensed into each well of a 96-well microplate. The prepared plates were incubated at 37°C for 48 and 72 hours, respectively. The

exposure durations were established using a previously performed biofilm detection assay [38]. After the incubation period, the plates were rinsed with distilled water to remove free-floating cells and then treated with 0.1% crystal violet for 15 minutes. Following this process, any excess dye was removed by an additional wash with distilled water. Subsequently, a 7:3 mixture (70% ethanol: 30% acetone) was added to dissolve the strain. In the final step, the optical density of the liquid in each well was assessed at 550 nanometers. The experiment was performed in triplicate [39].

2.4.5 Determination of antioxidant activity

The ability of the *P. lanceolata* ethanol extract to neutralize free radicals was assessed by monitoring the decolorization of the persistent DPPH radical. This approach is based on the capacity of antioxidant compounds to neutralize DPPH radicals, leading to a reduction in the intense purple coloration observed at a wavelength of 515 nanometers.

For this purpose, 0.0039 g of DPPH preapared in 50 mL ethanol. Prepared DPPH was added to the specified columns with the serial dilution method [40]. The mixture was kept at ambient temperature in the absence of light for 30 minutes. After this period, the optical measurement was recorded at 515 nanometers using a microplate reader (Biotek Microplate Spectrophotometer). Ascorbic acid, a commercially available antioxidant, was used as the positive control. All tests were repeated three times.

The percentage of DPPH radical neutralization was determined using the following formula:

$$\text{DPPH Radical Scavenging (\%)} = \left(\frac{A_1 - A_0}{A_0}\right) \times 100$$

In the equation, A_0 refers to the initial optical density of the DPPH mixture (control), while A_1 represents the optical density of the extract-treated samples. This calculation quantifies the percentage of DPPH radicals scavenged by the *P. lanceolata* ethanol extract, providing an assessment of its antioxidant potential [21].

2.6 Biochemical composition analysis

To analyze the biochemical profile of the plant extract, GC-MS analyses were conducted using an Agilent 8890 GC system coupled with an Agilent 5977B mass spectrometer (Agilent Technologies Inc.) [41]. An HP-5MS capillary column (30 m × 0.25 mm i.d., 0.25 μm film thickness) was used for the separation of volatile compounds. Helium (99.999% purity) was employed as the carrier gas at a constant flow rate of 1.0 mL/min. The injection volume was 1 μL with a split ratio of 1:10, and the injector temperature was set at 250 °C. The oven temperature was initially set at 50 °C (held for 2 minutes), then increased by 10 °C/min to 280 °C and held for 10 minutes, resulting in a total run time of

approximately 35 minutes. The MS detector operated in electron ionization (EI) mode at 70 eV, scanning a mass range of m/z 50–550. The ion source temperature was maintained at 230 °C. The obtained mass spectra and retention times were compared with entries in the Wiley-NIST mass spectral library for compound identification. The data were analyzed multiple times to verify the presence and quantity of the identified compounds. Depending on the solvent system, certain analytical parameters were adjusted as needed. In this study, compounds constituting at least 0.5% of the total composition were classified and reported as predominant components. The results obtained through this approach provide a comprehensive profile of the extract's fundamental chemical composition [42].

2.7 Statistical analysis

Data from three independent experiments for each antioxidant activity were reported as the mean ± standard deviation (SD). EC_{50} values were subsequently estimated through the Four-Parameter Logistic Regression method with a 95% confidence interval [43]. Statistical analyses were performed in R Studio **(**version 2024.09.0**)** using One-Way Analysis of Variance (ANOVA) and the Pearson correlation test. The level of statistical significance was set at $p \leq 0.05$.

3. RESULTS

3.1 Antimicrobial activity test

The ethanol extract of *P. lanceolata* was tested for antimicrobial activity against various bacterial and yeast strains using the disk diffusion method. Gentamicin and Tobramycin were employed as positive controls, and the inhibition zone measurements for extract-containing disks are provided in Tables 1–4. These antibiotics were included in the assay to facilitate comparative evaluation.

To evaluate the differences among independent trials, an ANOVA test was applied, resulting in a p-value of 0.00111. Since this value is below 0.05, it demonstrates a notable variation among the dose groups. However, Pearson correlation analysis revealed a low correlation coefficient ($r = 0.0365$, $p = 0.4491$) between extract concentration (50 microliters, 100 microliters, and 150 microliters) and inhibition zone diameter. This result suggests that the increase in extract concentration did not produce a clear dose-dependent effect on the inhibition zone.

TABLE 2. The disk diffusion method was employed to assess the antimicrobial response of food-isolated strains, with results recorded in millimeters. A value of (0.00±0.00) indicates no inhibition. Data are presented as mean ± standard deviation (n = 3), derived from three independent trials that yielded consistent results

Strains	50µL	100µL	150µL	Gentamicin	Tobramycin
Bacillus subtilis DSMZ 1971	7.33± 0.58	7.00± 0.00	7.33± 0.58	30.00± 0.00	26.00± 0.00
Candida albicans DSMZ 1386	7.33± 0.58	0.00± 0.00	8.00± 0.00	12.00± 0.00	13.00± 0.00
Enterobacter aerogenes ATCC 13048	0.00± 0.00	0.00± 0.00	0.00± 0.00	24.00± 0.00	18.00± 0.00
Enterococcus faecalis ATCC 29212	0.00± 0.00	0.00± 0.00	0.00± 0.00	12.00± 0.00	8.00± 0.00
Escherichia coli ATCC 25922	0.00± 0.00	0.00± 0.00	0.00± 0.00	22.00± 0.00	20.00± 0.00
Listeria monocytogenes ATCC 7644	0.00± 0.00	0.00± 0.00	0.00± 0.00	28.00± 0.00	24.00± 0.00
Pseudomonas aeruginosa DSMZ 50071	0.00± 0.00	0.00± 0.00	0.00± 0.00	15.00± 0.00	22.00± 0.00
Pseudomonas fluorescens P1	0.00± 0.00	0.00± 0.00	0.00± 0.00	13.00± 0.00	12.00± 0.00
Salmonella enteritidis ATCC 13076	7.00± 0.00	7.00± 0.00	7.33± 0.58	21.00± 0.00	20.00± 0.00
Salmonella typhimurium SL1344	0.00± 0.00	0.00± 0.00	0.00± 0.00	24.00± 0.00	15.00± 0.00
Staphylococcus aureus ATCC 25923	0.00± 0.00	0.00± 0.00	0.00± 0.00	21.00± 0.00	14.00± 0.00
Staphylococcus epidermidis DSMZ 20044	7.67± 0.58	9.00± 1.00	10.00± 1.00	22.00± 0.00	20.00± 0.00
Staphylococcus hominis ATCC 27844	8.33± 0.58	8.00± 1.00	9.00± 1.00	18.00± 0.00	16.00± 0.00
Staphylococcus warneri ATCC 27836	0.00± 0.00	0.00± 0.00	0.00± 0.00	23.00± 0.00	18.00± 0.00
Bacillus cereus RSKK 863	0.00± 0.00	0.00± 0.00	0.00± 0.00	24.00± 0.00	18.00± 0.00
Shigella flexneri RSKK 184	0.00± 0.00	0.00± 0.00	0.00± 0.00	18.00± 0.00	17.00± 0.00
Acinetobacter baumannii CECT 9111	0.00± 0.00	0.00± 0.00	0.00± 0.00	13.00± 0.00	22.00± 0.00

TABLE 2. The disk diffusion method was employed to assess the antimicrobial response of food-isolated strains, with results recorded in millimeters. A value of (0.00±0.00) indicates no inhibition. Data are presented as mean ± standard deviation (n = 3), derived from three independent trials that yielded consistent results

Strains	50µL	100µL	150µL	Gentamicin	Tobramycin
Enterococcus durans	0.00±0.00	0.00±0.00	0.00±0.00	11.00± 0.00	13.00± 0.00
Enterococcus faecium	0.00±0.00	0.00±0.00	0.00±0.00	28.00± 0.00	15.00± 0.00
Klebsiella pneumoniae	0.00±0.00	0.00±0.00	0.00±0.00	19.00± 0.00	23.00± 0.00
Listeria innocua	0.00±0.00	0.00±0.00	0.00±0.00	13.00± 0.00	15.00± 0.00
Salmonella infantis	0.00±0.00	0.00±0.00	0.00±0.00	17.00± 0.00	14.00± 0.00
Salmonella kentucky	0.00±0.00	0.00±0.00	0.00±0.00	12.00± 0.00	16.00± 0.00
Escherichia coli	0.00±0.00	0.00±0.00	0.00±0.00	0.00±0.00	0.00± 0.00

TABLE 3. The disk diffusion method was used to evaluate the antimicrobial response of clinically isolated strains, with results expressed in millimeters. A value of (0.00±0.00) signifies no inhibition. Data are presented as mean ± standard deviation (n = 3), based on three independent trials that demonstrated consistent results

Strains	50µL	100µL	150µL	Gentamicin	Tobramycin
Staphylococcus aureus	7.67±0.58	9.00±1	10.00±0.00	22.00± 0.00	18.00± 0.00
Streptococcus mutans	7.00±0.00	8.00±0.00	9.00±5.20	22.00± 0.00	24.00± 0.00
Staphylococcus hominis	0.00±0.00	0.00±0.00	0.00±0.00	9.00± 0.00	11.00± 0.00
Staphylococcus haemolyticus	0.00±0.00	7.00±0.00	8.00±0.00	10.00± 0.00	10.00± 0.00
Staphylococcus lugdunensis	0.00±0.00	0.00±0.00	0.00±0.00	17.00± 0.00	18.00± 0.00
Shigella boydi	0.00±0.00	0.00±0.00	0.00±0.00	20.00± 0.00	18.00± 0.00
Acinetobacter baumannii	0.00±0.00	0.00±0.00	0.00±0.00	18.00± 0.00	16.00± 0.00
Shigella flexneri	0.00±0.00	0.00±0.00	0.00±0.00	16.00± 0.00	14.00± 0.00
Staphylococcus aureus	0.00±0.00	0.00±0.00	0.00±0.00	22.00± 0.00	16.00± 0.00
Enterococcus faecalis	8.33±0.58	9.00±1	9.67±0.58	12.00± 0.00	10.00± 0.00
Klebsiella pneumoniae	0.00±0.00	0.00±0.00	0.00±0.00	18.00± 0.00	18.00± 0.00
Candida tropicalis	0.00±0.00	0.00±0.00	0.00±0.00	0.00± 0.00	0.00± 0.00
Candida glabrata	0.00±0.00	0.00±0.00	0.00±0.00	7.00± 0.00	8.00± 0.00

TABLE 4. The disk diffusion method was employed to evaluate the antimicrobial activity against multi-drug-resistant strains, with results expressed in millimeters. A value of (0.00±0.00) denotes the absence of inhibition. Data are reported as mean ± standard deviation (n = 3), based on three separate trials that yielded consistent results

Strains	50µL	100µL	150µL	Gentamicin	Tobramycin
Escherichia coli	0.00± 0.00	0.00± 0.00	0.00± 0.00	8.00± 0.00	9.00± 0.00
Klebsiella pneumoniae	8.33± 0.58	8.00± 0.00	8.00± 1.00	15.00± 0.00	20.00± 0.00
Acinetobacter baumannii	0.00± 0.00	0.00± 0.00	0.00± 0.00	0.00± 0.00	0.00± 0.00
Enterobacter aerogenes	0.00± 0.00	0.00± 0.00	0.00± 0.00	16.00± 0.00	18.00± 0.00
Serratia odorifera	0.00± 0.00	0.00± 0.00	0.00± 0.00	7.00± 0.00	9.00± 0.00
Proteus vulgaris	0.00± 0.00	0.00± 0.00	0.00± 0.00	11.00± 0.00	11.00± 0.00
Streptococcus pneumonia	0.00± 0,00	0.00± 0.00	0.00± 0.00	10.00± 0.00	8.00± 0.00
Staphylococcus aureus MRSA	9.33± 0.58	10.00± 1.00	11.00± 0.00	0.00± 0.00	7.00± 0.00
Staphylococcus aureus MRSA+MDR	10.00± 1.00	11.00± 0.00	11.67± 0.58	22.00± 0.00	21.00± 0.00
Providencia rustigianii	0.00± 0.00	0.00± 0.00	0.00± 0.00	16.00± 0.00	19.00± 0.00
Achromobacter sp.	8.00± 0.00	9.00± 0.00	9.67± 0.58	9.00± 0.00	0.00± 0.00

These results indicate that *P. lanceolata* ethanol extract exhibited inhibition effects against 13 out of 48 tested strains, demonstrating significant antimicrobial activity against specific microorganisms. Among standard isolated bacteria (Table 1), *S. epidermidis* DSMZ 20044 showed a 10 mm inhibition zone, while *S. hominis* ATCC 27844 exhibited a 9 mm inhibition zone. No antimicrobial activity was observed among food isolated strains (Table 2). In clinical isolates (Table 3), the highest inhibition zone was recorded for *S. aureus*, measuring 10 mm. Among multidrug-resistant (MDR) strains (Table 4), *S. aureus* MRSA, *S. aureus* MRSA+MDR, and *Achromobacter* sp. showed the greatest sensitivity to the applied extract concentrations. However, the extract's efficacy varied among different microorganisms, emphasizing the importance of strain-specific susceptibility.

TABLE 5. Evaluation of MIC, MBC, and MFC values of *P. lanceolata*: Unveiling its antimicrobial and antifungal efficacy

Strains	**MIC (mg/ml)**	**MBC/MFC (mg/ml)**
Bacillus subtilis DSMZ 1971	> 22,867	> 22,867
Candida albicans DSMZ 1386	> 22,867	> 22,867
Salmonella enteritidis ATCC 13076	> 22,867	> 22,867
Staphylococcus epidermidis DSMZ 20044	> 22,867	> 22,867
Staphylococcus hominis ATCC 27844	> 22,867	> 22,867
Klebsiella pneumoniae	> 22,867	> 22,867
Staphylococcus aureus MRSA	0,175	0,179
Staphylococcus aureus MRSA +MDR	5,717	5,717
Achromobacter sp.	> 22,867	> 22,867
Staphylococcus aureus	0,175	0,715
Streptococcus mutans	0,175	0,179
Staphylococcus haemolyticus	0,175	11,433
Enterococcus faecalis	> 22,867	> 22,867

MIC and MBC values were also determined (Table 5). MIC values varied between, 0.175 to 22.867 milligrams per milliliter. The microorganisms with the lowest MIC values were *S. aureus* MRSA, *S. aureus*, *S. mutans*, and *S. haemolyticus*, each with an MIC of 0.175 mg/mL. MBC values ranged between 0.179 and 11.433 mg/mL. Notably, *S. aureus* MRSA and *S. mutans* exhibited the lowest MBC values (0.179 mg/mL), indicating high susceptibility to bactericidal effects. For other strains, such as *B. subtilis* DSMZ 1971, *S. epidermidis* DSMZ 20044, and *C. albicans* DSMZ 1386, MIC and MBC values were recorded as >22.867 mg/mL, suggesting that the required extract concentration for antimicrobial activity exceeded the tested range.

These findings demonstrate that *P. lanceolata* ethanol extract is effective against *S. aureus* MRSA, *S. mutans*, and *S. haemolyticus* even at low concentrations. The notable antimicrobial effect detected at minimal concentrations indicates that *P. lanceolata* could be a strong natural antimicrobial agent.

3.2 Anti-biofilm activity

The antibiofilm activity of *P. lanceolata* ethanol extract against different bacterial strains was evaluated. Biofilm activity was determined through OD550 absorbance measurements, and percentage changes were calculated relative to the control group. This research evaluated the antibiofilm activity of the tested plant solution against various bacterial species.

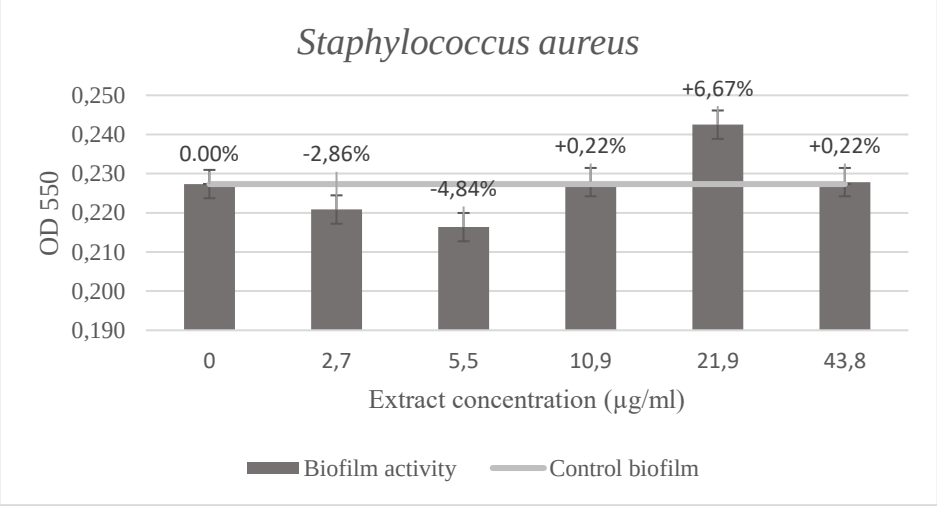

FIGURE 1. Effects of *Plantago lanceolata* on inhibition of biofilm formation. The line is normal amount of biofilm observed-positive controls. *S. aureus* from clinically isolated strain

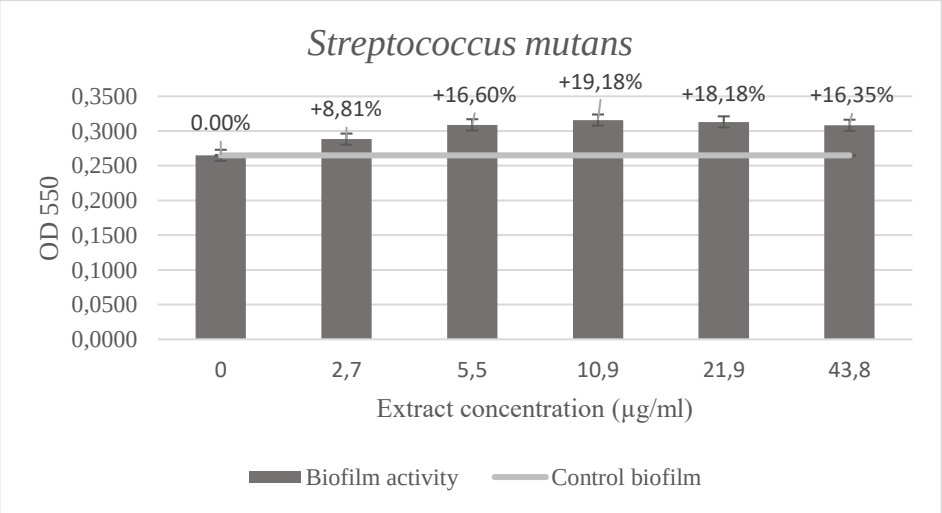

FIGURE 2. Impact of *Plantago lanceolata* on Biofilm Development Inhibition. The line is normal amount of biofilm observed-positive controls. *S. mutans* from clinically isolated strain

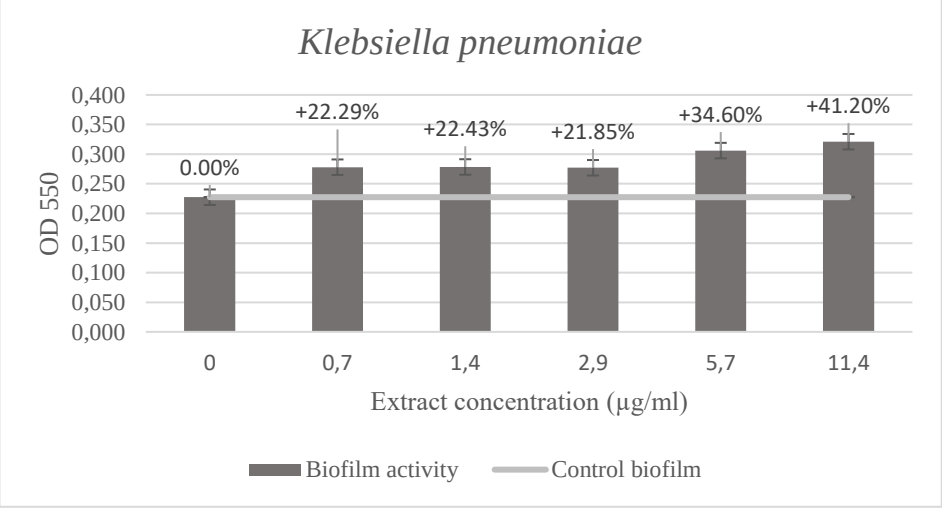

FIGURE 3. Impact of *Plantago lanceolata* on Biofilm Development Inhibition. The line is normal amount of biofilm observed-positive controls. *K. pneumoniae* from strains with multi-drug resistance

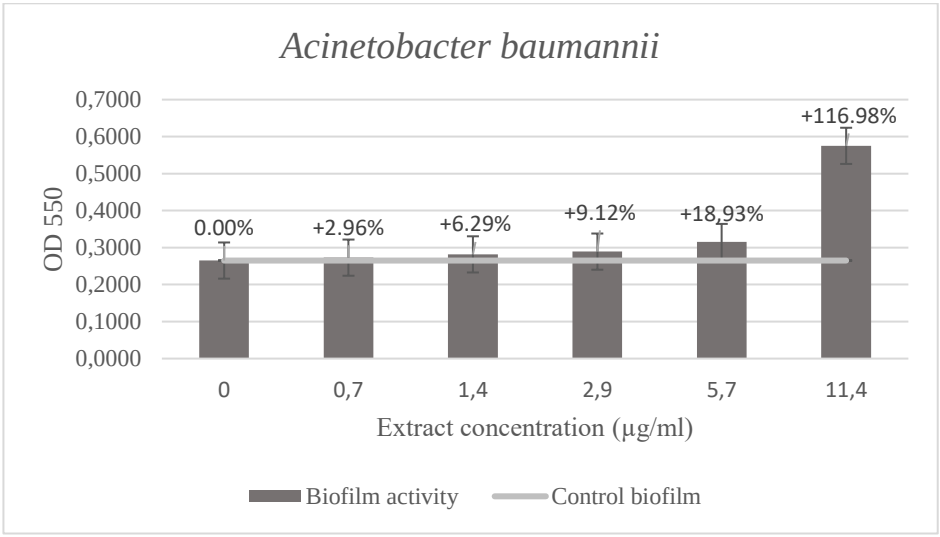

FIGURE 4. Impact of *Plantago lanceolata* on Biofilm Development Inhibition. The line is normal amount of biofilm observed-positive controls. *A. baumannii* from strains with multi-drug resistance

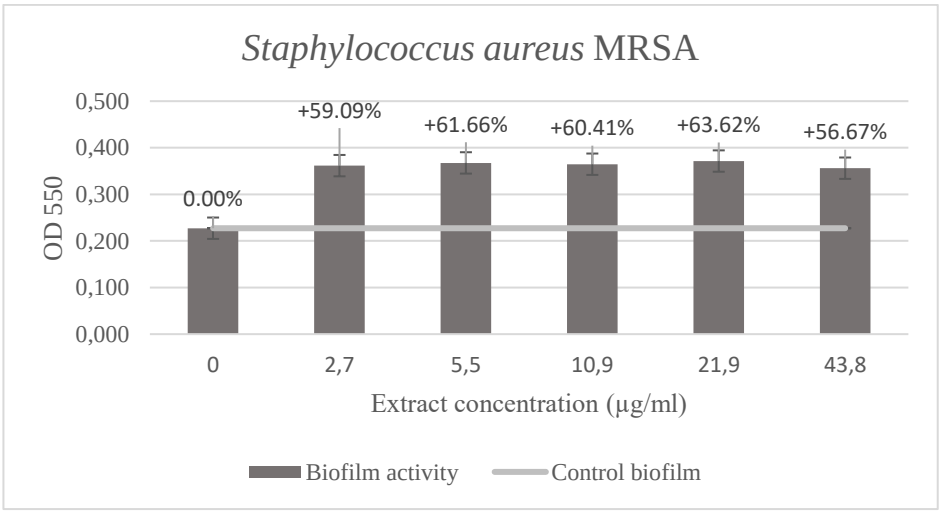

FIGURE 5. Impact of *Plantago lanceolata* on Biofilm Development Inhibition. The line is normal amount of biofilm observed-positive controls. *S. aureus* MRSA from strains with multi-drug resistance

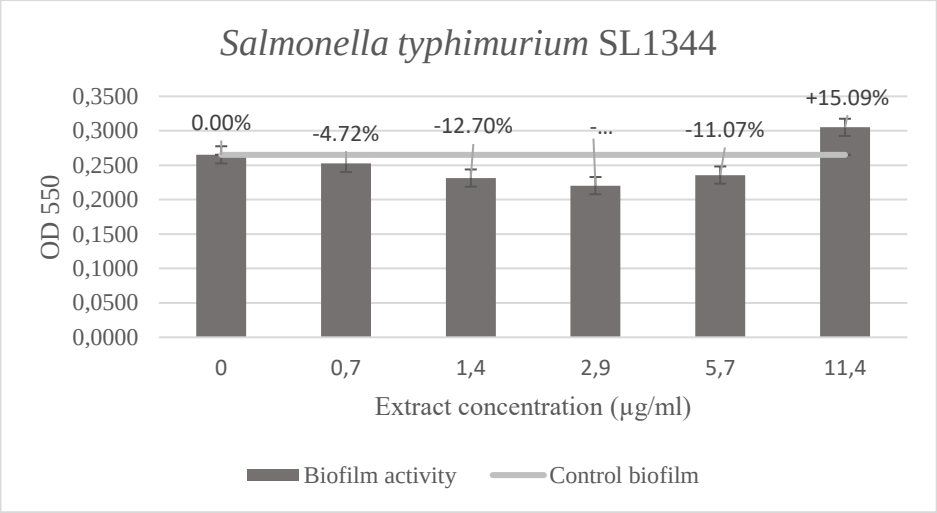

FIGURE 6. Effects of *Plantago lanceolata* on inhibition of biofilm formation. The line is normal amount of biofilm observed-positive controls. *S. typhimurium* SL1344 from standart isolates

In *S. aureus* (Figure 1) and *S. typhimurium* SL1344 (Figure 6) strains, biofilm inhibition was observed at lower extract concentrations, whereas an increase in biofilm formation was recorded at higher concentrations. Specifically, in *S. aureus*, biofilm production decreased by 4.84% at 5.5 µg/mL, while an increase of 6.67% was observed at 21.9 µg/mL. Similarly, *S. typhimurium* was the only strain where biofilm formation was suppressed at lower concentrations (16.86% reduction), yet at the highest concentration, biofilm production increased by 15.09%. These findings indicate that the solution may act in a dose-dependent manner, demonstrating antibiofilm properties at low concentrations while potentially promoting biofilm formation once specific threshold concentrations are exceeded.

In contrast, *S. mutans* (Figure 2), *K. pneumoniae* (Figure 3), *A. baumannii* (Figure 4), and methicillin-resistant *S. aureus* (MRSA) (Figure 5) exhibited a significant increase in biofilm formation upon treatment with the extract. The highest increase in *S. mutans* was observed at 10.9 µg/mL (19.18%), while in *K. pneumoniae*, biofilm production increased by 41.20% at 11.4 µg/mL. In the Gram-negative pathogen *A. baumannii*, biofilm formation dramatically increased by 116.98% at 11.4 µg/mL. Similarly, in *S. aureus* MRSA, biofilm activity significantly increased across all tested concentrations, with a 61.66% increase at 5.5 µg/mL and reaching 63.62% at 21.9 µg/mL.

These findings suggest that *P. lanceolata* extract may induce different biofilm responses depending on the bacterial species and applied concentration.

3.3 Antioxidant activity

The antioxidant activity of *P. lanceolata* ethanol extract was measured using the DPPH free radical neutralization test. Ascorbic acid was employed as the positive control, and ethanol without the extract was used as the negative control.

TABLE 6. DPPH free radical neutralization activity of *Plantago lanceolata* ethanol extract and ascorbic acid (%) expressed as mean ± SD

Concentration (µg/mL)	**DPPH Radical Neutralization Activity of *P. lanceolata* (%)**	**DPPH Radical Neutralization Activity of Ascorbic Acid (%)**
1000	62.70 ± 0.21	94.70 ± 0.00
500	60.80 ± 0.56	94.30 ± 0.05
250	63.20 ± 1.01	92.40 ± 0.01
125	41.00 ± 1.87	91.00 ± 0.01
62.5	23.40 ± 6.91	73.00 ± 0.04
31.25	18.90 ± 2.65	40.20 ± 0.07
15.625	10.60 ± 1.71	23.20 ± 0.27
7.81	0.51 ± 1.14	11.80 ± 0.04

Upon examining the antioxidant activity of the extract, the highest inhibition rate was determined to be 62.7% ± 0.21. Furthermore, the EC_{50} value was determined to be 0.0858 milligrams per milliliter. In contrast, the EC_{50} value of ascorbic acid was determined to be 0.04 milligrams per milliliter, indicating that the antioxidant capacity of the extract is lower than that of ascorbic acid. To assess the statistical significance of differences between concentrations, an ANOVA test was conducted, yielding a *p*-value of $p < 2 \times 10^{-16}$. This outcome confirms a statistically significant difference between ascorbic acid and the extract. Furthermore, Pearson correlation analysis was conducted to assess the correlation between extract concentration and DPPH scavenging activity, yielding an r value of 0.753 ($p = 2.335 \times 10^{-14}$). This strong positive correlation indicates that as the extract concentration increases, the ability to neutralize DPPH radicals increases proportionally. In conclusion, while *P. lanceolata* ethanol extract exhibits notable antioxidant activity, its efficacy is not as strong as that of ascorbic acid. However, a significant increase in antioxidant capacity was observed with increasing extract concentrations.

3.4 Biochemical composition analysis (GC-MS)

The biochemical profile of the *P. lanceolata* ethanol extract was examined through GC-MS analysis. Compounds present in concentrations above 0.5% were categorized as primary components. Table 7 outlines the identified chemical constituents, including their chemical structure, molecular formula, and molecular weight.

TABLE 7. GC-MS analysis of *Plantago lanceolata* ethanol extract profile

Retention Time	Area %	Compound Name	Formula	Molecular Weight (g/mol)
35.005	0.31	Myristic acid	$C_{14}H_{28}O_2$	228.37
36.532	4.10	Neophytadiene	$C_{20}H_{38}$	278.50
39.794	17.95	Hexadecanoic acid	$C_{16}H_{32}O_2$	256.42
44.189	5.14	Linoleic Acid	$C_{18}H_{32}O_2$	280.40
44.357	26.46	Linolenic Acid	$C_{18}H_{30}O_2$	278.40
44.484	7.95	Linolenyl alcohol	$C_{18}H_{32}O$	264.40
44.621	26.37	Linolenic Acid	$C_{18}H_{30}O_2$	278.40
44.881	4.64	cis,cis,cis-7,10,13-Hexadecatrienal	$C_{16}H_{26}O$	234.38
45.208	2.26	Octadecanoic acid	$C_{18}H_{36}O_2$	284.5
47.906	0.19	Sorbitol	$C_6H_{14}O_6$	182.17
49.331	0.26	Eicosanoic acid	$C_{20}H_{40}O_2$	312.5
53.985	0.34	Docosanoic acid	$C_{22}H_{44}O_2$	340.6
56.723	0.22	Eicosane	$C_{20}H_{42}$	282.5
65.710	0.32	1-Nonadecene	$C_{19}H_{38}$	266.5
70.871	0.23	1-Docosene	$C_{22}H_{44}$	308.6
72.875	0.61	Phytyl stearate	$C_{38}H_{74}O_2$	563.0

The major components identified in the GC-MS analysis were Neophytadiene ($C_{20}H_{38}$) – 4.10%, Hexadecanoic acid ($C_{16}H_{32}O_2$, Palmitic Acid) – 17.95%, and Linolenic acid ($C_{18}H_{30}O_2$) – 52.83%, as detailed in Table 7.

This analysis indicates that *P. lanceolata* ethanol extract possesses a composition rich in lipid derivatives and fatty acids. Notably, hexadecanoic acid is a well-known compound with reported antimicrobial and antioxidant properties [44].

Among the compounds identified in the GC-MS analysis, sorbitol ($C_6H_{14}O_6$) was detected at 0.19%. Sorbitol metabolism plays a crucial role in plants as a sugar

alcohol with various biological functions [45]. It is involved in the plant's defense mechanisms against environmental stress factors. To sum up, the major components identified in *P. lanceolata* ethanol extract provide significant insights into the plant's potential pharmacological and biological activities.

4. DISCUSSION

Bacteria pose significant risks in the modern world and have become one of the greatest threats of our time. The resistance mechanisms that bacteria have developed against antibiotics and antimicrobial agents have driven scientists to focus on discovering novel antimicrobial compounds. In this search for alternative bioactive compounds, plants play a crucial role. Plants contain important biochemical compounds that contribute to various physiological and ecological processes, including environmental adaptation. These biochemical compounds, classified as secondary metabolites, exhibit diverse biological properties, including antimicrobial, antioxidant activities [46].

Our comprehensive study on *P. lanceolata* offers an in-depth evaluation of its antimicrobial, antibiofilm, and antioxidant properties. The results of the chemical composition analysis offer valuable insights into the plant's potential antimicrobial and antioxidant effects. The findings align with previous studies in existing literature, further supporting the pharmacological capability of *P. lanceolata*. This study was conducted using a broad-spectrum microorganism collection, ensuring a comprehensive evaluation of its bioactive properties.

The antimicrobial activity of *P. lanceolata* ethanol extract was initially evaluated using the disk diffusion test. To ensure the consistency of the results across replicates, ANOVA statistical analysis was performed, yielding a *p*-value of 0.00111. This result indicates a statistically significant similarity among repeated replicates. The correlation coefficient between the extract doses (50 microliters, 100 microliters, and 150 microliters) and inhibition zone diameters was found to be low, suggesting that increasing extract concentration did not have a clear dose-dependent effect on inhibition zones. The extract was tested against 48 microorganism strains, with the most pronounced inhibitory effects observed among multidrug-resistant and clinically relevant strains. *P. lanceolata* extract exhibited the highest antimicrobial effectiveness against multidrug-resistant *S. aureus* MRSA+MDR, forming a 12 mm inhibition zone, while among clinical isolates, it demonstrated a 10 mm inhibition zone against *E. faecalis***.** The Gram-positive bacterium *S. aureus* has shown significant susceptibility to *P. lanceolata* in previous studies [47]. A study in existing literature investigated the differences in the antimicrobial effectiveness of *P. lanceolata* extracts prepared using different solvents. The results demonstrated that the same bacterial strains exhibited varying susceptibilities depending on the solvent used [48]. Antimicrobial activity studies with different solvents are conducted to explore how each solvent's unique chemical properties influence the extraction and bioactivity of plant compounds.

In antimicrobial activity assays, bacterial growth in response to varying concentrations of the plant extract was assessed using the MIC test. The obtained results showed that the extract displayed strong antimicrobial activity against specific microorganisms. Among the tested strains, the most susceptible bacteria were multidrug-resistant *S. aureus* MRSA, clinically isolated *S. aureus*, and *S. haemolyticus*, with an MIC of 0.175 milligrams per milliliter. This finding indicates that *P. lanceolata* extract is effective against these strains even at low concentrations. Evaluation of the MBC test revealed that the MBC value for *S. aureus* MRSA and *S. mutans* was 0.179 mg/mL, suggesting strong bactericidal activity. In contrast, the MIC value for *S. haemolyticus* was recorded as 11.433 mg/mL, indicating a higher concentration requirement for antimicrobial efficacy against this strain. The observation of low MIC and MBC values against antibiotic-resistant strains such as *S. aureus* MRSA suggests that the plant extract has potential for further investigation as an antimicrobial agent. Among the standard strains, microorganisms such as *B. subtilis* DSMZ 1971 and *S. enteritidis* ATCC 13076 exhibited resistance beyond the tested extract concentrations.

The results obtained from the MIC and MBC experiments indicate that the antimicrobial activity of *P. lanceolata* extract aligns with findings from previous studies in the literature [48]. Similarly, studies available have explored the antimicrobial properties of other members of the *Plantaginaceae* family, such as *P. lanceolata* and *P. major*. The findings suggest that the presence of antioxidant activity within this plant family may contribute to its potential applications in various fields [49].

The antibiofilm activity of *P. lanceolata* ethanol extract was evaluated against different microorganism strains, revealing that biofilm inhibition varied with the type of bacterial species and extract concentration. The analyses indicated that the extract exhibited a selective effect on biofilm inhibition. While biofilm suppression was observed at low concentrations in certain strains, such as clinically isolated *S. aureus* and standard strain *S. typhimurium* SL1344, an increase in biofilm formation was detected in pathogenic strains including *S. mutans*, *K. pneumoniae*, *A. baumannii*, and *S. aureus* MRSA.

The presence of saturated fatty acids detected in the GC-MS analysis was investigated because of their potential influence on biofilm formation, which may be either positively or negatively affected. This effect appears to be dependent on environmental conditions [50]. The findings suggest that *P. lanceolata* extract exhibits a selective effect on biofilm inhibition, acting as a suppressor in some bacterial species while promoting biofilm formation in others. Research has examined the antimicrobial properties of species within the *Plantago* genus. Studies have examined how extracts obtained from different plant organs using various solvents can influence biofilm formation in bacteria, highlighting the impact of solvent selection on antimicrobial activity [51]. In the literature, the antibiofilm activity of *P. lanceolata* extract has been investigated

against *K. pneumoniae* and *E. coli* bacteria [52]. In our antibiofilm study, the analysis of multidrug-resistant strains suggested the presence of certain factors that may promote biofilm formation. This finding provides a valuable contribution to the literature by offering a deeper understanding of the biofilm-modulating effects of *P. lanceolata* extract.

The antioxidant property of *P. lanceolata* ethanol extract was assessed using the DPPH assay. The free radical neutralization capacity of DPPH was compared with that of vitamin C (ascorbic acid). The results showed that the extract exhibited antioxidant activity, although its effectiveness was less than ascorbic acid. To quantify the antioxidant activity, the EC_{50} value was used. The EC_{50} represents the concentration of the plant extract needed to neutralize half of the DPPH free radicals. The EC_{50} value of *P. lanceolata* ethanol extract was determined as 0.0858 mg/mL, whereas for ascorbic acid, this value was 0.0400 mg/mL. The higher EC_{50} value of the plant extract indicates that a higher amount is needed to produce the same antioxidant effect as ascorbic acid.

To determine whether the antioxidant activity of *P. lanceolata* extract is concentration-dependent, Pearson correlation analysis was performed, yielding an r value of 0.753 ($p < 0.0001$). This strong positive correlation indicates that as the concentration of the extract rises, the DPPH scavenging capacity also increases proportionally. Additionally, ANOVA analysis confirmed statistically significant differences among the different extract concentrations.

While ascorbic acid is identified as a pure compound, the plant extract exhibits a complex composition. Antioxidant effects can occur in synergistic or antagonistic interactions among its constituents. This suggests that the bioactivity of *P. lanceolata* extract could be enhanced through the isolation of its compounds into purer fractions. *P. lanceolata* extract presents potential as a natural antioxidant source.

Several studies have assessed the antioxidant capacity of *P. lanceolata* obtained from different sources using the DPPH assay [53]. The obtained results indicated that *P. lanceolata* extracts from different locations exhibited varying antioxidant activities. In the literature, the total antioxidant capacity of *P. lanceolata* extracts has been measured using both the DPPH and ABTS assays [54]. These studies suggest that the antioxidant activity of *P. lanceolata* has potential applications in various fields.

The biochemical profiling of *P. lanceolata* ethanol extract was analyzed using GC-MS. The results indicated that the extract primarily consists of lipid derivatives, fatty acids, aliphatic hydrocarbons, and terpenoids. A study in the literature [55] reported the presence of fatty acids in *P. lanceolata* extract based on GC-MS analysis. Among the dominant components, fatty acids such as linolenic acid ($C_{18}H_{30}O_2$) (26.46% and 26.37%) and hexadecanoic acid ($C_{16}H_{32}O_2$, palmitic acid) (17.95%) were identified. Linolenic acid has previously been shown to exhibit strong antioxidant, cardiovascular protective

effects [56]. Hexadecanoic acid, detected in the GC-MS analysis, is a fatty acid known for its antibacterial properties [57]. The compound has been reported to exhibit antibacterial effects against pathogens such as *S. aureus* and *P. aeruginosa*. In our study, the low MIC values observed against *S. aureus* MRSA and *S. mutans* may be associated with the presence of this compound. Additionally, Neophytadiene ($C_{20}H_{38}$) (4.10%) has been documented in the literature as a compound capable of inhibiting biofilm formation in certain bacterial species [58]. This compound is considered a significant secondary metabolite with the potential to contribute to the inhibitory effects observed in plant extracts against microorganisms. The results suggest that the components identified in the GC-MS analysis of *P. lanceolata* ethanol extract may be associated with its antioxidant and antimicrobial activities.

According to the literature, P. lanceolata is a plant with high drought tolerance, fast growth and deep rooting [59]. Plantago lanceolata's tolerance to drought conditions and deep rooting ability make it an important candidate for forage production and environmental sustainability. The inhibitory effect of aucubin compound on nitrification in the soil indicates the potential of this species to reduce nitrogen losses and N_2O emissions. The genotype and seasonal variability of aucubin content in leaves and roots reveals the importance of genotype selection for this purpose [60].

5. CONCLUSIONS

As a poster with the title “Antimicrobial Activity of *Plantago lanceolata* L. (Ribwort Plantain) with Ethnobotanical Significance” a part of this study was presented in International Congress of New Searches in Multidisciplinary Studies. This study extends the findings summarized in our presentation 'Antimicrobial Activity of *Plantago lanceolata* L. (Ribwort Plantain) with Ethnobotanical Significance' by analyzing them in more detail and compares them with existing information in the literature.

This study extends the findings summarized in our presentation 'Antimicrobial Activity of *Plantago lanceolata* L. (Ribwort Plantain) with Ethnobotanical Significance' by analyzing them in more detail and compares them with existing information in the literature.

This study demonstrates that *Plantago lanceolata* L. possesses antimicrobial, antibiofilm, and antioxidant properties. The plant extract exhibited significant antimicrobial activity, particularly against *S. aureus* MRSA, *S. mutans*, and *S. aureus* MRSA+MDR strains. The antioxidant capacity, determined by the DPPH assay, indicated a strong free radical scavenging potential.

GC-MS analysis revealed a volatile compound profile rich in fatty acid derivatives, particularly linolenic acid and hexadecenoic acid. The study employed a broad-spectrum microorganism collection, contributing valuable

data to the literature. The findings suggest that *P. lanceolata* represents a promising natural resource for pharmaceutical, food, and cosmetic applications.

Acknowledgement This study was funded by the TÜBİTAK 2209 project.

Author Contribution Statements Idea/Concept: ME, DT, AB, KC; Conceptualization and design: ME, DT, AB, KC; Auditing consulting: DT, EG, ED; References: AB, KC; Materials: EG, ED, GG; Data Collection and/or processing: ME, DT, KC, EG; Analysis and/or interpretation: ME, DT, KC; Literature search: ME, KC, EG, ED, GG; Writing: ME, DT; Critical review: DT, KC, AB.

Declaration of Competing Interests The authors declare that there is no conflict of interest related to the content of this study.

Ethical Statement This research did not involve human participants or animals. Therefore, no ethical approval was required.

Use of Artificial Intelligence No artificial intelligence-based tools or applications were used in the preparation of this study. The entire content of the study was produced by the author(s) in accordance with scientific research methods and academic ethical principles.

REFERENCES

[1] Flint, H.J., Why Gut Microbes Matter. Springer International Publishing: Aberdeen, UK, 2020. https://doi.org/10.1007/978-3-030-43246-1

[2] Soni, J., Sinha, S., Pandey, R., Understanding bacterial pathogenicity: a closer look at the journey of harmful microbes. *Frontiers in Microbiology*, 15 (2024). https://doi.org/10.3389/fmicb.2024.1370818

[3] Panthee, B., Gyawali, S., Panthee, P., Techato, K., Environmental and Human Microbiome for Health. *Life*, 12 (2022). https://doi.org/10.3390/life12030456

[4] Ryan, M.P., Sevjahova, L., Gorman, R., White, S., The Emergence of the Genus Comamonas as Important Opportunistic Pathogens. *Pathogens*, 11 (2022), 1032. https://doi.org/10.3390/pathogens11091032

[5] Urban-Chmiel, R., Marek, A., Stępień-Pyśniak, D., Wieczorek, K., Dec, M., Nowaczek, A., Osek, J., Antibiotic Resistance in Bacteria—A Review. *Antibiotics*, 11 (2022), 1079. https://doi.org/10.3390/antibiotics11081079

[6] Zhang, F., Cheng, W., The Mechanism of Bacterial Resistance and Potential Bacteriostatic Strategies. *Antibiotics*, 11 (2022), 1215. https://doi.org/10.3390/antibiotics11091215

[7] WHO, WHO's first global report on antibiotic resistance reveals serious, worldwide threat to public health, WHO: Geneva, 2014. https://www.who.int/southeastasia/news/detail/30-04-2014-who-s-first-global-report-on-antibiotic-resistance-reveals-serious-worldwide-threat-to-public-health.

[8] Canlı, K., Yetgin, A., Benek, A., Bozyel, M.E., Murat Altuner, E., *In Vitro* Antimicrobial Activity Screening of Ethanol Extract of *Lavandula stoechas* and Investigation of Its Biochemical Composition. *Advances in Pharmacological Sciences*, (2019). https://doi.org/10.1155/2019/3201458

[9] Aslam, B., Wang, W., Arshad, M.I., Khurshid, M., Muzammil, S., Rasool, M.H., Nisar, M.A., Alvi, R.F., Aslam, M.A., Qamar, M.U., Salamat, M.K.F., Baloch, Z., Antibiotic resistance: a rundown of a global crisis. *Infection and Drug Resistance*, 11(2018), 1645–1658. http://dx.doi.org/10.2147/IDR.S173867

[10] Centers for Disease Control and Prevention (CDC), *Antibiotic Resistance Threats in the United States*. CDC: Atlanta, Georgia, 2019. Available online: https://www.cdc.gov/antimicrobial-resistance/data-research/threats/index.html

[11] Giacomini, E., Perrone, V., Alessandrini, D., Paoli, D., Nappi, C., Degli Esposti, L., Evidence of Antibiotic Resistance from Population-Based Studies: A Narrative Review. *Infection and Drug Resistance*, 14 (2021). http://doi.org/10.2147/IDR.S289741

[12] Baran, A., Kwiatkowska, A., Potocki, L., Antibiotics and Bacterial Resistance—A Short Story of an Endless Arms Race. *International Journal of Molecular Sciences*, 24 (2023), 5777. https://doi.org/10.3390/ijms24065777

[13] Breijyeh, Z., Jubeh, B., Karaman, R., Resistance of Gram-Negative Bacteria to Current Antibacterial Agents and Approaches to Resolve It. *Molecules*, 25 (2020), 1340. https://doi.org/10.3390/molecules25061340

[14] Canlı, K., Turu, D., Benek, A., Bozyel, M.E., Şimşek, Ö., Altuner, E.M., Biochemical and Antioxidant Properties as well as Antimicrobial and Antibiofilm Activities of Allium scorodoprasum subsp. jajlae (Vved.) Stearn. *Current Issues in Molecular Biology*, 45 (2023), 4970–4984. https://doi.org/10.3390/cimb45060316

[15] Bailly, C., Traditional uses, pharmacology and phytochemistry of the medicinal plant *Flueggea virosa* (*Roxb. ex Willd.*) *Royle*. *Future Pharmacology*, 4 (2024), 77–102. https://doi.org/10.3390/futurepharmacol4010007

[16] Yazarlu, O., Iranshahi, M., Kashani, H.R.K., Reshadat, S., Habtemariam, S., Iranshahy, M., Hasanpour, M., Perspective on the application of medicinal plants and natural products in wound healing: A mechanistic review. *Pharmacological Research*, 174 (2021), 105841. https://doi.org/10.1016/j.phrs.2021.105841

[17] Salmerón-Manzano, E., Garrido-Cardenas, J.A., Manzano-Agugliaro, F., Worldwide research trends on medicinal plants. *International Journal of Environmental Research and Public Health*, 17 (2020), 3376. https://doi.org/10.3390/ijerph17103376

[18] Angelini, P., Plant-derived antimicrobials and their crucial role in combating antimicrobial resistance. *Antibiotics*, 13 (2024), 746. https://doi.org/10.3390/antibiotics13080746

[19] Turu, D., Bozyel, M.E., Candan, K., Yakan, M.A., Benek, A., Canlı, K., In vitro antimicrobial and antioxidant activities of *Pyracantha coccinea* fruits ethanol extract. *International Journal of Academic Multidisciplinary Research*, 4 (2020).

[20] Xu, Z., Ullah, N., Duan, Y., Hou, Z., Liu, A., Xu, L., Editorial: Plant secondary metabolites and their effects on environmental adaptation based on functional genomics. *Frontiers in Genetics*, 14 (2023). https://doi.org/10.3389/fgene.2023.1211639

[21] Bozkurt, S.D., Turu, D., Gül, G., Yaman, C., Benek, A., Canlı, K., Determination of antioxidant activity and biochemical content of *Homalothecium philippeanum* (*Spruce*) *Schimp. Anatolian Bryology*, 10 (2024), 169–178. https://doi.org/10.26672/anatolianbryology.1576833

[22] Ji, X., Hou, C., Guo, X., Physicochemical properties, structures, bioactivities and future prospective for polysaccharides from *Plantago* L. (*Plantaginaceae*): A review. *International Journal of Biological Macromolecules*, 135 (2019), 637–646. https://doi.org/10.1016/j.ijbiomac.2019.05.211

[23] Kolak, U., Boğa, M., Uruşak, E.A., Ulubelen, A., Constituents of *Plantago major* subsp. *intermedia* with antioxidant and anticholinesterase capacities. *Turkish Journal of Chemistry*, (2011). https://doi.org/10.3906/kim-1102-990

[24] Gonçalves, S., Romano, A., The medicinal potential of plants from the genus *Plantago* (*Plantaginaceae*). *Industrial Crops and Products*, 83 (2016), 213–226. https://doi.org/10.1016/j.indcrop.2015.12.038

[25] Pol, M., Schmidtke, K., Lewandowska, S., *Plantago lanceolata* – An overview of its agronomically and healing valuable features. *Open Agriculture*, 6 (2021), 479–488. https://doi.org/10.1515/opag-2021-0035

[26] Bahadori, M.B., Sarikurkcu, C., Kocak, M.S., Calapoglu, M., Uren, M.C., Ceylan, O., *Plantago lanceolata* as a source of health-beneficial phytochemicals: Phenolics profile and antioxidant capacity. *Food Bioscience*, 34 (2020), 100536. https://doi.org/10.1016/j.fbio.2020.100536

[27] Abate, L., Bachheti, R.K., Tadesse, M.G., Bachheti, A., Ethnobotanical uses, chemical constituents, and application of *Plantago lanceolata* L. *Journal of Chemistry*, 2022 (2022), 1–17. https://doi.org/10.1155/2022/1532031

[28] Ranjbari, A., Nazer, M., A review of medicinal plants effective on wound healing in the western part of Iran based on ethnobotanical documents. *Plant Biotechnology Persa*, 6 (2024), 88–92. https://doi.org/10.61186/pbp.6.1.88

[29] Abate, L., Bachheti, R.K., Tadesse, M.G., Bachheti, A., Ethnobotanical uses, chemical constituents, and application of Plantago lanceolata L. *Journal of Chemistry*, 2022 (2022), 1532031. https://doi.org/10.1155/2022/1532031

[30] Jiru, T.M., Getahun, M., Antifungal activity of *Plantago lanceolata* and *Sida ovata* leaf extracts against dermatomycotic fungi. *Evidence-Based Complementary and Alternative Medicine*, (2023), 9957892. https://doi.org/10.1155/2023/9957892

[31] Laanet, P.R., Bragina, O., Jõul, P., Vaher, M., *Plantago major* and *Plantago lanceolata* Exhibit Antioxidant and *Borrelia burgdorferi* Inhibiting Activities. *International Journal of Molecular Sciences*, *25* (2024), 7112. https://doi.org/10.3390/ijms25137112

[32] Murat Altuner, E., Canlı, K., Akata, I., Antimicrobial screening of *Calliergonella cuspidata, Dicranum polysetum* and *Hypnum cupressiforme*. *Journal of Pure and Applied Microbiology*, 8 (2014).

[33] Benek, A., Canlı, K., Murat Altuner, E., Antimicrobial and antioxidant activities of some mosses. *Anatolian Bryology*, 9 (2023), 42–49. https://doi.org/10.26672/anatolianbryology.1300126

[34] Andrews, J.M., BSAC standardized disc susceptibility testing method (version 6). *Journal of Antimicrobial Chemotherapy*, 60 (2007), 20–41. https://doi.org/10.1093/jac/dkm110

[35] Moniharapon, E., Hashinaga, F., Antimicrobial activity of Atung (*Parinarium glaberrimum* Hassk) fruit extract. *Pakistan Journal of Biological Sciences*, 7 (2004), 1057–1061. https://doi.org/10.3923/pjbs.2004.1057.1061

[36] Rodríguez-Melcón, C., Alonso-Calleja, C., García-Fernández, C., Carballo, J., Capita, R., Minimum inhibitory concentration (MIC) and minimum bactericidal concentration (MBC) for twelve antimicrobials (biocides and antibiotics) in eight strains of *Listeria monocytogenes*. *Biology (Basel)*, 11 (2021), 46. https://doi.org/10.3390/biology11010046

[37] Krishnan, R., Arumugam, V., Vasaviah, S.K., The MIC and MBC of silver nanoparticles against *Enterococcus faecalis* - A facultative anaerobe. *Journal of Nanomedicine & Nanotechnology*, 6 (2015), 285. http://dx.doi.org/10.4172/2157-7439.1000285

[38] Benek, A., Determination of the moss flora of Izmir Bozdaglar range and investigation of the biological activities of some samples, PhD Thesis, Kastamonu University, Kastamonu, Turkey, 2024.

[39] Benek, A., Turu, D., Canlı, K., Determination of biological activity and biochemical content of ethanol extract from fruiting body of *Tricholoma bufonium* (*Pers.*) *Gillet*. *Journal of Fungi*, 10 (2024), 761. https://doi.org/10.3390/jof10110761

[40] Kosakowska, O., Węglarz, Z., Pióro-Jabrucka, E., Przybył, J.L., Kraśniewska, K., Gniewosz, M., Bączek, K., Antioxidant and antibacterial activity of essential oils and hydroethanolic extracts of Greek oregano (*O. vulgare* L. subsp. *hirtum* (*Link*) *Ietswaart*) and common oregano (*O. vulgare* L. subsp. *vulgare*). *Molecules*, 26 (2021), 988. https://doi.org/10.3390/molecules26040988

[41] Kaurinovic, B., Popovic, M., Vlaisavljevic, S., Trivic, S., Antioxidant capacity of *Ocimum basilicum* L. and *Origanum vulgare* L. extracts. *Molecules*, 16 (2011), 7401–7414. https://doi.org/10.3390/molecules16097401

[42] Canlı, K., Bozyel, M.E., Turu, D., Benek, A., Şimşek, O., Murat Altuner, E., Biochemical, antioxidant properties and antimicrobial activity of steno-endemic *Origanum onites*. *Microorganisms*, 11 (2023), 1987. https://doi.org/10.3390/microorganisms11081987

[43] Chen, Z., Bertin, R., Froldi, G., EC_{50} estimation of antioxidant activity in DPPH assay using several statistical programs. *Food Chemistry*, 138 (2013), 414–420. https://doi.org/10.1016/j.foodchem.2012.11.001

[44] Ganesan, T., Subban, M., Christopher Leslee, D.B., Kuppannan, S.B., Seedevi, P., Structural characterization of *n*-hexadecanoic acid from the leaves of *Ipomoea eriocarpa* and its antioxidant and antibacterial activities. *Biomass Conversion and Biorefinery*, 14 (2024), 14547–14558. https://doi.org/10.1007/s13399-022-03576-w

[45] Pleyerová, I., Hamet, J., Konrádová, H., Lipavská, H., Versatile roles of sorbitol in higher plants: luxury resource, effective defender or something else?. *Planta*, 256 (2022), 13. https://doi.org/10.1007/s00425-022-03925-z

[46] Rahman, Md. M., Rahaman, Md. S., Islam, Md. R., Hossain, Md. E., Mannan Mithi, F., Ahmed, M., Multifunctional therapeutic potential of phytocomplexes and natural extracts for antimicrobial properties. *Antibiotics*, 10 (2021), 1076. https://doi.org/10.3390/antibiotics10091076

[47] Fayera, S., Babu, G.N., Dekebo, A., Bogale, Y., Phytochemical investigation and antimicrobial study of leaf extract of *Plantago lanceolata*. *Natural Products Chemistry & Research*, 6 (2018), 0311. https://doi.org/10.4172/2329-6836.1000311

[48] Rahamouz-Haghighi, S., Kh, B., Mohsen-Pour, N., Sharafi, A., *In vitro* evaluation of cytotoxicity and antibacterial activities of ribwort plantain (*Plantago lanceolata* L.) root fractions and phytochemical analysis by gas chromatography-mass spectrometry. *Archives of Razi Institute*, 77 (2022), 2131. https://doi.org/10.22092/ARI.2022.358045.2143

[49] Zhakipbekov, K., Turgumbayeva, A., Issayeva, R., Kipchakbayeva, A., Kadyrbayeva, G., Tleubayeva, M., et al., Antimicrobial and other biomedical properties of extracts from *Plantago major*, *Plantaginaceae*. *Pharmaceuticals*, 16 (2023), 1092. https://doi.org/10.3390/ph16081092

[50] Kim, H., Cha, E., Ham, S., Park, J., Nam, S., Kwon, H., Linoleic acid inhibits *Pseudomonas aeruginosa* biofilm formation by activating diffusible signal factor-mediated quorum sensing. *Biotechnology and Bioengineering*, 118 (2021), 82–93. https://doi.org/10.1002/bit.27552

[51] Bouali, A., Spissu, Y., Barberis, A., Fadda, A., Azara, E., Orrù, G., Ouarda, H.E. F., Phytochemical evaluation and exploration of some biological activities of aqueous and ethanolic extracts of two species of the genus *Plantago* L. *PLos One*, 19 (2024), e0298518. https://doi.org/10.1371/journal.pone.0298518

[52] Amer, F., Algabar, A., Abdalameer Baqer, B., Sawsan, A., Authman, H., The Lepidoptera Research Foundation. *Journal of Research on Lepidoptera*, 50 (2019), 50–62.

[53] Akbalık, C., Kireçci, O.A., Fırat, M., Şahin, İ., Çelikezen, F.Ç., Bitlis yöresinde yetişen *Plantago lanceolata* (yılan otu) bitkisinin antioksidan ve antimikrobiyal özelliklerinin araştırılması. *Bitlis Eren Üniversitesi Fen Bilimleri Dergisi*, 10 (2021), 287–295. https://doi.org/10.17798/bitlisfen.827636

[54] Sanna, F., Piluzza, G., Campesi, G., Molinu, M. G., Re, G. A., Sulas, L., Antioxidant contents in a Mediterranean population of *Plantago lanceolata* L. exploited for quarry reclamation interventions. *Plants*, 11 (2022), 791. https://doi.org/10.3390/plants11060791

[55] Rahamouz-Haghighi, S., Sharafi, A., Bagheri, K., *In vitro* organogenesis from transformed root cultures of *Plantago lanceolata* and phytochemical analysis by HPLC and GC-MS. *Journal of BioScience and Biotechnology*, 10 (2021), 87–97.

[56] Yuan, Q., Xie, F., Huang, W., Hu, M., Yan, Q., Chen, Z., The review of alpha-linolenic acid: Sources, metabolism, and pharmacology. *Phytotherapy Research*, 36 (2022), 164–188. https://doi.org/10.1002/ptr.7295

[57] Joujou, F.M., El Darra, N., Rajha, H.N., Sokhn, E.S., Alwan, N., Evaluation of synergistic/antagonistic antibacterial activities of fatty oils from apricot, date, grape, and black seeds. *Scientific Reports*, 14 (2024), 6532. https://doi.org/10.1038/s41598-024-54850-y

[58] Maheswari, B.U., Kalaiselvi, G., Exploring neophytadiene from *Ampelocissus araneosa*: A molecular docking approach to inhibit biofilm formation in *Staphylococcus aureus*. *Uttar Pradesh Journal of Zoology*, 45 (2024), 59–70. https://doi.org/10.56557/upjoz/2024/v45i33875

[59] Pol, M., Schmidtke, K., Lewandowska, S., Plantago lanceolata–An overview of its agronomically and healing valuable features. *Open agriculture*, 6 (2021), 479-488. https://doi.org/10.1515/opag-2021-0035

[60] Pol, M., Potterat, O., Tröber, F., Lewandowska, S., Schmidtke, K., Rooting patterns and aucubin content in *Plantago lanceolata*. *Agriculture*, 14 (2024), 1352. https://doi.org/10.3390/agriculture14081352

http://communications.science.ankara.edu.tr

Communication Ankara Biology
Volume 34, Number 1, Pages 104-153 (2025)
ISSN 1303-6025 E-ISSN 2651-3749
DOI: 10.53447/communc.1491834

Review Article; Received: May 29, 2024; Accepted: August 29, 2024

OVERVIEW OF PLANT-DERIVED BIOMATERIALS

Ahmet Aşkın YILMAZ[1], İlker BÜYÜK[1]

Keywords

Plants
Biomaterials
Biocompatible
Recent developments

To cite this article

Yilmaz, A.A., Büyük, I., Overview of plant-derived biomaterials. *Commun.Fac.Sci.Univ.Ank.Ser.C Biology*, 34 (1) (2025), 104-153. https://doi.org/10.1111/communc.1491834

Affiliations

[1] Department of Biology, Faculty of Science, Ankara University, Ankara, TÜRKİYE

Abstract

Humans have been using plant-derived biomaterials throughout the history and they have an important place in today's daily life. They have a wide range of uses, from biotechnological to medical purposes. Plant-derived biomaterials possess various implementation in many fields including food industry, health care, biomedical science, cosmetics, energy science, environmental health and drug-gene delivery. Biomaterials have evolved to tissue-specific smart polymers since their discovery. Many biotechnological applications have allowed the production of biomaterials with different structures and shapes. Furthermore, latest studies demonstrated that constitutive organization and surface topographies of plants might also be beneficial for many biomaterial production processes. In this article, the history, classification, properties and application areas of biomaterials are explained by supporting studies. As a conclusion, it is inescapable for scientists to realise that plants are affordable, maintainable and regenerative platforms, and thus, they are optimal resources for generation of organic biomaterials. In this review, important current developments in the field of plant-derived biomaterials are also discussed.

1. INTRODUCTION

According to the Consensus Conference of the European Society of Biomaterials-II, a biomaterial is defined as the desired interface material in biological systems, utilized to assess processes aimed at enhancing, treating, or modifying the functioning of any body, tissue, or organ. Biomaterials are recognized for their biocompatibility with living tissues [1]. Biomaterials are typically categorized based on their material properties including polymeric materials, biopolymers, ceramic materials, certain active metals, and their composites. These materials are also classified based on their interactions with living tissues and responses against. Hence, biomaterials can be classified into non-bioactive or bioactive, biomimetic and biodegradable materials. When biomaterials are directly employed in living tissues, they can interact with the biological system in a controlled manner and thus they be utilized for diagnostic or therapeutic purposes [2, 3]. Biomaterials are extensively utilized in biological systems and medical devices. These biomaterials include ceramic materials,

ahmetaskinyilmaz@gmail.com- 0000-0001-8523-8939 https://ror.org/01wntqw50
buyuki@ankara.edu.tr- Corresponding author; 0000-0002-0843-8299 https://ror.org/01wntqw50

certain metals and their alloys, specific bioactive glasses, polymeric materials and their composites, biopolymers and their composites, as well as materials synthesized from animal-derived sources [4].

Biomaterials can be inserted into tissues like tendons, intraocular ligaments, heart valves, dental implants, and vascular transplants. Through the biomaterials, damaged or deteriorated organs and tissues can be fully replaced [5, 6]. The main materials used as biomaterials are: biodegradable polymeric materials, ceramic materials, alloys of some materials, biopolymers, composite materials, biocomposite materials reinforced with natural fibers, some other filling materials [7]. According to the literature findings, how a qualified biomaterial should have is listed below (Table 1).

At the present time, conventional materials are replaced by materials obtained from sustainable sources, and important steps are being taken for the development and design of these materials. Therefore, sustainable biomaterial applications exhibit an increasing trend compared to other conventional materials. There are several advanced techniques for synthesizing different types of biomaterials. These techniques also include thermal or hydrothermal synthesis Table 1 shows how biomaterials should be manufactured and utilized to ensure that they are more sustainable for our environment [4].

While various techniques are employed for nanomaterials in biological applications, one of the most commonly utilized methods is hydrothermal carbonization conducted in an aquatic environment under moderate pressure and temperature conditions. The resulting material from this technique finds utility in numerous applications including drug delivery, CO_2 separation, catalysis in various organic synthesis, sensors, and chemical vapor deposition [4].

TABLE 1. Properties of a good biomaterial [4]

Characteristics which a qualified biomaterial should possess	**Manufacturing for sustainability**
Biomaterials are available in solid or liquid forms, and they can be synthesized artificially or derived naturally from biological sources.	In addition to reducing the quantity of raw materials utilized, there is a pressing need to decrease the materials employed in packaging and prioritize the quality of the product
Biomaterials are generally non-living in nature or in combination with other substances	Disposable items that cannot be recycled or composted should be actively avoided.
Newly produced materials can be successfully applied to structurally and functionally regenerate, replace or repair any part of the body (organ, tissue).	Fossil fuel-based products and their derivatives must be avoided, and products obtained from renewable resources must always be preferred.

Biomaterials improve quality of people's life	Sustainability must be ensured in the potential use of product materials in the life cycle of products, in the recycling from materials from residue and in raw material growth. In addition, the sustainability factor should be internalized in the medical, social, financial and all other relevant environmental areas
	Products must be recyclable, reusable, or biodegradable.
	Government must promote sustainable farming facilities for farmers and other communities.
	The use of genetically modified organisms (GMOs) must be prohibited in raw material manufacturing
	Chemicals that comply with the twelve principles of green chemistry must be used on agricultural farms
	Chemicals and nanomaterial products that cause environmental problems and harm public health must be limited
	The different stages of the fabrication procedure must be distributed in a multi-centre way

The searching for a biomaterial in which biological and mechanical factors are in balance is difficult. Synthetic materials have traditionally excelled at providing the mechanical properties needed to support tissue growth. The most important handicap of such materials is their limited bioactivity. Due to their limited cell adhesion and inability to replace the extracellular matrix, synthetic materials become limited in supporting biological ingredients of cell proliferation. Moreover, synthetic materials typically lack degradability, thereby posing risks such as extrusion, immunogenicity, and hindrance in the formation of new tissues. The non-degradable ones may have a toxic affect to humans by spreading [8].

With the emergence and development of nanotechnology, there is an increasing demand for the use the natural materials for different biomedical applications. In addition, this rapidly expanding sector has made the requirement for eco-friendly biomaterials. For example, because of their chemical modifiability and ease of hydrogel formation, plants-derived biomaterials also function as potential bioinks (Figure 1). Therefore, these abundant, natural, renewable new generation bioinks have attracted considerable interest in 3D bioprinting investigations [8].

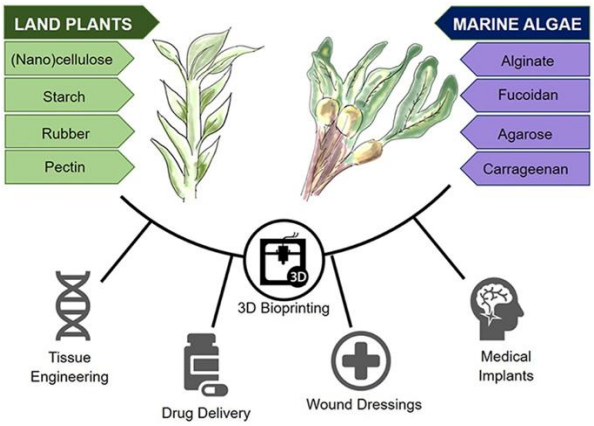

FIGURE 1. Plant-derived biomaterials obtained from terrestrial and sea creatures and their uses [8]

Concerns are growing about the depletion of natural resources, the growth of global populations and the release of large amounts of waste in our oceans and atmosphere [9]. Issues such as electronic waste, resource depletion, human health, the costs of medical systems and environmental problems lead people to work in the field of renewable, sustainable and flexible electronics. In order to cope with these challenges, it is needed to improve environmentally friendly, sustainable and biocompatible devices [10].

Plant-based products including cotton, wood, linen, and hemp have been used for countless of purposes for thousands of years [9]. Plants are living organisms with important parts such as wood, leaf and flower that host many natural materials in nature. The hierarchical structures of plant-based materials are displayed in Figure 2 [10].

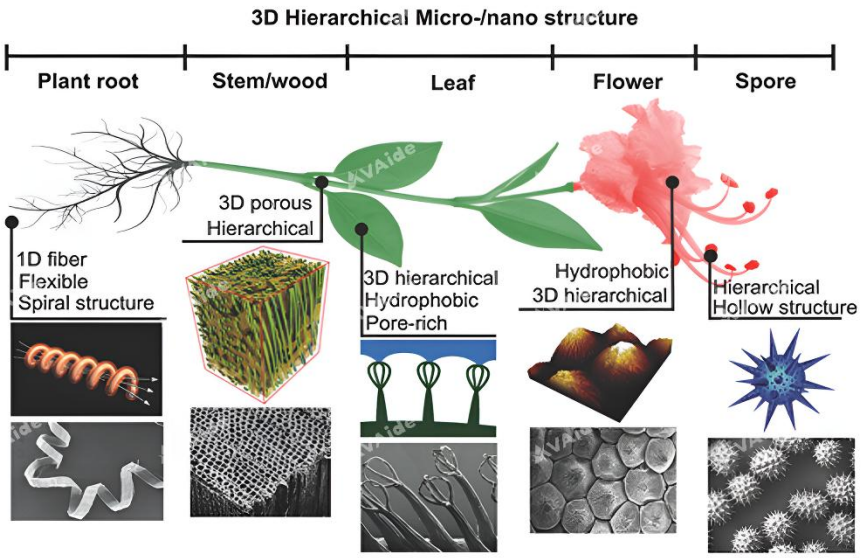

FIGURE 2. Hierarchical structure of materials in plants [11]

The names "biomaterials science" and "biomaterials field" refer to two distinct but related research disciplines. Examining the structure, evolutionary processes, and adaptive mechanisms that enable these materials to carry out a particular function is the focus of biological materials field. Biomaterials science, on the other hand, tries to make material scaffolds that mimic the desired properties of biological tissues. As a result, its goal is to replace damaged tissue [10].

Biomaterials applied for different areas need to have some specific properties. Also it should have good functionality for special applications. After the biomaterials are applied in the human body, they must restore function in the damaged part or in the tissues affected by the disease. Moreover it can be used to diagnose the diseases. Biomaterials possess many different medical properties [4]. These features can be listed as in Table 2.

TABLE 2. Some medical properties of a good biomaterial [12]

Medical properties which biomaterials can provide	**Requirements of a implanted biomaterial**
Filling gaps in plastic surgery operations,	It should be compatible with blood
Bone replacement, load transmission and stress distribution,	It should not be toxic and dangerous when it is applied for delivering the drug to the target organ or for eradicating cancerous cells
Stabilizing mechanical abrasion on joint implants which have high lubricity	Non-inflammatory, non-mutagenic, -non-carcinogenic, non-allergenic, non-pyrogenic in nature biomaterial should be selected
Good light transmittance and correct refractive value in the intraocular lens for clarity	Biomaterials should not affect the surrounding tissues and organs
Good sound conduction in cochlear implantation,	
In pacemakers, biomaterials must have a suitable stimulant for electrical conductivity	
The membrane made of biomaterial for dialysis has a high permeability	

Good biomaterial should be biocompatible and not harmful to host organisms after implantation. Therefore, the implanted biomaterial is required to fulfill the characteristics in Table 2.

Biological understanding, which integrates with the principles of engineering technology to meet medical needs, has a very important contribution to the creation of life-changing and life-saving therapeutic products like artificial organ pacemaker surgical robot systems ECG. Moreover, tissue engineering with biomimetic 3D cell-core scaffolds is seen as a favorable approach for the restoration of tissue-oriented inventions such as 3D printing of bioorganisms.

2. HISTORY OF BIOMATERIALS

Since ancient times, humankind have been addicted on herbal products for their basic needs. Plants were used for crop, fuel, garment and medical needs [13, 14]. The usage of plant tissue as a biomaterial in humans dates back to 3000 BC. Historians and archaeologists have found proof that ancient Egyptian doctors utilized coconut shells to renovate fractures and imperfections in sick skulls [15]. Moreover, the Romans and Ancient Egyptians could sculpt wooden prostheses for limb and exploit vegetable fibers to suture the skin around the lesions. Some

of the earliest applications of biomaterials are the usage of gold wires to fixate loose teeth with synthetic ones by the Phoenicians [13, 14].

From antiquity to the industrial revolution in the 19th century, plant biomaterials were commonly selected as materials for crafting external prosthetics. Materials capable of meeting the physical demands of the altered tissues are prioritized. For example, wooden prostheses were used instead of bone, and the teeth were replaced by ivory or gold. Insufficient attention was paid to the use of internal biomaterials due to lack of anesthetic because this deficiency limited the complexity of the surgeries that can be performed at those times [15]. Early in the 20th century, bone plates were a useful tool for stabilizing fractured bones and shortening the healing time. In clinical trials conducted in the 1950s and 1960s, hip articulations, prosthetic heart valves, and blood vessel repair were all improved [13, 14].

The field of biomaterials has changed with the establishment of materials science in the 20th century. In later stages, scientists began to focus on the internal microarchitecture of biomaterials to figure out the significance of the biomaterial-tissue interface at cellular level [15]. Traditional tissue repair methods have many disadvantages, including various surgeries, increased risk of infection, harmful procedures, and donor shortage. As a result of increasing population and urbanization, the demand for bio-repairment needs is increasing. The industrial revolution facilitated the production of a range of artificial biomaterials, initially metallic and later polymers, possessing highly advantageous properties for the advancement of medical equipment. Synthetic biomaterials have minimum biocompatibility and scarce capacity for tissue remodeling. In recent years, both nature-based materials and artificial biomaterials have become integral components of regenerative therapeutics and tissue engineering technologies. Only a small fraction of the approximately 300,000 plant species worldwide—about 5000—have been investigated for their potential medicinal applications. There remains a vast reservoir of plant-based natural materials existing purpose of medicinal use, with many yet to be discovered [16].

2.1 First generation biomaterials

The first known scientific endeavor in the subject of biomaterials occurred during World War II, when military surgeon and ophthalmologist Dr. Harold Ridley treated an aviator who had been struck by machine gun fire and had particles of polymethacrylate in his eyes. Dr. Ridley investigated the possibility that acrylic particles would impair a pilot's sight, and remarkably, the pilot showed no reaction to the synthetic, foreign material that had been lodged in his eyes. Because of this incident, Dr. Ridley developed the first artificial intraocular lens in 1950 to replace a patient's whole natural lens [17, 18]. In 1981, the US Food and Drug Administration (FDA) approved intraocular lens replacement, and since then, it has become one of the most common procedures performed worldwide [19].

In company with the emergence of the field of materials science, several unique internal biomaterials were developed from the 1960s to 1980s. These include materials which are derived from various biological materials that form the basis of first-generation internal prostheses. The first principle on first-generation biomaterials is to reduce the biological response of host against a foreign matter for creating bioinert scaffolds. The aim is to obtain a biomaterial that does not cause a chronic Foreign Body Response (FBR) and does not form a fibrous capsule between it and the host once it is implanted. Otherwise this process will result in implant inefficacy and rejection of the biomaterial [20].

Prolonged implantation of first generation biomaterials will eventually cause to over-absorption of host proteins and ultimate implant fault, predisposing patients to serious infection. Consequently, additional surgical intervention is required to remove the failed implant [20].

FBR is an immunological response to a biomaterial characterized as the final stage of chronic inflammation, massive cell occurrence and fibrotic capsule formation around the implanted biomaterial, and is prominent in first generation biomaterials. Therefore, researchers turned to developing second-generation biomaterials to tackle problems such as degradation and surface modifications in the host [21].

2.2 Second generation biomaterials

Researchers have tried to eradicate the incidence of implant ineffectiveness and multiple operations by designing biomaterial that decomposes inside the transplanted host [20]. Next-generation biomaterials are engineered to incorporate a three-dimensional (3D) structure that supports host cell integrity [22]. Important features of second generation biomaterials are that the material is slowly degraded to be replaced by host tissue, reducing the risk of secondary surgery, and any by-product fragments are eliminated by the host phagocyte cells. Second-generation biomaterials are designed to be bioactive, promoting decomposition and minimizing the environmental impact of biomaterials [20]. They still generate byproducts, though, such glycolic and lactic acids. This constant release lowers local pH levels and causes an inflammatory reaction, which can damage delicate tissue after surgery or injury [23].

2.3 Engineered biomaterials (Introduction to the modern age)

From 1935 to 1978, researchers concentrated on developing synthetic biomaterials with tailored properties to substitute naturally occurring biomaterials. During this period, various biomaterials emerged, including synthetic polymers, silicones, ceramics, hydrogels, metal alloys, polyurethanes, Teflon, polyethylene glycol (PEG), poly (lactic-co-glycolic acid) (PLGA), hydroxyapatite, titanium, and bioglass [24].

2.4 The modern age of biomaterials

Initially, first-generation biomaterials primarily focused on providing structural support during the early stages of biomaterial improvement. Researchers aimed to modify the function of replaced tissue within the host. This initial phase of biomaterials development aligned with the rise of materials science, leading to the adaptation of existing industrial materials for biomedical applications. Researchers have created a temporary host tissue interface that facilitates the reduction of foreign biomaterial to by-products, owing to the degradable biomaterial. Researchers have started to enhance degradable biomaterials to optimize essential properties like durability and flexibility. The increasing level of programmable control over biomaterials has facilitated numerous applications in various fields. Controlled drug delivery and gene therapy are the good examples of them. The researchers designed the chemical composition of the biomaterials to ideally suit the microenvironment of the intended replacement tissue [15].

2.4.1 Smart polymers

Polymers are extensively utilized in biomaterial implementations. As researchers have developed polymers capable of responding to diverse stimuli, they have started utilizing polymers as an innovative therapeutic delivery system. Smart polymers are designed to release their contents in response to a range of internal and external stimuli, with the inclusion of chemical, physical, and biological cues. Consequently, these polymers can be tailored to discharge a drug solely in response to a specific trigger, including internal cues like enzymatic activation or alterations in local pH levels. Likewise, external stimuli may involve electromagnetic radiation, light, or activation through acoustic energy. Such advancements enable the utilization of drug-loaded smart polymers to precisely release compounds into tissue in patients [25, 26].

2.4.2 Natural biomaterials

These natural biomaterials are sourced from endogenous proteins and serve as delivery vectors for a range of therapeutic agents. Endogenous protein-based materials possess the ability to undergo enzymatic or hydrolytic degradation by the host. Typically, an immunogenic response may arise from allogeneic protein or tissue derived from animal sources [15].

3. CLASSIFICATION OF PLANT BASED BIOMATERIALS

There are various methods for the classification of biomaterials which are shown in Table 3 [27].

TABLE 3. Basic biomaterial classification

Classification Basics	**Biomaterials in Different Classes**
Chemical Composition	Ceramic materials, Polymeric Materials, Metals and Composite Materials
Occurrence or Origin	Natural, Semi-Synthetic, Synthetic, Hybrid Materials
Dimensional Stability	Nano, Micro and Macro Forms of Biomaterials
Interaction with Living Body Tissues	Absorbable, Non-Absorbable, Bioactive and Biological Inertia
Biodegradability	Biodegradable and Biostable
Structural View	Porous and Non-Porous
Application	Diagnostic, Therapeutic, Restorative, Preventive and Regenerative
Field of Application	Interbody, Extracorporeal
Contact Time with Body Tissue	Limited, Long-Term and Permanent

Biomaterials used mostly in medicinal applications are categorized into two types [27].

3.1 Absorbable materials

They are materials that undergo degradation after being implanted into the human body and are subsequently absorbed by body tissues. Such materials are degraded slowly and their micro or nano sized fragments are released into the body. Eventually, they are absorbed by the body fluids and dissolve completely by the time of progress.

3.2 Non-absorbable materials

Biomaterials that do not disintegrate and are not absorbed by the tissues after being implanted in the human body are non-absorbable materials [27, 28].

Biomaterials can be categorized based on their properties and applications, including bio-inert materials, bioactive materials, biocompatible materials,

biodegradable materials, and biostable materials. Bioactive materials have significant interactions with living tissues, whereas non-bioactive materials possess minimal interactions with human tissue. Metals employed as biomaterials typically exhibit inert behavior towards body tissues. Ceramic and polymeric materials can be inert or absorbable, with ceramics often exhibiting bioactive properties as well. In specific applications of biomaterials, the design and selection of biological, chemical, physical and mechanical properties are very important for better functioning of the raw materials [29].

3.3 Carbon materials and renewable resources

There are numerous biopolymers found in the nature and biosynthesized from different living organisms. The main examples of these biopolymers are cellulose obtained from plants, chitin obtained from fungi and arthropods. Additionally, numerous other biopolymers, such as agar, chitosan, zein, dextrin, and alginate, originated from organic materials, along with carbon-based materials. These biopolymers and their composites find applications across various fields owing to their biocompatibility, bioactivity, biodegradability and non-toxic nature [30, 31].

The production and development of biologically-derived materials from natural resources and nanocomposites with biocompatibility are important for various sectors. Many conventional methods have been implemented to design and develop sustainable biomaterials by controlling particle size, temperature, pressure, biomaterial morphology, mechanical and thermal stability and pH. Biomaterials designed by conventional methods are applied in many different fields, but in the design of sustainable biomaterials, there are many parameters to be overcome such as reproducibility, high porosity, stability, controllable properties of the material. Therefore, modification is essential in nanomaterial production [4].

3.4 Classification of biomaterials by their nature and tissue responses

Naturally derived biomaterials can be divided into many groups according to their structure. Protein-based biomaterials (silk, gelatin, collagen etc.), polysaccharide-based biomaterials (chitin, cellulose, glucose, etc.) and biomaterials obtained from decellularised tissue (decellularized blood vessels, heart valves) are good examples of this category [32].

3.4.1 Biologically inert biomaterials

Once a material is implanted into the human body, the surrounding tissue begins to interact with it. Any material with even the slightest degree of this interaction is called 'bioinert'. Titanium, stainless steel, partially stabilised zirconia, alumina and ultra-high molecular weight polyethylene are some examples of the bioinert materials. A fibrous capsule can expand surrounding bioinert implants. Therefore, the operability of the implant depends on its integrity with the surrounding tissue.

3.4.2 Biologically active biomaterials

A substance that interacts with peripheral tissue after insertion into a human body is referred to as bioactive. This is a surface kinetic shift brought on over time by its implantation in live bone. A "carbonate apatite" stratum is created in the bone as a result of ion exchange between a bioactive implant and the surrounding body fluid. Some of the main biologically active biomaterials are synthetic hydroxyapatite, glass ceramic and bioglass materials.

3.4.3 Bio-absorbable biomaterials

Bioabsorbable refers to a substance that, after being placed in the human body, starts to break down (be absorbed) and is gradually replaced by growing tissue, such as bone or cartilage. Polylactic-polyglycolic acid copolymers and tri calcium phosphate are the main bioabsorbable materials. Other common materials used in recent years are calcium oxide, calcium carbonate and gypsum [16].

4. PROPERTIES OF PLANT-DERIVED BIOMATERIALS

Plant-derived materials are known to provide increased mechanical steadiness, bioactivity, biocompatibility, and biodegradability [8]. Plant-derived biomaterials have gained priority in the field of bioprinting due to their desirable properties (Figure 3). Polysaccharides such as agar, alginate, cellulose are commonly utilized in the structure of scaffold installations. Numerous researchers have extensively examined the appropriateness of these polysaccharides within the realm of regenerative medicine [33].

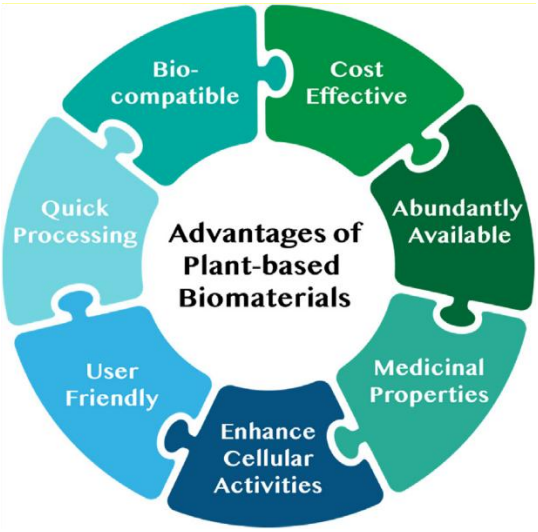

FIGURE 3. Advantages of plant-derived biomaterials [33]

4.1 Agarose

Agarose is a biomaterial obtained from red algae. Its capability to reversibly transition into a gel form with temperature has sparked attention in the realm of plant-based 3D bioprinting [34]. It behaves like alginate with its high water uptake and resemblance to extracellular matrix. It has also the advantage of self-gelation through hydrogen bonding without the requirement of possibly toxic cross-linking compounds like genipin [35]. Cells in agarose interfere with the cross-linking process and the hydrogen bonding required for gel formation. This can be overcome by increasing cell affinity through combination with other polymers such as collagen, chitosan and cellulose [36]

4.2 Alginate

Alginate stands as a member of the most extensively employed materials in 3D bioprinting. Alginate is commonly obtained from brown algae species such as *Laminaria digitate*, *Laminaria hyperborean*, *Laminaria japonica*, *Ascophyllum nodosum* and *Macrocystis pyrifera* [37]. In terms of structure, polysaccharides are copolymers consisting of β-D-Mannuronic acid (M) and β-D-Mannuronic acid (G). Alginates contain β-D-Mannuronic acid and β-D-Mannuronic acid residue blocks in varying proportions. In the copolymer, β-D-Mannuronic acid and β-D-Mannuronic acid-β-D-Mannuronic acid (together) residues increase flexibility. β-D-Mannuronic acid residues enhance both rigidity and gelling capability [38]. The natural proportion of β-D-Mannuronic acid to β-D-Mannuronic acid fluctuates depending on the species of seaweed from which the alginate is sourced. The ratio exhibits environmental and seasonal variability. Therefore, anionic compounds are obtained from different combinations for usage in diverse biomedical implementations [39, 40].

4.3 Cellulose

Globally, the most abundant biopolymer is cellulose, comprised of recurring monomer units of d-anhydroglucopyranose. These units are interconnected via β-(1-4) glycosidic bonds [4].

The acidic hydrolysis of cellulose leads to the cleavage of the glycosidic bond, resulting in the formation of nanocrystalline cellulosic materials, often known as nanocellulose. Cellulose nanocrystals have been successfully used as flocculants, supercapacitors, raw materials for some types of advanced paper, polymer composites and hydrogels. Industrially, it functions as a co-catalyst in conjunction with catalysts such as palladium, silver and gold nanoparticles [41].

Carboxymethyl cellulose provides mechanical strength for the hydrogel system and acts as excellent fillers in order to overcome obstacles related to shape accuracy [33].

4.4 Starch

Starch, a polysaccharide, is sourced from cereals and tuber crops like potatoes. It is stored in large quantities [42]. The composition of starch molecules typically comprises around 30% amylose and 70% amylopectin. However, the specific ratio between amylose and amylopectin can vary naturally depending on the source from which the starch is extracted [43]. Starches containing a higher proportion of amylose offer increased crystallinity and firmness. Their hygroscopic properties enable reversible hydration. Consequently, it supports continuous hydrogel spraying in extrusion-based printing methods [8].

There are several mechanical variables that determine the viscoelastic characteristics of starch. These characteristics primarily include concentration, extrusion temperature, storage modulus, elasticity, and flow stress [22].

Starch is widely recognized for its high biocompatibility, making it a promising material for scaffolds in tissue engineering and drug delivery implementations. Research has indicated that the encapsulation of cells in hydrogels based on starch results in enhanced cell adherence and vitality. Starch's rheological characteristics make it simple to modify the hydrogel's composition, which makes it easier to replicate the architecture of real tissues. Thus, it fulfils the various mechanical requirements for different cell types [44].

4.5 Nanocellulose

Nanocellulose, a highly versatile and abundant natural biopolymer, possesses remarkable mechanical strength, unique surface chemistry, and favorable biological properties such as high biocompatibility, low biodegradability, and non-toxicity. Additionally, it is an affordable material which may be used for a variety of purposes [8]. In general, architecture of nanocellulose consists of a complex arrangement of polymeric cellulose chains (about 1 nanometre) and macroscopic fibrillar structures with a diameter of about 5-20 μm (micrometres) in hierarchical order. In the microfibrillar structure, there is a pattern of well-organized crystalline regions alternated with less structured amorphous domains [45]. This arrangement ultimately determines the mechanical properties of cellulose. It provides flexibility and plasticity to amorphous regions. In addition, this configuration causes the formation of regular (crystalline) fraction, which contributes to the strength and flexibility of the substance [46].

Generally, there are three primary types of nanocellulose: cellulose nanocrystals, nanofibrillated cellulose, and bacterial cellulose. Generally, there have been significant research studies on plant-derived components which are largely favoured for their sustainability. Sources for cellulose nanocrystals and nanofibrillated cellulose extraction contain wood, hemp, cotton, potato tubers and algae [46].

4.6 Fucoidan

Fucoidan, a sulfated polysaccharide derived from brown algae and seaweeds like Kombu and Wakame, is water-soluble and exhibits the capacity to improve both the hydrophilic and mechanical properties of original polycaprolactone scaffolds [47] and additionally, this polymer possesses the capability to merge with other substances like alginate, gelatin, chitosan, calcium phosphates, and hydroxyapatite. Naturally, this situation renders it a favourable polysaccharide for developing new bioink formulations [48]. The material has potential anti-inflammatory, antioxidant and angiogenic properties for tissue engineering purposes [8]. Fucoidan's rheological characteristics also seem favorable for bioprinting; at concentrations less than 1.5% weight-volume, it exhibits shear-thinning tendency [49].

The rheological characteristics of fucoidan subtypes, both linear and branching, varied. Indeed, it seems that the type of seaweed used to extract the fucoidan affects the variations in viscosity. These discrepancies are due to changes in uronic acids, sulfate ratios, and molecular weight [8]. A direct correlation is noted between fucoidan concentration and dynamic viscosity. However, a decline in viscoelasticity is observed at elevated temperatures. The addition of substances like NaCl or $CaCl_2$ to the hydrogel leads to a gradual rise in the dynamic modulus, thereby enhancing the mechanical resilience of the hydrogel. Moreover, the viscoelastic properties of fucoidan are found to remain consistent across a broad pH spectrum [49]. Fucoidan has numerous medicinal properties. It is used in preclinical research studies for its antioxidant, anti-inflammatory and anti-cancer properties [50]. Besides, it has been found to stimulate the differentiation of osteoblast-like cells (MG-63) and adipose-derived stem cells in vitro. In other studies, angiogenesis-inducing properties of fucoidan have been shown through regulation of protein kinase B and matrix metalloproteinase-2. Fucoidan also prevents disruption of the FGF-2-FGF-receptor (Fibroblast Growth Factor-2) complex and induces angiogenesis in endothelial cells. Fucoidan can be utilized for bone tissue regeneration because of these two characteristics [51]. Using freeze-drying technique, Puvaneswary et al. (2015) created composite scaffolds included tricalcium phosphate, fucoidan, and chitosan to be used for bone tissue engineering applications. When fucoidan was added, human mesenchymal stem cells secreted more osteocalcin in vitro—a direct indicator of osteogenic differentiation. Chitosan-fucoidan, chitosan-nano hydroxyapatite-fucoidan, and chitosan-nano hydroxyapatite were among the combinations of scaffolds that were created. Among them, the most successful scaffold for periosteum-derived mesenchymal stem cell proliferation and differentiation was found to be the chitosan-nano hydroxyapatite-fucoidan composite, which showed a favorable architecture [52, 53].

4.7 Karagenan

Carrageenan is a polygalactone extracted from red seaweeds (algae, Rhodophyceae). It is a biopolymer classified as a sulfated polysaccharide. The substance comprises alternating lengthy chains of ester sulfated α-1,3 D-galactose and β-1,4 3,6-anhydro-galactose, resembling the structure of mammalian glycosaminoglycans found in natural extracellular matrices such as glucosaminoglycans [33, 8].

Carrageenan is crosslinkable and can gel both thermally and ionically. To create a bioprinting bioink, it is mixed with other substances such as nanosilicates and polymethacrylic anhydride. The precision, pliability, and stiffness of this ink allow the creation of layered tissue architectures [8]. Carrageenan-based bioinks showed an affinity for osteogenesis in addition to their high cell viability and adhesion capacity [54, 55]. Moreover, it boosted the compressive strength of collagen-hydroxyapatite-based composite gels, making them suitable for applications in bone tissue engineering [56]. The sulfated structure of carrageenan closely resembles the naturally occurring sulfated glycosaminoglycans found in the cartilage extracellular matrix [57, 58]. Therefore, this structure shows chondrogenic, non-toxic and mechanical features resembling natural cartilage [58]. Due to its easy crosslinking and similarity to glycosaminoglycan, carrageenan is of great importance for cartilage bio-inks [8].

4.8 Pectin

The primary component of pectin, a heteropolysaccharide, is D-galactosyluronic acid bound by an α-1→4-glycosidic linkage. Citrus fruit cell walls are the primary source of it. Depending on how much the residues of galaturonic acid have been esterified, it is categorized as having either high or low methoxy pectin. Due to its ability to be adjusted and refined by polymer concentration or crosslinking, pectin is a very adaptable substance. As a result, it may replicate a variety of natural textures [59].

Pectin naturally occurs as a component of plant cell walls. Due to its high molecular weight and hydrophilicity, it is well-suited for forming hydrogels and is considered an excellent candidate for 3D bioprinting. Pectin is also a versatile hydrogel. Since it has an adhesive cell ligand, it has rheological and viscoelastic properties which are suitable for independent modulation [59]. By adjusting polymer and/or crosslinker concentration, the elastic modulus of pectin can be modulated to biomechanically mimic a broad spectrum of natural human tissue types [60].

Pectin is extracted from waste materials derived from the fruit juice, apple, and cider industries through acidic and heat extraction methods [61]. Gelling is more likely to occur with highly densed solutions of pectin. Moreover, gelation occurs when pectin is subjected to acidic conditions along with the presence of divalent or trivalent cations [62]. Pectin, like alginate, is easily cross-linked when divalent calcium ions are present, forming links between homogalacturonic chains [63]. However, compared to other natural polymers, pectin has not been extensively

studied for its potential in tissue engineering and regenerative applications [62]. Poor ability of pectin to bind cells is one of its main drawbacks. However, its potential as a scaffold in bone tissue creation has been investigated by several researchers. Improved cell adhesion has been attained by combining it with some other substances such as polyvinyl alcohol [64, 65, 66].

4.9 Ulvan

Ulvan is a naturally occurring bio-polysaccharide consisting of glucuronic, iduronic, sulphated rhamnose, and xylose acids. It can be naturally isolated from the cell wall of green algea including *Ulva lactuca* and *Ulva rotundata*. Its distinct makeup, which contains iduronic acid—a component seldom seen in other modern algal polysaccharides such as alginates and agar—is what distinguishes ulvan from other similar products. Ulvan exhibits structural properties similar to mammalian glucosaminoglycans such as heparin and chondroitin sulfate, attributed to the presence of sulphated sugar residues. As a result, research endeavors have been directed towards exploring its potential in regenerative applications [67].

This water-soluble thermosensitive polymer may be mixed with other materials to create a milieu that is tailored to a particular tissue. Moreover, ulvan demonstrates both biocompatibility and biodegradability, making it a promising candidate for incorporation into bioink formulations [68 ,69].

4.10 Other ımportant biomaterials

Plants are a source of many elements, including proteins, sugars, essential oils, and secondary metabolites, each with its own special qualities. Of them, proteins have garnered a great deal of attention for tissue engineering endeavors because of their inherent biocompatibility. In addition, they have been widely used in these studies because they support cell adhesion and proliferation [70]. Compared to animal proteins, plant-based proteins are safer and less immunogenic. Additionally, they are more soluble in water due to their low molecular weight. Furthermore, these proteins are incredibly inexpensive and need very little processing [71]. Considering these characteristics, plant-based proteins emerge as promising candidates for tissue engineering applications. Moreover, their primarily edible nature makes them highly advantageous for the development of meat substitutes and related products.

The examples of proteins employed in the fabrication of tissue engineering scaffolds were given in Table 4. Furthermore, subsequent sections will elaborate on various alternative plant-based materials utilized in similar applications [33].

TABLE 4. Proteins used in tissue engineering [33]

Plant Protein	Technic	Scaffolding Component	Article	Potential Applications
Soya Protein	3D Bioprinting	Soya Protein	Edible bioink composed of soya protein for the production of bovine skeletal muscle is described Cell Studies/ Animal research (Bovine Satellite Cells)	Cell Based Meat
	Electrospinning	Soya Protein	Pre-clinical experiments in pigs in which the scaffold promotes re-epithelialisation and collagen synthesis are described Cell Studies/ Animal research (Pigs)	Wound Healing
	Freeze Drying	Soya Protein	Scaffolding is described as supporting the growth and viability of HMSCs Cell Studies/ Animal research (MSC)	Tissue Engineering
Tofu	Casting	Tofu-Soybean Protein	Observation of healthy cell growth was noted. Moreover, in vivo animal research has shown that the scaffold is well tolerated by the body Cell Studies/ Animal research (Animal Model)	Wound Healing
Wheat Protein	Chemical Precipitation	Magnesium Phosphate - Wheat protein	The scaffold utilized in the in vivo model has been demonstrated to enhance the differentiation of osteogenic cells. Cell Studies/ Animal research (Rabbits)	Bone
Zein Protein	Electrospinning	Gelatin - Zein	During the study, the scaffold facilitated both the growth and differentiation of PDLS cells. Cell Studies/ Animal research (PDLSC's)	Bone
	Freeze Drying	Chitosan- nano-HA- Zein	In the study, enhanced adhesion, growth and proliferation of MG-63 cells in the scaffold were observed Cell Studies/ Animal research (MG-63)	Bone
	Solvent Casting Technique	PCL- Zein	In the study, the analysis of physical parameters and the potential of scaffolding in implications of tissue engineering are described	Bone

4.10.1 Gum

Gums are intricate carbohydrates sourced from trees or shrubs. In the food industry, they serve as thickening agents. Moreover, it is also used to advance the structure of food products [72]. They are also used as adhesives. Gums exhibit remarkable efficiency in forming colloidal solutions in aqueous environments. They enhance the viscoelastic characteristics of hydrogels, thereby functioning as thickening agents and conferring essential mechanical resilience. Being hydrophilic, gums readily blend with other biomaterials and bioactive substances. Their shear-thinning behavior is particularly advantageous in bioprinting applications, making them vital components in extrusion-based bioprinting processes. Owing to their natural origin and exceptional properties, gums are invaluable for scaffold fabrication [73].

4.10.2 Essential oils

Essential oils are highly concentrated extracts obtained from plants, typically acquired through distillation. The oils, frequently employed in traditional complementary and alternative medicine, are extracted from different plant parts including flowers, leaves, and roots [74]. They reduce infection and inflammation. Also they have pain relieving properties and can accelerate the healing process by preventing wound formation [75]. Essential oils aid improve the polymer blends' processability throughout the scaffold-building process and can be used in place of some synthetic materials, such as PVA (PolyVinyl Alcohol), which are commonly utilized as plasticizers [76]. Additionally, certain oils, like cinnamon oil, improve the blend's pliability. As a result, they are crucial to the production of hydrophobic bioinks [77]. Due to their diverse medicinal properties, essential oils are being employed in regenerative medicine. Clove oil has been integrated into scaffolds for wound healing purposes because of its antimicrobial characteristics. Lavender oil, on the other hand, has demonstrated utility in bone tissue engineering [78, 79]. Table 5 lists a few instances of essential oils that have been researched for use in polymer composites for tissue engineering applications [33].

TABLE 5. Some of the essential oils utilized in tissue engineering [33]

Oil	Technic	Scaffolding Component	Cell Studies/ Animal Research	Usefulness
Almond Oil	Electrospinning	Polyurethane (PU)	Red blood cells (RBCs)	Bone Tissue Engineering
Basil Oil	Electrospinning	PU-TiO2	RBCs	Cardiovascular Applications
Castor Oil	Electrospinning	PU	RBCs	Cardiovascular Applications
	Electrospinning	PU-Kitosan	L929 Fibroblasts	Suturing and Wound Healing
	4 Dimensional Printing	PCL	Human bone marrow-derived MHC	Regenerative Medicine
Clove Oil	Hydrogel	Cellulose Nanofibres	Human Gingival Fibroblast Cells	Tissue
	Super Critical Foaming	PCL	MSCs	Implantation
Cinnamon Oil	Electrospinning	PVP	-	Biomedical Applications
Coconut Oil	Electrospinning	PU	RBCs	Vascular
Cardamom Oil	Nano-Encapsulation	Gelatine	Human Corneal Epithelial Cells and HepG2	Antibiotics
Corn Oil	Electrospinning	PU-Nim oil	Human Dermal Fibroblasts (HDFs)	Bone

4.10.3 Plant extracts

The utilization of plant extracts and various botanical components in the realm of healthcare dates back to ancient eras. Traditional medicine and plants have a very strong connection with each other. Tissue engineering and regenerative medicine render considerable use of bioactive components generated from plant extracts. They may be utilized efficiently to produce bioinks, which increases the medicinal quality and causes the sample to establish a biological reaction.

Among the various qualities of the extracts are their ability to stimulate multi-line cells' differentiation and proliferation [80, 81]. Moreover, biodegradable scaffolds produced using polycaprolactone were embedded with extracts of plants such as *Azadirachta indica*, *Memecylonedule*, *Myristica adamania*. It was found to have a great potential for use as wound dressings for burns [82]. Plant extracts have several uses in regenerative medicine, including the capacity to cross-link and have antibacterial properties. These extracts have furthermore been applied pharmacologically. For instance, extract from *Panax ginseng* has been utilized to slow down the process of radical generation [83]. *Ginkgo biloba* extract has also been observed to improve nerve tissue function in vivo [84]. It has been noted that extracts obtained from plants such as *Achillea Millefolium* stimulate the proliferation of human fibroblast cells. It has been noticed that *Prunus mume* extract exhibits a complete antibacterial activity against *Porphyromonas gingivalis* and *Streptococcus mitis* [85, 86].

4.10.4 Plant secondary metabolites

Secondary metabolites present in plants play a vital role in their defense mechanisms. These include various bioactive compounds such as alkaloids, glycosides, flavonoids, phenolics, and terpenoids, which are highly valued in pharmaceutical applications. They demonstrate antioxidant properties crucial for a wide range of nutraceutical uses. Additionally, these metabolites exhibit natural anti-fungal, anti-viral, anti-microbial, anti-cancer, and anti-inflammatory characteristics. They interact directly with cell receptors, membranes, and nucleic acids [87]. These adaptable characteristics enable them to boost cell adhesion, proliferation, and attachment. Research has demonstrated that secondary metabolites, such proline and ascorbic acid, boost collagen production, speed up the development of MHC (major histocompatibility complex) into osteoblasts, and improve cellular activity [33].

Promising results have been obtained when secondary metabolites are added as crosslinking agents. These secondary metabolites have the capability to link together two or more polymeric strands through both non-covalent pathways and chemical crosslinking methods. The crosslinking mechanism of secondary metabolites is graphically shown in Figure 4 [88].

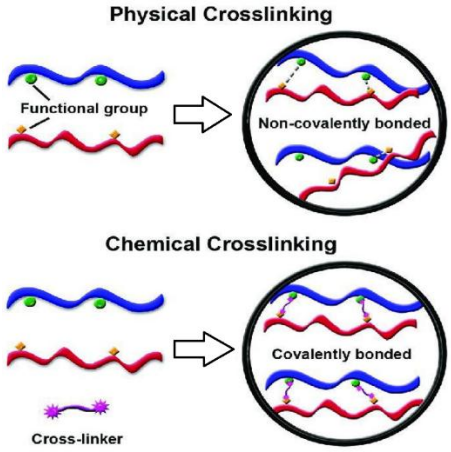

FIGURE 4. Cross-linking mechanism of secondary metabolites (adapted from Ramachandran et al. 2019) [89]

Cross-linking allows the construction of the desired architecture of scaffolds. Additionally, it strengthens the structure mechanically and makes it more stable against bodily fluid hydrolysis. Comparing plant-based secondary metabolites to chemical crosslinkers like glutaraldehyde, their negative effects are minimal, making them safe, biocompatible, and cost-effective choices. For example, in a study with genipin (extracted from Genipa americana), crosslinking of collagen, gelatin and chitosan polymers was successfully achieved [88]. Furthermore, it was discovered that polyvinyl alcohol enhances the tensile strength of hydrogels produced using silk and nano-hydroxyapatite in comparison to crosslinkers such as calcium chloride or carbodiimide [90].

Plant-derived biomaterials show promise for using plant microarchitecture as well as for their inherent biological function as cell growth boosters [91].

5. APPLICATION AREAS OF PLANT-DERIVED BIOMATERIALS AND TECHNOLOGIES USED

5.1 Tissue engineering applications

The utilization of plant-derived materials has been a consistent focus throughout human history [92]. Plant-derived materials, including polysaccharides, gums, essential oils, proteins, and secondary metabolites hold substantial promise for use in tissue engineering applications [33].

Biomaterials used in manufactoring; basically regulate the physical, rheological, chemical and biological properties of the scaffolds produced. The ideal biomaterial should have the following properties:

- Be able to produce tissue with sufficient mechanical strength and durability,

- It should have biocompatibility to resemble ECM (extracellular matrix),

- Biodegradability should be maintained to be suitable for natural ECM secretion synthesised by cells,

- It should be amenable to chemical modifications to fulfill tissue-specific needs.,

- It should have large-scale production potential [33].

The significant mechanical strength of synthetic biomaterials is necessary to promote tissue development. Nevertheless, these substances impede cellular proliferation, trigger immunogenicity, and discharge hazardous byproducts into the surroundings upon deterioration. They also have poor cell adhesion [93, 94, 95, 96]. On the other hand, natural materials of plant origin show both mechanical strength and biocompatibility to promote cell growth. Further, these materials have the added benefit of being more affordable due to their intrinsic biodegradability and therapeutic qualities, such as their antibacterial activities [97].

Bioprinting can revolutionize tissue engineering because the arrangement of cells and biologically active molecules in 3D space makes it possible to produce tissue through additives. Tissue engineering relies on cell-seeded biomimetic 3D scaffolds. Additionally, tissue engineering emerges as a promising future strategy and a viable alternative for promoting tissue repair. However, to achieve success, a thorough understanding of biomaterial properties and the potential synergies of their combinations is undoubtedly essential [98, 99, 100].

5.2 3D bioprinting technologies

The exact deposition of cells into a viscous biomaterial in a preset spatial arrangement using computer-aided printers is known as "bioprinting," a fast developing topic in biomedicine. It combines 3D printing technology, materials science, and tissue engineering to produce living biological structures with unique spatial configurations. Bioprinting has a wide range of possible uses, including improvements in medication delivery, surgery for transplantation and reconstruction, and the creation of implanted medical devices. This approach surpasses conventional 3D printing by adding biological properties to the ink, such as cell adhesion and proliferation, as well as the required mechanical properties. Bioinks are used at significantly lower temperatures because of the incorporated biological ingredients. In order to maintain the viability and functionality of cells, they need to be crosslinked using slightly non-toxic techniques [99]. What makes plant-based proteins supremely attractive is their gelling capacity, hydrophilicity, and inherent stiffness, which closely mimic the properties of the extracellular matrix. These characteristics make them ideal candidates for both biological and mechanical aspects in bioprinted tissues, organs, and biomedical applications [8].

Three main forms of printing technologies are used in 3D bioprinting: extrusion, laser-assisted, and inkjet (Table 6). Inkjet bioprinting is achieved by depositing cell suspensions at high shear rates, ejecting droplets with a diameter of approximately 50 μm (micrometres). In addition, low viscosity solutions are used

[101]. On the contrary, in laser-assisted bioprinting, a laser is directed onto a laser-absorbing layer of biomaterial, creating localized pressure which induces ink deposition [102]. Extrusion-based bioprinting, also referred to as bioplotting, works by using a nozzle powered by a screw, piston, or pneumatic force to deposit cells and bioink [103, 104]. Extrusion bioprinting operates at a slower pace compared to laser and inkjet printing but, it allows for structural deposition and solidification with each layer deposition [102, 105]. Different viscosities of bioinks are needed for each type of printing process in order to achieve good deposition [106]. Therefore, bioinks with adjustable viscosity gain versatility by utilising different technologies [8].

The primary challenge confronting bioprinting for medical applications is the identification of suitable, biocompatible materials [107]. Throughout history, a wide array of materials, encompassing alloys, ceramics, metals, and composites, have been instrumental in advancing biomedicine [108]. While the specific properties sought in materials for biomedical applications may vary, the fundamental prerequisites for in-vivo usage remain consistent. An ideal scaffold for facilitating cell growth and interfacing with biological systems is indispensable for successful tissue engineering endeavors. Simultaneously, such a scaffold should be biocompatible, non-toxic, and capable of offering mechanical support to replicate the natural macro-micro architecture of tissues [109, 110]. There are requirements for candidate biomaterials in the process of turning a biomaterial into a bioink. To produce live tissues, organs, and biological materials, the material must be able to hold its structure after printing and permit extrusion as a liquid bioink [8].

Apart from rheological and biological characteristics, bioinks need to support de novo tissue formation in order for in vivo tissue changes to be robust. The mechanical properties necessary for bioinks include compression, storage, elastic modulus, residual, and maximum compressive stresses [111].

The field of tissue technology has taken on dimension with the emergence of 3D cell culture technologies. With the further researches, the scale of use has expanded from the delivery of substances and drugs to provide a 3D environment for cell biomaterials used as scaffolds. Cellulose, alginate, Matrigel, Collagen I, fibrin, hyaluronic acid, gelatin, or natural biomaterial mixtures are commonly employed in the fabrication of 3D cell cultures. Synthetic polymers such as polyurethane, polyethylene glycol, and polyvinyl alcohol are also utilized in 3D cell cultures.

Tissue models are created during the bioprinting process using a hydrogel-based biomaterial mixture or a biomaterial solution that contains the necessary cell types (bioink) [98, 99, 100].

TABLE 6. Main types of 3D bioprint [8]

Bioprinting Technology	Key Components	Advantages	Disadvantages
Inkjet-Based	-Liquefied droplets deposited on a solid platform -The droplets need to solidify before the next layer is added -Droplet size 1-300 picolitres; rates 1-10,000 droplets per second	-High print speeds - Cheap - Ready -High resolution (about 10μm tunability in one cell)	-Low viscosity liquid required (Viscosity-3.5^{-12} mPas/s) -The possibility that heat ultrasound and shear pressure may impair cell viability -Risk of breast obstruction with the use of biomaterial -Only low cell counts (Cell Density-Low-<106 cells/ml) -Limited print height
Laser Based	-The energy absorber utilizes a laser pulse to heat and position the biomaterial -High-precision cell and material deposition without nozzle	-Multiple cell types can be deposited simultaneously for composite tissue engineering -Solutions with wide viscosity(Viscosity-1^{-300}mPa/s) ratios and high cell density can be printed (Cell Density- Moderate-<108 cells/ml)	-Slow process -Laser-induced cell damage -Low cell deposition accuracy -Metal pollution -Restrictive in the use of suitable biomaterials
Extrusion Based	-Material deposited through a nozzle/injector -Both high and low temperature settings are provided	-Cheap -Interchangeable platform, nozzles and environmental controls allow for a wide range of biomaterials -Mainly open-access hardware and software platforms -High cell (spheroids) density(Viscosities-30^{-6}x107 mPa)	-Slower than other technologies -High temperature settings may not be suitable for cellular material

5.2.1 Very important component of biological printing: bioinks

The method of bioprinting, also called three-dimensional bioprinting, entails building a biological structure or a biological model by assembling different materials, cells, and biomolecules using a material transfer procedure [112]. By layer-by-layer deposition, bioprinting uses additive manufacturing and fast prototyping to create complex systems. Initially, with the assistance of computer-aided design, it can be created and modeled the prototype of the construction. This model is divided into several 2D layers by the bioprinter's software, and each layer is then produced. The end product of this iterative procedure is a three-dimensional (3D) structure.

5.3 E-skin

The concept of e-skin refers to a sensor that replicates the properties of human skin, translating pressure, temperature, humidity, and other physiological factors into electronic signals [113, 114]. Studies on e-skins are popular in areas such as human-machine interfaces, artificial intelligence and health monitoring [115, 116, 117]. The emerging concept of "green e-skins" is particularly noteworthy. The primary focus should be on identifying compounds derived from natural resources and developing methods to produce environmentally friendly, biocompatible synthetic materials suitable for the device [118, 11]. The vast array of natural substances remains largely untapped by researchers, offering abundant possibilities. These materials offer diverse avenues for developing sustainable e-skins, utilizing cost-effective, renewable, and plentiful resources that are environmentally friendly. Consequently, green and flexible electronics can emerge as a supplementary technology in emerging markets, mitigating the demand for conventional electronics [11].

Natural plant materials like wood, leaves, and flowers are abundant biomaterials that biodegrade naturally in soil. These materials possess diverse structures that provide unique mechanical properties, making them suitable for creating high-performance and biocompatible e-skins (see Figure 5). The growing field of green electronics is the integration of materials obtained from plants or other biological sources into a variety of electronic devices intended for human body-to-machine interfaces [11].

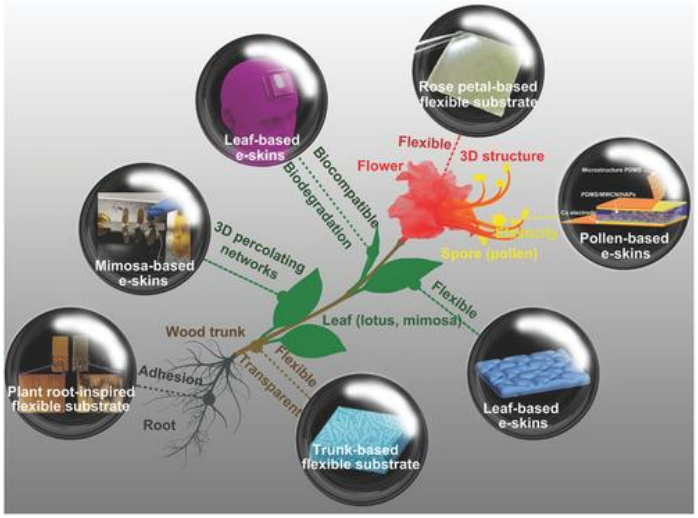

FIGURE 5. Schematic representation of plants in e-skin applications [11]

5.3.1 New design for green e-skins

A sensing layer including a entirely biodegradable film sensitized with organic compounds was presented by Prof. Bao's group in 2010. These organic materials exhibit high pressure sensitivity and rapid response times, making them suitable for cardiovascular monitoring. Moreover, this film has the added benefit of effectively reducing electronic waste [11].

The production of flexible, safe, compatible materials for wearable electronic devices from plant-based biomaterials is extremely important during the creation of green e-skins [119].

5.3.2 Plants as modular building blocks for green e-skins

Natural plant materials, developed over millions of years with 3D properties and mechanical characteristics, have been shown to be adaptable to conventional electronic materials [120, 121, 122]. Nonetheless, accurately replicating natural 3D structures presents challenges, making it difficult to adapt such materials for e-skin applications. Green materials developed for sustainable e-skins should exhibit the following characteristics (Figure 6):

I. Sustainability (abundant and renewable raw materials),

II. High performances (hierarchical structures with the desired mechanical and transport properties,

III. Environmentally sensitive (biocompatible, biodegradable and non-toxic materials)

IV. Large-scale, economical, and effective production [11]

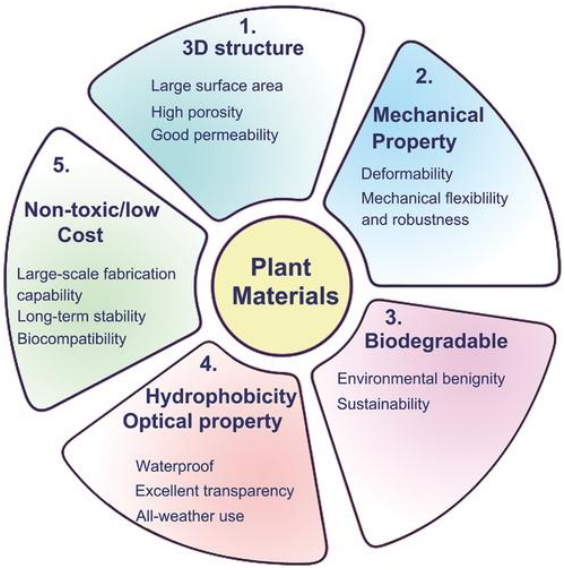

FIGURE 6. Benefits of potential e-skin applications with plant materials [11]

Cellulose, the primary component of plant biomass, is a natural polymer composed of numerous d-glucan units linked together through β-1-4 linkages. In addition to cellulose exhibiting exceptional tensile strength, its precursor derivatives possess rare optical properties. As a result, cellulose-based films find extensive applications in various industries including aerospace, automotive, comfort fabrics, specialty sports textiles, commercial membranes, wearable batteries, sensors, and electronics markets [11].

5.4 Structural layouts

In plants, the micro/nano structure frequently plays a vital role in dictating mechanical properties such as stability, flexibility, and elasticity, along with various functionalities like superhydrophobicity/superhydrophilicity, structural coloration, anti-reflective properties, selective filtration potential, and directional adhesion [11]. Strategies for the fabrication of multiscale hierarchical surfaces or 3D structures are known through studies [123, 124]. Materials characterized by low density, extensive surface areas, interlocking microstructures, and well-developed nanostructures hold significant promise across various fields including medicine, optics, electronics, and energy [11]. Fan et al. published a study by using natural plant leaves as biological samples from which they prepared Pt/N-doped TiO_2 nanomaterials. This nanomaterial has high porosity, large surface area and unique hierarchy (Figure 7a-c) [125]. Highly organized, three-dimensional micro and nanostructures derived from plant leaves exhibit notable photocatalytic activities [11].

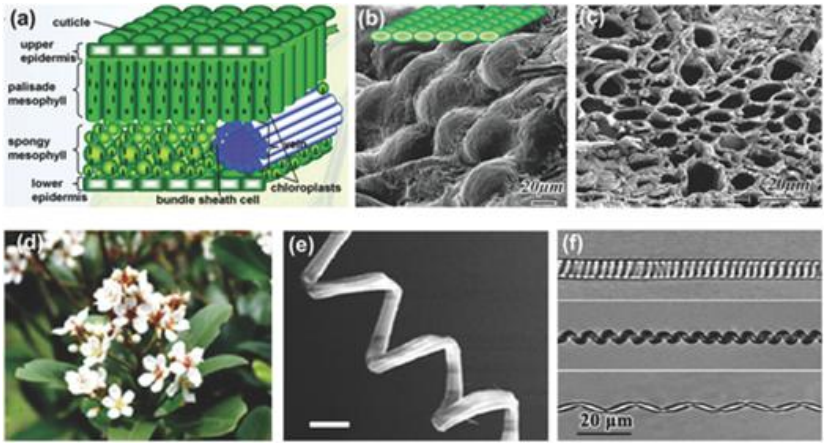

FIGURE 7. TiO_2 nanomaterial [126, 127]

Apart from biomaterials shaped like spheres or sheets, natural spiral containers are crucial elements in creating innovative nanomaterials with distinct morphologies. However, achieving 1D micro helical structures through conventional synthetic methods poses significant challenges. Kamata group (2011) pioneered the use of spiral cups from lotus roots as bio-molds for fabricating silver microcoils [128]. Subsequently, Wang et al. created magnetically repelling spiral cups by incorporating magnetic nickel onto the surface of spiral cups (Figure 7d,e) in 2014. In contrast to traditional 1D nanowires, helical veins from sheets with helical structures were able to maintain their size even under tensile stress due to their superior mechanical properties (Figure 7f). Further advantages of 1D helical materials are that they are biodegradable and biocompatible. They are easily scalable in terms of production. Consequently, 1D micro-wound wires are crucial for the advancement of bio-sustainable electronics in the future [129, 81].

Within plants, 3D structures play a pivotal role in amplifying and transmitting tactile signals to receptors, facilitating precise recognition of diverse external stimuli, including pressure and tactile signals [80, 130]. For example, a polymer substrate fabricated using plant leaves as a mould pattern can significantly increase the stretchability of a conductive Cu (Copper) layer on the surface of the substrate. Vein-shaped designs offer opportunities for introducing new or enhanced functionalities to fabricated devices, while also enhancing their stretchability and flexibility [130]. Likewise, in 2015, Su et al. developed 3D polydimethylsiloxane (PDMS) substrates using mimosa leaves as templates for design [131]. PDMS substrates showed an uneven pattern of microdomains in their examination, with an average diameter of 18.4 ± 6.1 μm and a height of 16.1 ± 3.7 μm (Figure 8). These protruding microdomains facilitated significant changes in the electrical signal upon light touch with the finger. Additionally, they utilized other plant leaves such as *Populus lasiocarpa* or *Cymbopogon citratus* as design templates and observed a similar level of amplification and transfer of tactile signals [131].

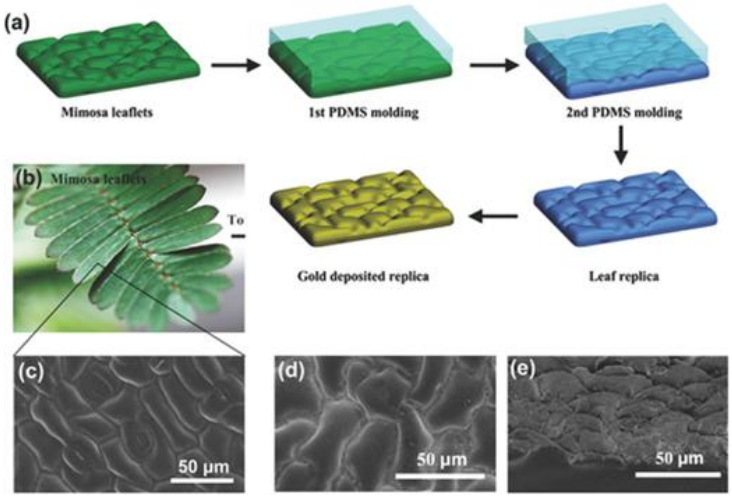

FIGURE 8. PDMS films obtained from mimosa leaves and SEM images [132, 131]

5.4.1 Cellulose based films

The primary component of biomass from plants is cellulose. About 40–45% of the weight of wood is made up of cellulose [133]. The cellulose content varies depending on the plant species. It stands as the most prevalent natural polymer globally, with an estimated annual production of cellulose ranging from 75 to 100 billion tonnes [134].

5.4.1.1 Cellulose derived membranes

Finely porous cellulose structures with exceptional transparency are seen in natural plants. In a study conducted in 2018, researchers reported on a flexible film composed of cellulose-based membranes. While cellulose films derived from wood pulp typically feature porous structures and rough surfaces, compressing these films resulted in a 80% deformation. In contrast, conventional materials like poly(3,4-ethylenedioxythiophene):poly(4-styrenesulfonate) lacking cellulose demonstrate lower deformation due to their brittleness and stiffness, often breaking under minimal force. This study highlights how a cellulose-based film can enhance the properties of high-performance flexible pressure sensors [135].

To enhance mechanical flexibility, Isogai (2013) successfully produced carboxylated cellulose nanofibrils through treatment with 2,2,6,6-tetramethylpiperidine-1-oxyl/sodium bromide/sodium hypochlorite in an aqueous alkaline environment (Figure 9a) [136]. Following the conversion of hydroxyl groups to carboxyl groups, carboxylated cellulose nanofibrils exhibit small diameters (approximately 5-10 nm) and demonstrate excellent optical transparency (see Figure 9b-c). Moreover, these carboxylated cellulose nanofibrils, characterized by long fibrous structures, have the capability to self-align, forming plywood-like nanolayer structures, thereby achieving high mechanical strength (Figure 9c-d) [137, 137, 139].

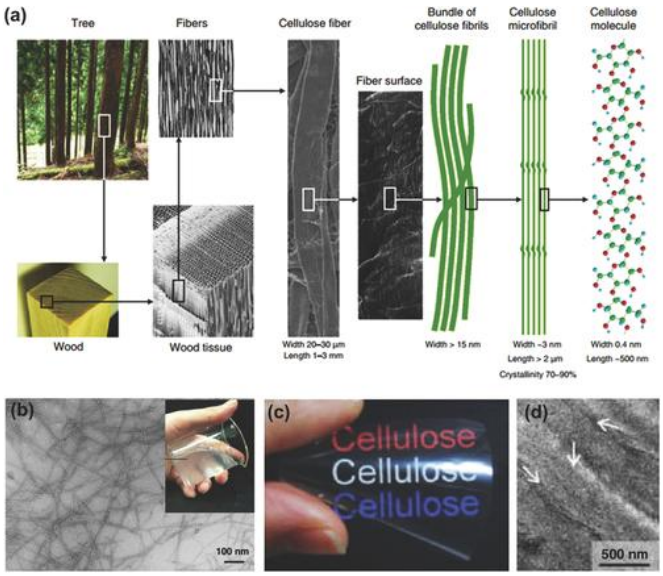

FIGURE 9. Carboxylated cellulose nanofibrils [136]

Papers made of cellulose have been used to create flexible screens, optical sensors, electronic skins (e-skins), and energy storage devices [11]. The performance of green plant-based, paper-based, flexible devices is promising. In 2014, Fang et al. first achieved the production of transparent paper with a light transmittance exceeding 90% from wood pulp through the oxidation of 2,2,6,6-tetramethylpiperidine-1-oxyl (TEMPO) (Figure 10a) [140]. When wood fibres are oxidised by TEMPO, they become shorter and have brittle, hollow fibrous structures (Figure 10b). This method enables the creation of dense fibrous networks in sheet form, which effectively reduces backward light scattering (see Figure 10c-d). Following this, Jung et al. achieved the groundbreaking feat of producing a biodegradable, transparent paper for the first time using carbon nanofibers derived from wood (Figure 10e) [141]. They proved that this optically transparent carbon nanofibre film biodegraded in wood with a fungus after disposal (Figure 10f-g). Materials like polysaccharides, silk, and resin can also be utilized to create biocompatible, optically clear paper as well as paper derived from vegetable cellulose. Furthermore, starch-based optically transparent sheets have been commercially manufactured as biodegradable polymers [11].

5.5 Plants as building blocks (3D bioshapes-moulds)

Electronic skins, or "e-skins," frequently use dielectric elastomers as sensing materials. These elastomers can be high dielectric constant (high-k) polymers, conducting polymers or semiconductor and metallic nanomaterials that can be embedded in elastomers. However, viscoelastic conduction elastomers typically produce significant hysteresis and sluggish reaction times (up to 10 seconds) [11].

In addition, thermal expansion of polymers leads to modifications in intrinsic electrical properties which vary with temperature. To address the primary limitations of conventional e-skins, which are typically prepared with monofunctional and planar structures, integrating advanced geometric designs is proposed as a solution. Through this approach, e-skin structures can effectively convert external pressure into electrical signals [11].

5.5.1 3D bioframes

In reaction to changes in the environment, natural biological systems have skillfully modified their micro- and nanostructures. Fibers significantly impact the complexity of plants' hierarchical architecture. Such morphologies include the hollow, chestnut-like structures of sunflower pollen, the tubular structures found in poplar catkins, the microstructures found in wood, and the cellular arrangement seen in *Lycopodium clavatum* spores [142, 143, 144, 145]. From this point of view, owing to the robust, hierarchical structures and mechanical properties of plant-based materials, it can be said that e-skins can be used as biocompatible templates or bioframes. For example, by simple heat treatment of plant fibres and freeze-drying of these fibres, 3D plant fibre-based material with desired pore sizes can be obtained (Figure 11a) [146]. Very good 3D network structures and low density were observed in poplar catkin fibres placed in ethanol. When fibres with these properties are used as sensing materials in e-skin, materials with high electrical conductivity can be produced.

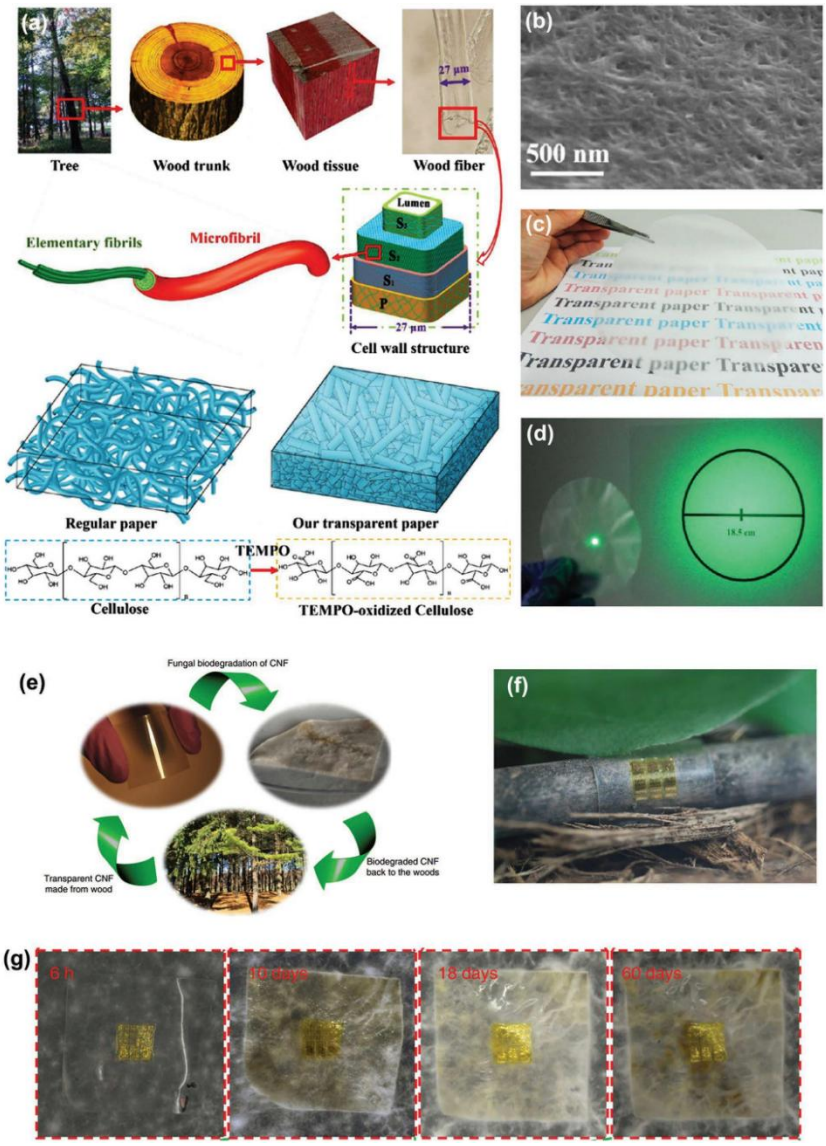

FIGURE 10. Transparent paper [140, 141]

When poplar catkin fibers are treated with sodium chloride, it allows for further adjustment of the morphology and porous structure of the synthesized carbon materials (Figure 11b). Poplar catkin fibres are prone to produce 2-dimensional carbon nanosheets due to their hollow, tubular structure. By subjecting the electrode to activation and carbonization processes, a significantly increased specific surface area was achieved during its manufacturing (Figure 11c). Microporous aerogels made from carbon were produced utilizing raw poplar catkin fibers. Additionally, these aerogels were employed as sensing layers in flexible pressure sensors, showcasing both high electrical conductivity and compressibility (Figure 11d) [146]. Ding et al. introduced Konjac glucomannan

derived carbon nanofibre aerogel to the world of science with similar methods (Figure 11e-f) [147]. Associated with this material, hierarchical carbon aerogels with their unique structure and adjustable size can be reproduced (Figure 11g). Carbonaceous nanofibrous aerogels exhibit great properties. These characteristics include low density, great compressibility, high conductivity, excellent thermal stability, zero toxicity, and high sensitivity to pressure (Figure 11h) [11].

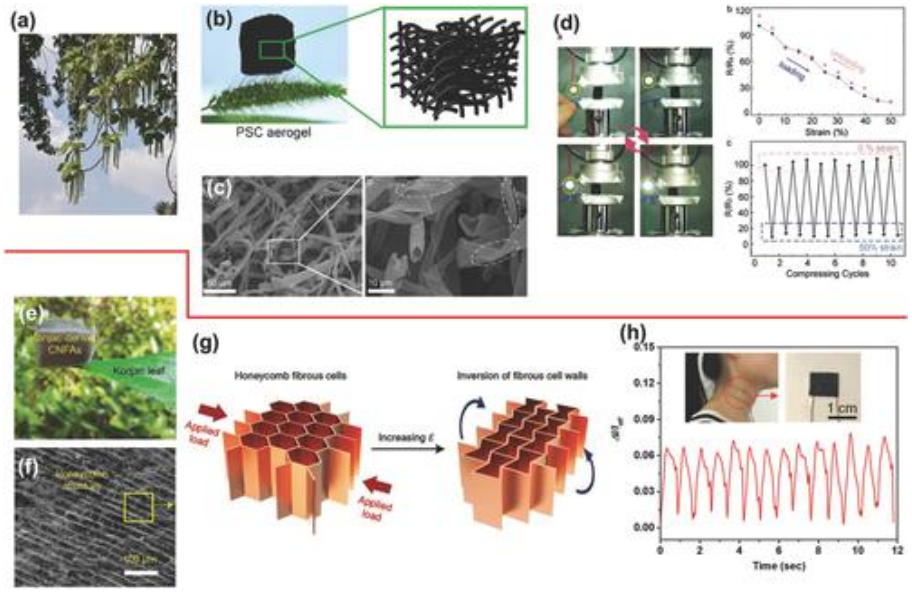

FIGURE 11. Biocompatible Templates [146, 147]

The configuration, form, and elasticity of artificially produced organic polymers can be customized by modifying the ligands. However, modifying natural plant materials is more complex due to their inherent, naturally existing morphology and internal arrangement. Many research efforts have focused on identifying the most suitable plants and natural resources to achieve specific functionalities. These functionalities include a 3D hierarchical structure, mechanical adaptability, self-repairing abilities, structural coloration, hydrophobicity/hydrophilicity balance, biocompatibility, and exceptional performance [11].

Enhancing the electrical conductivity of natural plant and plant-derived materials is crucial for improving the sensing capabilities and transport properties of electronic skins (e-skins). Therefore, studies on the development or design of conductive composite biomaterials for green flexible electronics can be carried further [11].

5.6 Plant derived biomaterials and their uses in bioengineering

Tissue regeneration and the construction of artificial organs can reduce the gap between the number of donated organs and people's needs. Bone implants and hip replacements are dangerous procedures. An infection can cause a rejection reaction. Biomaterial implant coatings allow easier osseointegration (integration into the surrounding bone), promote bone growth and prevent rejection reaction. In 2010, Kokkonen and collaborators isolated sugar subgroups from the primary carbon columns in enzyme-treated apples. They subsequently applied coatings of apple pectins onto nanometer-thick titanium dental implants. Their experiments showed favourable results in rat bone tissue culture. Rejection reactions were reduced and osseointegration was promoted in rat bone tissue culture [148].

5.6.1 3D biomedical applications

Due to their plentiful availability, gelling properties, and biological activity, biomaterials sourced from plants perform an essential function as bioinks in 3D bioprinting. The application potential of alginate and nanocellulose as frameworks for tissue engineering has undergone thorough examination. Consequently, the subsequent section of this review will concentrate on the latest research concerning these two biomaterials, which are leading the way in bioprinting advancements [8].

5.6.2 Hydrogels and their use in biomedical field

Hydrogels are composed of plant cell wall constituents and are cross-linked, water-swelling hydrophilic polymeric networks. Because of their structural similarity to extracellular cellular matrix (ECM), hydrogels have gained recognition as sophisticated materials with a broad variety of applications in the last 20 years. Hydrogels serve as an actual three-dimensional medium for cell development and presence in cell culture.

Hydrogels derived from biologically renewable polymers are extensively utilized in biomedical applications owing to their low toxicity, environmental friendliness, biocompatibility, accessibility, and cost-effectiveness. However, the primary challenge lies in identifying an ideal plant-based green hydrogel capable of replicating the key structural, functional, and performance properties of human tissues in tissue engineering. Additionally, these natural polymers often require optimization to ensure controllable chemistry and physical effects for applications such as drug delivery and tissue regeneration [149]. When bioprinting technologies are integrated, polymers are naturally generated for personalized and biological treatments. These applications include medication delivery, implanted medical devices, and wound dressing [8].

Ngoenkam et al. introduced injectable thermosensitive hydrogel for delivery of chondrocytes in cartilage tissue engineering [150]. Ciolacu et al. prepared lower density hydrogels containing cellulose/lignin to inject high drug content. Encapsulating bioactive compounds intended for intestinal delivery within

pectin hydrogels is a dependable method to safeguard them from degradation induced by the high acidity of gastric and intestinal enzymes. Certain types of pectins exhibit promising in vitro anti-inflammatory properties, rendering them valuable in the formulation of health products [151]. A new class of nanoscale particles of cellulose-based substances and polymers (hairy) has been able to overcome the structural limitations of conventional nanocellulose and also provide extra resistance to mechanical tissue engineering materials [152]. In vivo experiments conducted by Hadebe et al. (2014) on type 1 diabetic animal models, the administration of insulin-filled hydrogel particles composed of amidated pectin resulted in lower blood glucose levels [153].

5.6.3 Biomaterials as scaffolding

In recent times, tissue engineering scaffolds and hydrogels based on cellulose have been developed as a result of developing 3D printing technology. The attractive alternative scaffold that closely resembles human tissues in both structure and function is the plant tissue vasculature. Zadegan et al. (2011) pioneered the development of a cellulose/hydroxylapatite nanocomposite scaffold for bone tissue engineering, which notably enhanced the viability and proliferation of chondrocyte cells. Additionally, Andrew Pelling from the University of Ottawa and colleagues successfully created apple cellulose scaffolds, providing an additional method for culturing in vitro of mammalian cells within a 3D environment. These scaffolds were produced from a simple, cost-effective, and renewable source [154, 155].

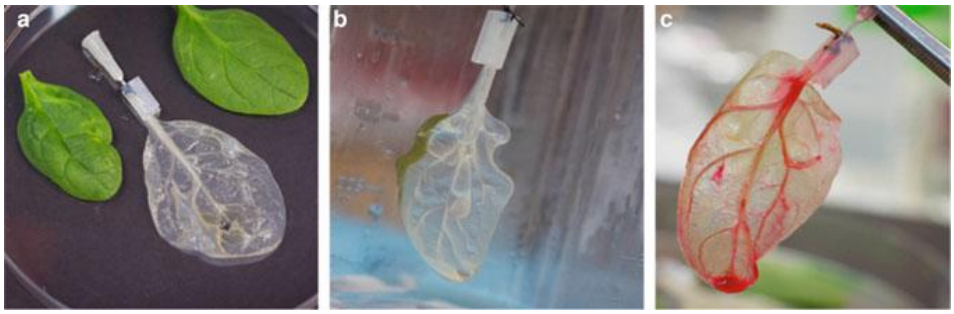

FIGURE 12. Artificial leaf (Source https://thebiochemistblog.com/2018/03/07/plant-based-biomaterials-engineering-the-future/) [156]

The production of decellularized plants by the Gaudette group for scaffolds in tissue perfusion marks the inception of a novel research avenue in the interdisciplinary field exploring the artificial interface between different taxa, namely plants and animal. The tissue of the plant vasculature mimics the mammalian vasculature. The central xylem and phloem transport water and nutrients to the peripheral cells, similar to blood vessels in humans. Spinach leaves from local markets were decellularised and the leaf was tested with red dye which indicated low fluid leakage. Then it was recellularised with human

cells. Human endothelial cells were placed in the lumen of the plant vasculature and mesenchyme cells in the outer tissue. These were glued and found to grow rapidly. Cardiomyocytes were also seeded on the leaf surfaces. Cardiomyocytes are specialized cells crucial for heart function, as they have the ability to beat autonomously. Remarkably, when planted on spinach, these cardiomyocytes demonstrated exceptional capability to develop independently (Figure 12) [91].

5.6.4 Hybrid implants in bioengineering

Researchers have engineered composite scaffolds by combining diverse biomaterials. This combination of biocompatibility, biodegradability and mechanical strength is important for technological and industrial application [157]. As a general rule, natural hydrogels are typically less toxic and better tolerated by the body compared to synthetic counterparts [158].

Pasqui et al. (2014) devised a hybrid hydrogel composed of natural cellulose and hydroxyapatite for bone tissue engineering projects. Additionally, Gilabert Chirivella et al. (2017) created a coating material by blending silver and chitosan for coating titanium dental implants. These particles were observed to exhibit inhibitory effects on dental pathogens such as Streptococcus mutans and Porphyromonas gingivalis, effectively preventing biofilm formation and subsequent adhesion [159, 160].

6. CONCLUSIONS

Plant-based biomaterials have special qualities that make them stand out, making them excellent for creating matrices in tissue engineering. In the field of tissue engineering, the effective applications of plant-based biomaterials have greatly risen in the last few decades. These materials are abundant, affordable, biocompatible, and have therapeutic properties that make them good replacements for synthetic counterparts and those derived from animal sources.

Materials made of sustainable hybrid nanocellulose can be utilized to clean up the environment. The creation of sustainable biomaterials requires the use of cost-effective and environmentally friendly technologies. This is vital for ensuring the well-being of future generations and preventing pollution in the environment.

Plant-derived products present promising candidates for biomaterial applications, particularly in the realm of 3D bioprinting. Their botanical origin eliminates ethical concerns and they are often readily available and cost-effective. While they typically exhibit low immunogenicity and are non-harmful at low concentrations, they still possess bioactive properties. Optimization of bioinks is crucial, necessitating combinations with other materials to meet the biological and mechanical requirements of diverse tissue types. Prior to in vivo application, thorough toxicity analysis of the material is essential. Hybridization of polymers with varied properties offers significant advantages in enhancing functionality and overcoming limitations in biomaterial formation. A comprehensive understanding of polymers and their applications is vital for

advancing plant-based hydrogels through modern and applicable research studies, given the increasing importance of plant-derived compounds in ongoing discussions.

The outcomes from high-efficiency e-leathers derived from natural plant materials demonstrate the feasibility of fully green electronics. Their practicality underscores the positive impact they are poised to have in the future.

Boosting the sustainability and adaptability of e-skins requires elucidating the precise structure-property interactions between natural materials and e-skin devices. Numerous of the natural materials that have been widely used in numerous industries over the past ten years have not yet been tried in e-skins. In order to fully comprehend the mechanisms behind these materials and their practical applications, establishing a connection between structure and function is essential.

Author Contribution Statements AAY- literature search, manuscript writing, IB- supervising, manuscript editing

Declaration of Competing Interests The authors declare no conflict of interest.

Ethical Statement This research did not involve human participants or animals. Therefore, no ethical approval was required.

Use of Artificial Intelligence No artificial intelligence-based tools or applications were used in the preparation of this study. The entire content of the study was produced by the author(s) in accordance with scientific research methods and academic ethical principles.

REFERENCES

[1] Naderi, H., Matin, M.M., Bahrami, A.R., Critical issues in tissue engineering: biomaterials, cell sources, angiogenesis, and drug delivery systems. *Journal of Biomaterials Applications*, 26 (4) (2011), 383–417. https://doi.org/10.1177/0885328211408946

[2] Campoccia, D., Montanaro, L., Arciola, C.R.A., Review of the biomaterials technologies for infection-resistant surfaces. *Biomaterials*, 34 (2013), 8533–8554. https://doi.org/10.1016/j.biomaterials.2013.07.089

[3] Pradhan, D., Sukla, L.B., Thin film of yttria stabilized zirconia on NiO using vacuum cold spraying process for solid oxide fuel cell. *IJNBM*, 7 (1) (2017), 38–47. https://doi.org/10.1504/IJNBM.2017.089322

[4] Biswal, T., BadJena, S.K., Pradhan, D., Sustainable biomaterials and their applications: A short review. *Materials Today Proceedings*, 30 (2020), 274–282. https://doi.org/10.1016/j.matpr.2020.01.437

[5] Kulinets, I., Biomaterials and their applications in medicine, In: Amato, S.F., Ezzell Jr, R.M. (Eds.). *Regulatory Affairs for Biomaterials and Medical Devices*. Woodhead Publishing Series in Biomaterials, (2015), 1–10. https://doi.org/10.1533/9780857099204.1

[6] Stoddart, A., Cleave, V., The evolution of biomaterials. *Nature Materials*, 8 (2009), 444–445. https://doi.org/10.1038/nmat2447

[7] Jebakumar, A.Z., Idrees, M., Nondo, H.S., A review on application of biomaterial in medical sciences. *Journal of Science*, 4 (2014), 390–393.

[8] Jovic, T.H., Kungwengwe, G., Mills, A.C., Whitaker, I.S., Plant-derived biomaterials: A review of 3D bioprinting and biomedical applications. *Frontiers in Mechanical Engineering*, 5 (2019), 19. https://doi.org/10.3389/fmech.2019.00019

[9] Shogren, R., Wood, D., Orts, W., Glenn, G., Plant-based materials and transitioning to a circular economy. *Sustainable Production and Consumption*, 19 (25) (2019), 194-215. https://doi.org/10.1016/j.spc.2019.04.007

[10] Hudecki, A., Kiryczynski, G., Los, M.J. Biomaterials, Definition, Overview. In: Los, M.J., Hudecki, A., Wiechec E. *Stem Cells and Biomaterials for Regenerative Medicine*. Academic Press, (2018), 85–98. https://doi.org/10.1016/B978-0-12-812258-7.00007-1

[11] Wang, L., Wang, K., Lou, Z., Jiang, K., Shen, G., Plant-based modular building blocks for "green" electronic skins. *Advanced Functional Materials*, 28 (51) (2018), 1804510 (1-16). https://doi.org/10.1002/adfm.201804510

[12] Walker, B.W., Lara, R.P., Mogadam, E., Yu, C.H., Kimball, W., Annabi, N., Rational design of microfabricated electroconductive hydrogels for biomedical applications. *Progress in Polymer Science*, 92 (2019), 135–157. https://doi.org/10.1016/j.progpolymsci.2019.02.007

[13] Karunamoorthi, K., Jegajeevanram, K., Vijayalakshmi, J., Mengistie, E., Traditional medicinal plants: a source of phytotherapeutic modality in resource-constrained health care settings. *Journal of Evidence-Based Integrative Medicine*, 18 (1) (2013), 67-74. https://doi.org/10.1177/2156587212460241

[14] Sen, R., Chatterjee, M., Plant derived therapeutics for the treatment of Leishmaniasis. *Phytomedicine*, 18 (12) (2011), 1056–1069. https://doi.org/10.1016/j.phymed.2011.03.004

[15] Modulevsky, D., Plant derived cellulose scaffolds as a novel biomaterial for 3d cell culture and tissue regeneration. PhD Thesis, University of Ottawa, Ottawa, Canada, 2021. http://dx.doi.org/10.20381/ruor-26406

[16] Heness, G., Ben-Nissan, B. Innovative bioceramics. *Materials Forum*, 27 (2004), 104 –114.

[17] Moore, D.B., Harris, A., Siesky, B., The world through a lens: The vision of Sir Harold Ridley. *British Journal of Ophthalmology*, 94 (2010), 1277–1280. https://doi.org/10.1136/bjo.2009.163956

[18] Sarwar, H., Modi, N., Sir Harold Ridley: Innovator of cataract surgery. *The Journal of Perioperative Practice*, 24 (9) (2014), 210–212. https://doi.org/10.1177/1750458914024009

[19] Patel, A.S., Intraocular Lens Implants: A Scientific Perspective. In: Ratner, B.D., Hoffman, A.S., Schoen, F.J., Lemons, J.E. Biomaterials Science: An Introduction to Materials in Medicine. Academic Press, (2013), 917-930. https://doi.org/10.1016/B978-0-08-087780-8.00078-4

[20] Hench, L.L., Thompson, I., Twenty-first century challenges for biomaterials Subject collections Twenty-first century challenges for biomaterials. *ournal of the Royal Society Interface*, 7 (2010), 379–391. https://doi.org/10.1098/rsif.2010.0151.focus

[21] Kattula, S., Brynes, J.R., Wolberg, A.S., Fibrinogen and fibrin in hemostasis and thrombosis. *Arteriosclerosis, Thrombosis, and Vascular Biology*, 37 (2017), e13–e21. https://doi.org/10.1161/ATVBAHA.117.308564

[22] Chen, H., Xie, F., Chen, L., Zheng, B., Effect of rheological properties of potato, rice and corn starches on their hot-extrusion 3D printing behaviors. *Journal of Food Engineering*, 244 (2019), 150–158. https://doi.org/10.1016/j.jfoodeng.2018.09.011

[23] Liu, H., Slamovich, E., Webster, T.J., Less harmful acidic degradation of poly (lactic- co-glycolic acid) bone tissue engineering scaffolds through titania nanoparticle addition. *International Journal of Nanomedicine*, 1 (4) (2006), 541–545. https://doi.org/10.2147/nano.2006.1.4.541

[24] Saini, M., Singh, Y., Arora, P., Arora, V., Jain, K., Implant biomaterials: A comprehensive review. *World Journal of Clinical Cases*, 3 (1) (2015), 52-57. https://dx.doi.org/10.12998/wjcc.v3.i1.52

[25] Heath, D.E., Cooper, S.L., Polyurethanes. In: Ratner, B.D., Hoffman, A.S., Schoen, F.J., Lemons, J.E. Biomaterials Science: An Introduction to Materials in Medicine. Academic Press, (2013), 79–82. https://doi.org/10.1016/B978-0-08-087780-8.00009-7

[26] Wells, C.M., Harris, M., Choi, L., Murali, V.P., Guerra, F.D., Jennings, J.A. Stimuli-responsive drug release from smart polymers. *Journal of Functional Biomaterials*, 10(3) (2019), 34. https://doi.org/10.3390/jfb10030034

[27] Sultana, M.J., Ahmed, F.R.S., Porous biomaterials: classification, fabrication and its applications in advanced medical science. *American Journal of Nano Research*, 4(2) (2018), 16-20. https://doi.org/10.11648/j.ajn.20180402.11

[28] Zybutz, M.D., Laurell, L., Rapoport, D. A., Persson, G.R., Treatment of intrabony defects with resorbable materials, non-resorbable materials and flap debridement. *Journal of Clinical Periodontology*, 27 (2000), 169–178. https://doi.org/10.1034/j.1600-051x.2000.027003169.x

[29] 3D Sheikh, Z., Najeeb, S., Khurshid, Z., Verma, V., Rashid, H., Glogauer, M., Biodegradable materials for bone repair and tissue engineering applications. *Materials*, 8(9) (2015), 5744–5794. https://doi.org/10.3390/ma8095273

[30] Varma, R.S., Biomass-derived renewable carbonaceous materials forsustainable chemical and environmental applications. *ACS Sustainable Chemistry & Engineering*, 7 (7) (2019), 6458–6470. https://doi.org/10.1021/acssuschemeng.8b06550

[31] Yang, H., Ye, S., Zhou, J., Liang, T., Biomass-derived porous carbon materials for supercapacitor. *Frontiers in Chemistry*, 7 (274) (2019), 1–17. https://doi.org/10.3389/fchem.2019.00274

[32] Andrades, J.A., Regenerative Medicine and Tissue Engineering. InTechOpen: Houston, TX, USA, 2013. https://doi.org/10.5772/55668

[33] Indurkar, A., Pandit, A., Jain, R., Dandekar, P., Plant-based biomaterials in tissue engineering. *Bioprinting*, 21 (2021), e00127. https://doi.org/10.1016/j.bprint.2020.e00127

[34] Zarrintaj, P., Manouchehri, S., Ahmadi, Z., Saeb, M.R., Urbanska, A.M., Kaplan, D.L., Mozafari, M., Agarose-based biomaterials for tissue engineering. *Carbohydrate Polymers*, 187 (2018), 66–84. https://doi.org/10.1016/j.carbpol.2018.01.060

[35] Campos, F., Bonhome-Espinosa, A.B., Vizcaino, G., Rodriguez, I.A., Duran-Herrera, D., Lopez-Lopez, M.T., Sanchez-Montesinos, I., Alaminos, M., Sanchez-Quevedo, M.C., Carriel, V., Generation of genipin cross-linked fibrin-agarose hydrogel tissue-like models for tissue engineering applications. *Biomedical Materials*, 13 (2) (2018), 025021. https://doi.org/10.1088/1748-605X/aa9ad2

[36] Annamalai, R.T., Mertz, D.R., Daley, E.L.H., Stegemann, J.P., Collagen Type II enhances chondrogenic differentiation in agarose-based modular microtissues. *Cytotherapy*, 18 (2016), 263–277. https://doi.org/10.1016/j.jcyt.2015.10.015

[37] Lee, K.Y., Mooney, D.J., Alginate: properties and biomedical applications. *Progress in Polymer Science*, 37 (2012), 106–126. https://doi.org/10.1016/j.progpolymsci.2011.06.003

[38] Axpe, E., Oyen, M.L., Applications of alginate-based bioinks in 3D bioprinting. *International Journal of Molecular Sciences*, 17 (12) (2016), 1976. https://doi.org/10.3390/ijms17121976

[39] Cardoso, M.J., Costa, R.R., Mano, J.F., Marine origin polysaccharides in drug delivery systems. *Marine Drugs*, 14 (2) (2016), 34. https://doi.org/10.3390/md14020034

[40] Maleki, S., Almaas, E., Zotchev, S., Valla, S., Ertesvag, H., Alginate biosynthesis factories in pseudomonas fluorescens: localization and correlation with alginate production level. *Applied and Environmental Microbiology*, 82 (2016), 1227–1236. https://doi.org/10.1128/AEM.03114-15

[41] Mishra, R.K., Sabu, A., Tiwari, S.K., Materials chemistry and the futurist ecofriendly applications of nanocellulose: status and prospect. *Journal of Saudi Chemical Society*, 22 (2018), 949–978. https://doi.org/10.1016/j.jscs.2018.02.005

[42] Lu, D.R., Xiao, C.M., Xu, S.J., Starch-based completely biodegradable polymer materials. *Express Polymer Letters*, 3 (2009), 366-375. https://doi.org/10.3144/expresspolymlett.2009.46

[43] Vengal, J.C., Srikumar, M., Processing and study of novel lignin-starch and lignin-gelatin biodegradable polymeric films. *Trends in Biomaterials and Artificial Organs*, 18 (2005), 2.

[44] Dong, D., Li, J., Cui, M.,Wang, J., Zhou, Y., Luo, L., Wei, Y., Ye, L., Sun, H., Yao, Y., In situ "Clickable" zwitterionic starch-based hydrogel for 3D cell encapsulation. *ACS Applied Materials & Interfaces*, 8 (2016), 4442–4455. https://doi.org/10.1021/acsami.5b12141

[45] Dumanli, A.G., Nanocellulose and its composites for biomedical applications. *Current Medicinal Chemistry*, 24 (2017), 512–528. http://dx.doi.org/10.2174/0929867323666161014124008

[46] Lin, N., Dufresne, A., Nanocellulose in biomedicine: current status and future prospect. *European Polymer Journal*, 59 (2014), 302–325. https://doi.org/10.1016/j.eurpolymj.2014.07.025

[47] Jin, G., Kim, G.H. Rapid-prototyped PCL/fucoidan composite scaffolds for bone tissue regeneration: design, fabrication, and physical/biological properties. *ournal of Materials Chemistry*, 21 (2011), 17710–17718. https://doi.org/10.1039/C1JM12915E

[48] Silva, S.S., Fernandes, E.M., Pina, S., Silva-Correia,J., Vieira, S., Oliveira, J.M., Reis, R.L., Polymers of biological origin. *Comprehensive Biomaterials*, 2 (2017), 228–252. https://doi.org/10.1016/B978-0-12-803581-8.10134-1

[49] Tako, M., Rheological characteristics of fucoidan isolated from commercially cultured *Cladosiphon okamuranus*. *Botanica Marina*, 46 (2003), 461–465. https://doi.org/10.1515/BOT.2003.047

[50] Collins, K.G., Fitzgerald, G.F., Stanton, C., Ross, R.P. Looking beyond the terrestrial: the potential of seaweed derived bioactives to treat non-communicable diseases. *Marine Drugs*, 14 (3) (2016), 60. https://doi.org/10.3390/md14030060

[51] Kim, B.S., Yang, S.S., You, H.K., Shin, H.I., Lee, J., Fucoidan-induced osteogenic differentiation promotes angiogenesis by inducing vascular endothelial growth factor secretion and accelerates bone repair. *Journal of Tissue Engineering and Regenerative Medicine*, 12 (2018), e1311–e1324. https://doi.org/10.1002/term.2509

[52] Lowe, B., Venkatesan, J., Anil, S., Shim, M.S., Kim, S.K., Preparation and characterization of chitosan-natural nano hydroxyapatite-fucoidan nanocomposites for bone tissue engineering. *International Journal of Biological Macromolecules*, 93 (2016), 1479–1487. https://doi.org/10.1016/j.ijbiomac.2016.02.054

[53] Puvaneswary, S., Talebian, S., Raghavendran, H.B., Murali, M.R., Mehrali, M., Afifi, A.M., Kasim, N.H.B.A., Kamarul, T., Fabrication and in vitro biological activity of βTCP-Chitosan-Fucoidan composite for bone tissue engineering. *Carbohydrate Polymers*, 134 (2015), 799–807. https://doi.org/10.1016/j.carbpol.2015.07.098

[54] Chimene, D., Peak, C.W., Gentry, J.L., Carrow, J.K., Cross, L.M., Mondragon, E., Cardoso, G.B., Kaunas R., Akhilesh, K., Gaharwar. A.K., Nanoengineered Ionic–Covalent Entanglement (NICE) bioinks for 3D bioprinting. *ACS Applied Materials & Interfaces*, 10 (2018), 9957–9968. https://doi.org/10.1021/acsami.7b19808

[55] Li, J., Yang, B., Qian, Y., Wang, Q., Han, R., Hao, T., Shu, Y., Zhang, Y., Yao, F., Wang, C., Iota-carrageenan/chitosan/gelatin scaffold for the osteogenic differentiation of adipose-derived MSCs in vitro. *Journal of Biomedical Materials Research Part B: Applied Biomaterials*, 103 (2015), 1498–1510. https://doi.org/10.1002/jbm.b.33339

[56] Feng, W., Qi, Y., Wang, S., Effects of short-range order on the magnetic and mechanical properties of FeCoNi(AlSi)x high entropy alloys. *Metals*, 7 (11) (2017), 482. https://doi.org/10.3390/met7110482

[57] Bhattacharyya, S., Liu, H., Zhang, Z., Jam, M., Dudeja, P.K., Michel, G., Linhardt, R.J., Tobacman, J.K., Carrageenan-induced innate immune response is modified by enzymes that hydrolyze distinct galactosidic bonds. *Journal of Nutritional Biochemistry*, 21 (2010), 906–913. https://doi.org/10.1016/j.jnutbio.2009.07.002

[58] Popa, E.G., Caridade, S.G., Mano, J.F., Reis, R.L., Gomes, M.E., Chondrogenic potential of injectable K-carrageenan hydrogel with encapsulated adipose stem cells for cartilage tissue-engineering applications. *Journal of Tissue Engineering and Regenerative Medicine*, 9 (5) (2015), 550–563. https://doi.org/10.1002/term.1683

[59] Pereira, R.F., Barrias, C.C., Bartolo, P.J., Granja, P.L., Cell-instructive pectin hydrogels crosslinked via thiol-norbornene photoclick chemistry for skin tissue engineering. *Acta Biomaterialia*, 66 (15) (2018), 282–293. https://doi.org/10.1016/j.actbio.2017.11.016

[60] Cui, S., Yao, B., Gao, M., Sun, X., Gou, D., Hu, J., Zhou Y., Liu, Y., Effects of pectin structure and crosslinking method on the properties of crosslinked pectin nanofibers. *Carbohydrate Polymers*, 157 (2017), 766–774. https://doi.org/10.1016/j.carbpol.2016.10.052

[61] Jayani, R.S., Saxena, S., Gupta, R., Microbial pectinolytic enzymes: a review. *Process Biochemistry*, 40 (2005), 2931–2944. https://doi.org/10.1016/j.procbio.2005.03.026

[62] Munarin, F., Tanzi, M.C., Petrini, P., Advances in biomedical applications of pectin gels. *International Journal of Biological Macromolecules*, 51 (4) (2012), 681–689. https://doi.org/10.1016/j.ijbiomac.2012.07.002

[63] Fang, Y., Al-Assaf, S., Phillips, G.O., Nishinari, K., Funami, T., Williams, P.A., Binding behavior of calciumto polyuronates: comparison of pectin with alginate. *Carbohydrate Polymers*, 72 (2008), 334–341. https://doi.org/10.1016/j.carbpol.2007.08.021

[64] Coimbra, P., Ferreira, P., de Sousa, H.C., Batista, P., Rodrigues, M.A., Correia, I.J., Gil, M.H., Preparation and chemical and biological characterization of a pectin/chitosan polyelectrolyte complex scaffold for possible bone tissue engineering applications. *International Journal of Biological Macromolecules*, 48 (2011), 112–118. https://doi.org/10.1016/j.ijbiomac.2010.10.006

[65] Kokkonen, H.E., Ilvesaro, J.M., Morra, M., Schols, H.A., Tuukkanen, J. Effect of modified pectin molecules on the growth of bone cells. *Biomacromolecules*, 8 (2) (2006), 509–515. https://doi.org/10.1021/bm060614h

[66] Yao, N., Huang, C., Jin, D., Evaluation of biocompatibility of a pectin/polyvinyl alcohol composite hydrogel as a new nucleus material. *Orthopaedic Surgery*, 1 (3) (2009), 231–237. https://doi.org/10.1111/j.1757-7861.2009.00036.x

[67] Robic, A., Gaillard, C., Sassi, J.F., Lerat, Y., Lahaye, M., Ultrastructure of Ulvan: a polysaccharide from green seaweeds. *Biopolymers*, 91 (8) (2009), 652–664. https://doi.org/10.1002/bip.21195

[68] Chiellini, F., Morelli, A., Ulvan: A versatile platform of biomaterials from renewable resources. In: Pignatello, R. Biomaterials-Physics and Chemistry. InTechOpen, (2011), 1-26. https://doi.org/10.5772/24901

[69] Morelli, A., Puppi, D., Chiellini, F., Perspectives on biomedical applications of ulvan. *Seaweed Polysaccharides: Isolation, Biological and Biomedical Applications*, 16 (2017), 305–330. https://doi.org/10.1016/B978-0-12-809816-5.00016-5

[70] Reddy, N., Yang, Y., Potential and properties of plant proteins for tissue engineering applications. In: Proceedings of the 13th International Conference on Biomedical Engineering, Singapore, 2008. https://doi.org/10.1007/978-3-540-92841-6_315

[71] Jahangirian, H., Azizi, S., Rafiee-Moghaddam, R., Baratvand, B., Webster, T.J., Status of plant protein-based green scaffolds for regenerative medicine applications. *Biomolecules*, 9 (10) (2019), 619. https://doi.org/10.3390/biom9100619

[72] Saha, D., Bhattacharya, S., Hydrocolloids as thickening and gelling agents in food: a critical review. *Journal of Food Science and Technology*, 47 (2010), 587–597. https://doi.org/10.1007/s13197-010-0162-6

[73] Indurkar, A., Bangde, P., Gore, M., Reddy, P., Jain, R., Dandekar, P., Optimization of guar gum-gelatin bioink for 3D printing of mammalian cells. *Bioprinting*, 20 (2020), e00101. https://doi.org/10.1016/j.bprint.2020.e00101

[74] Ehlers, M.R., Todd, R.M., Genesis and maintenance of attentional biases: the role of the locus coeruleus-noradrenaline system. *Neural Plasticity*, 2017 (2017), 6817349. https://doi.org/10.1155/2017/6817349

[75] Gushiken, L.F.S., Rozza, A.L.A., Vieira, A.J., Fernando, P., Essential oils and their use in skin wound healing. *Natural Products Research Reviews*, (2016), 501-513.

[76] Liu, P., Chen, W., Liu, C., Tian, M., Liu, P., A novel poly (vinyl alcohol)/poly (ethylene glycol) scaffold for tissue engineering with a unique bimodal open-celled structure fabricated using supercritical fluid foaming. *Scientific Reports*, 9 (2019), 1–12. https://doi.org/10.1038/s41598-019-46061-7

[77] Guler, H.K., Çallıoglu, F.C., Çetin, E.S., Antibacterial PVP/cinnamon essential oil nanofibers by emulsion electrospinning. *Journal of the Textile Institute*, 110 (2019), 302–310. https://doi.org/10.1080/00405000.2018.1477237

[78] Unalan, I., Endlein, S.J., Slavik, B., Buettner, A., Goldmann, W.H., Detsch, R., Boccaccini A.R., Evaluation of electrospun poly(ε-caprolactone)/gelatin nanofiber mats containing clove essential oil for antibacterial wound dressing. *Pharmaceutics*, 11 (2019), 570. https://doi.org/10.3390/pharmaceutics11110570

[79] Zhang, Z., Zheng, Y., Zhang, L., Mani, M.P., Jaganathan, S.K., In vitro blood compatibility and bone mineralization aspects of polymeric scaffold laden with essential oil and metallic particles for bone tissue engineering. *International Journal of Polymer Analysis and Characterization*, 24(6) (2019), 504–516. https://doi.org/10.1080/1023666X.2019.1611029

[80] Huang, Y.C., Chen, C.T., Chen, S.C., Lai, P.H., Liang, H..C, Chang, Y., Yu, L.C., Sung, H. W. A natural compound (Ginsenoside Re) isolated from Panax ginseng as a novel angiogenic agent for tissue regeneration. *Pharmaceutical Research*, 22 (2005), 636–646. https://doi.org/10.1007/s11095-005-2500-3

[81] Wang, P., Wei, X., Zhang, F., Yang, K., Qu, C., Luo, H, He, L., Ginsenoside Rg1 of *Panax ginseng* stimulates the proliferation, odontogenic/osteogenic differentiation and gene expression profiles of human dental pulp stem cells. *Phytomedicine*, 21 (2) (2014), 177–183. https://doi.org/10.1016/j.phymed.2013.08.021

[82] Jin, G., Prabhakaran, M.P., Kai, D., Annamalai, S.K., Arunachalam, K.D., Ramakrishna, S., Tissue engineered plant extracts as nanofibrous wound dressing. *Biomaterials*, 34 (2013), 724–734. https://doi.org/10.1016/j.biomaterials.2012.10.026

[83] Bak, M.J., Jun, M., Jeong, W.S., Antioxidant and hepatoprotective effects of the red ginseng essential oil in H2O2-treated HepG2 cells and CCl4-treated mice. *Int International Journal of Molecular Sciences*, 13 (2012), 2314–2330. https://doi.org/10.3390/ijms13022314

[84] Wu, Y., Sun, J., George, J., Ye, H., Cui, Z., Li, Z., Liu, Q., Zhang, Y., Ge, D., Liu, Y., Study of neuroprotective function of *Ginkgo biloba* extract (EGb761) derived-flavonoid monomers using a three-dimensional stem cell-derived neural model. *Biotechnology Progress*, 32 (3) (2016), 735–744. https://doi.org/10.1002/btpr.2255

[85] Ghobadian, Z., Ahmadi, M.R.H., Rezazadeh, L,, Hosseini, E., Kokhazadeh, T., Ghavam, S., In vitro evaluation of Achillea Millefolium on the production and stimulation of human skin fibroblast cells (HFS-PI-16). *Medical Archives*, 69(4) (2015), 212–217. https://doi.org/10.5455/medarh.2015.69.212-217

[86] Seneviratne, C.J., Wong, R.W.K., Hagg, U., Chen, Y., Herath, T.D.K., Samaranayake P L and Kao R (2011) Prunus mume extract exhibits antimicrobial activity against pathogenic oral bacteria. *International Journal of Paediatric Dentistry*, 21 (4), 299–305. https://doi.org/10.1111/j.1365-263X.2011.01123.x

[87] Velu, G., Palanichamy, V., Rajan, A.P., Phytochemical and pharmacological importance of plant secondary metabolites in modern medicine. *Bioorganic Phase in Natural Food: An Overview*, (2018), 135–156. https://doi.org/10.1007/978-3-319-74210-6_8

[88] Manickam, B., Sreedharan, R., Elumalai, M., 'Genipin' – the natural water soluble cross-linking agent and its importance in the modified drug delivery systems: an Overview. *Current Drug Delivery*, 11 (1) (2014), 139–145. https://doi.org/10.2174/15672018113106660059

[89] Ramachandran, R., Jung, D., Spokoyny, A. M., Cross-linking dots on metal oxides. *NPG Asia Materials*, 11 (1) (2019), 9–12. https://doi.org/10.1038/s41427-019-0119-9

[90] Zhou, H., Wang, Z., Cao, H., Hu, H., Luo, Z., Yang, X., Cui, M., Zhou, L., Genipincrosslinked polyvinyl alcohol/silk fibroin/nano-hydroxyapatite hydrogel for fabrication of artificial cornea scaffolds—a novel approach to corneal tissue engineering. *Journal of Biomaterials Science, Polymer Edition*, 30 (2019), 1604–1619. https://doi.org/10.1080/09205063.2019.1652418

[91] Gershlak, J.R., Hernandez, S., Fontana, G., Perreault, L.R., Hansen, K. J., Larson, S.A., Binder, B.Y.K., Dolivo, D.M., Yang, T., Dominko, T., Rolle, M.W., Weathers, P.J., Medina-Bolivar, F., Cramer, C.L., Murphy, W.L., Gaudette, G.R. Crossing kingdoms: using decellularized plants as perfusable tissue engineering scaffolds. *Biomaterials*, 125 (2017), 13–22. https://doi.org/10.1016/j.biomaterials.2017.02.011

[92] Kumar, S., Dobos, G.J., Rampp, T. The significance of ayurvedic medicinal plants. *Journal of Evidence-Based Complementary & Alternative Medicine*, 22 (3) (2017), 494–501. https://doi.org/10.1177/2156587216671392

[93] Kweon, H., Yoo, M.K., Park, I.K., Kim, T.H., Lee, H.C., Lee, H.S., Oh, J.S., Akaike, T., Cho, C.S., A novel degradable polycaprolactone networks for tissue engineering. *Biomaterials*, 24(5) (2003), 801–808. https://doi.org/10.1016/s0142-9612(02)00370-8

[94] Nijst, C.L.E., Bruggeman, J.P., Karp, J.M., Ferreira, L., Zumbuehl, A., Bettinger, C.J., Langer, R. Synthesis and characterization of photocurable elastomers from poly(glycerol-co-sebacate). *Biomacromolecules*, 8 (10) (2007), 3067–3073. https://doi.org/10.1021/bm070423u

[95] Smith, A., Hunneyball, I.M., Evaluation of poly(lactic acid) as a biodegradable drug delivery system for parenteral administration. *International Journal of Pharmaceutics*, 30 (1986), 215–220. https://doi.org/10.1016/0378-5173(86)90081-5

[96] Tessmar, J.K., Gopferich, A.M., Customized PEG-derived copolymers for tissueengineering applications. *Macromolecular Bioscience*, 7 (1) (2007), 23–39. https://doi.org/10.1002/mabi.200600096

[97] Iravani, S., Varma, R.S., Plants and plant-based polymers as scaffolds for tissue engineering. *Green Chemistry*, 21 (2019), 4839–4867. https://doi.org/10.1039/C9GC02391G

[98] Laternser, S., Keller, H., Leupin, O., Rausch, M., Graf-Hausner, U., Rimann, M. A Novel Microplate 3D Bioprinting Platform for the Engineering of Muscle and Tendon Tissues. *SLAS Technology*, 23(6) (2018), 599-613. https://doi.org/10.1177/2472630318776594

[99] Malda, J., Visser, J., Melchels, F.P., Jungst, T., Hennink, W.E., Dhert, W.J.A., Groll, J., Hutmacher, D.W., 25th Anniversary Article: Engineering Hydrogels for Biofabrication. *Advanced Materials*, 25 (36) (2013), 5011-5028. https://doi.org/10.1002/adma.201302042

[100] Rimann, M., Bono, E., Annaheim, H., Bleisch, M., Graf-Hausner, U., Standardized 3D Bioprinting of Soft Tissue Models with Human Primary Cells. *Journal of Laboratory Automation*, 21 (4) (2016), 496-509. https://doi.org/10.1177/2211068214567146

[101] Holzl, K., Lin, S., Tytgat, L., Van Vlierberghe, S., Gu, L., Ovsianikov, A. Bioink properties before, during and after 3D bioprinting. *Biofabrication*, 8 (3) (2016), 032002. https://doi.org/10.1088/1758-5090/8/3/032002

[102] Derakhshanfar, S., Mbeleck, R., Xu, K., Zhang, X., Zhong, W., Xing, M., 3D bioprinting for biomedical devices and tissue engineering: a review of recent trends and advances. *Bioactive Materials*, 3 (2018), 144–156. https://doi.org/10.1016/j.bioactmat.2017.11.008

[103] Jakab, K., Norotte, C., Damon, B., Marga, F.,Neagu, A., Besch-Williford, C.L., Kachurin, A., Church, K.H., Park, H., Mironov, V., Markwald, R., Vunjak-Novakovic, G., Forgacs, G., Tissue engineering by self-assembly of cells printed into topologically defined structures. *Tissue Engineering Part A*, 14 (2008), 413–421. https://doi.org/10.1089/tea.2007.0173

[104] Landers, R., Hubner, U., Schmelzeisen, R., Mulhaupt, RRapid prototyping of scaffolds derived from thermoreversible hydrogels and tailored for applications in tissue engineering. *Biomaterials*, 23 (2002), 4437–4447. https://doi.org/10.1016/S0142-9612(02)00139-4

[105] Smith, C.M., Stone, A.L., Parkhill, R.L., Stewart, R.L., Simpkins, M.W., Kachurin, A.M., Warren, W.L., Williams, S.K., Three-dimensional bioassembly tool for generating viable tissue-engineered constructs. *Tissue Engineering*, 10 (9-10) (2004), 1566–1576. https://doi.org/10.1089/ten.2004.10.1566

[106] Aljohani, W., Ullah, M.W., Zhang, X., Yang, G., Bioprinting and its applications in tissue engineering and regenerative medicine. *International Journal of Biological Macromolecules*, 107 (2018), 261–275. https://doi.org/10.1016/j.ijbiomac.2017.08.171

[107] Malkoc, V., Challenges and the Future of 3D Bioprinting. Available online at: http://www.alliedacademies.org/articles/challenges-and-the-futureof-3d-bioprinting.pdf (accessed on: December 31, 2018)

[108] Le May I., Lappi, V.G., White, W.E. Materials for biomedical applications. *Polymer Engineering & Science*, 15 (1975), 789–794. https://doi.org/10.1002/pen.760151105

[109] Drury, J.L., Mooney, D.J., Hydrogels for tissue engineering: scaffold design variables and applications. *Biomaterials*, 24 (2003), 4337–4351. https://doi.org/10.1016/S0142-9612(03)00340-5

[110] Gungor-Ozkerim, P.S., Inci, I., Zhang, Y.S., Khademhosseini, A., Dokmeci, M.R. Bioinks for 3D bioprinting: an overview. *Biomaterials Science*, 6 (2018), 915–946. https://doi.org/10.1039/C7BM00765E

[111] Chung, J.H.Y., Naficy, S., Yue, Z., Kapsa, R., Quigley, A., Moulton, S.E., Wallace, G.G., Bio-ink properties and printability for extrusion printing livingmcells. *Biomaterials Science*, 1 (2013), 763-773. https://doi.org/10.1039/C3BM00012E

[112] Gunatillake, P.A., Adhikari, R., Gadegaard, N., Biodegradable synthetic polymers for tissue engineering. *European Cells and Materials*, 5 (2003), 1–16. https://doi.org/10.22203/ecm.v005a01

[113] Hammock, M.L., Chortos, A., Benjamin, C., Tee, K., Jeffrey, B., Tok, H., Bao, Z., 25th anniversary article: the evolution of electronic skin (e-skin): a brief history, design considerations, and recent progress. *Advanced Materials*, 25 (2013), 5997-6038. https://doi.org/10.1002/adma.201302240

[114] Pan, L., Chortos, A., Yu, G., Wang, Y., Isaacson, S., Allen, R., Shi, Y., Dauskardt, R., Bao, Z., An ultra-sensitive resistive pressure sensor based on hollow-sphere microstructure induced elasticity in conducting polymer film. *Nature Communications*, 5 (2014), 3002. https://doi.org/10.1038/ncomms4002

[115] Lou, Z., Chen, S., Wang, L., Shi, R., Li, L., Jiang, K., Chen, D., Shen, G., Ultrasensitive and ultraflexible e-skins with dual functionalities for wearable electronics. *Nano Energy*, 38 (2017), 28-35. https://doi.org/10.1016/j.nanoen.2017.05.024

[116] Owens, R.M., Malliaras, G.G., Organic Electronics at the Interface with Biology. *MRS Bulletin*, 35 (2010), 449–456. https://doi.org/10.1557/mrs20

[117] Sekitani, T., Someya, T., Human-Friendly Organic Integrated Circuit. *Materials Today*, 14 (2011), 398-407. http://dx.doi.org/10.1016/S1369-7021(11)70184-5

[118] Irimia-Vladu, M. "Green" electronics: biodegradable and biocompatible materials and devices for sustainable future. *Chemical Society Reviews*, 43 (2014), 588-610. https://doi.org/10.1039/C3CS60235D

[119] Wang, L., Chen, D., Jiang, K., Shen, G., New insights and perspectives into biological materials for flexible electronics. *Chemical Society Reviews*, 46 (2017), 6764–6815. https://doi.org/10.1039/c7cs00278e

[120] Chen, Q., Pugno, N.M., Bio-mimetic mechanisms of natural hierarchical materials: a review. *Journal of the Mechanical Behavior of Biomedical Materials*, 19 (2013), 3-33. https://doi.org/10.1016/j.jmbbm.2012.10.012

[121] Hwang, S.W., Tao, H., Kim, D.H., Cheng, H., Song, J.K., Rill, E., Brenckle, M.A., Panilaitis, B., Won, S.M., Kim, Y.S., Song, Y.M., Yu, K.J., Ameen, A., Li, R., Su, Y., Yang, M., Kaplan, D.L., Zakin, M.R., Slepian, M.J., Huang, Y., Omenetto, F.G., Rogers, J.A., A physically transient form of silicon electronics. *Science*, 337 (6102) (2012), 1640–1644. https://doi.org/10.1126/science.122632

[122] Wegst, U.G.K., Bai, H., Saiz, E., Tomsia, A.P., Ritchie, R.O. Bioinspired structural materials. *Nature Materials*, 14 (2015), 23–36. https://doi.org/10.1038/nmat4089

[123] Zan, G., Wu, Q., Biomimetic and bioinspired synthesis of nanomaterials/nanostructures. *Advanced Materials*, 28 (11) (2016), 2099-2147. https://doi.org/10.1002/adma.201503215

[124] Zhang, P., Ma, Y., Zhang, Z., He, X., Zhang, J., Guo, Z., Tai, R., Zhao, Y., Chai, Z., Biotransformation of ceria nanoparticles in cucumber plants. *ACS Nano*, 6 (11) (2012), 9943–9950. https://doi.org/10.1021/nn303543n

[125] Zhou, H., Li, X., Fan, T., Osterloh, F.E., Ding, J., Sabio, E.M., Zhang, D., Guo, Q., Artificial inorganic leafs for efficient photochemical hydrogen production inspired by natural photosynthesis. *Advanced Materials*, 22 (2010), 951-956. https://doi.org/10.1002/adma.200902039

[126] Feng, L., Li, S., Li, Y., Li, H., Zhang, L., Zhai, J., Song, Y., Liu, B., Jiang, L., Zhu, D., Super-Hydrophobic Surfaces: From Natural to Artificial. *Advanced Materials*, 14 (2002), 1857–1860. https://doi.org/10.1002/adma.20029002

[127] Diah, S.Z.M., Karman, S.B., Gebeshuber, I.C. Nanostructural colouration in Malaysian plants: Lessons for biomimetics and biomaterials. *Journal of Nanomaterials*, 2014 (2014), 1-15. https://doi.org/10.1155/2014/878409

[128] Kamata, K., Suzuki, S., Ohtsuka, M., Nakagawa, M., Iyoda, T., Yamada, A., Fabrication of left-handed metal microcoil from spiral vessel of vascular plant. *Advanced Materials*, 23(46) (2011), 5509-5513. https://doi.org/10.1002/adma.201103605

[129] Gao, W., Feng, X., Pei, A., Kane, C.R., Tam, R., Hennessy, C., Wang, J., Bioinspired helical microswimmers based on vascular plants. *Nano Letters*, 14 (1) (2014), 305-10. https://doi.org/10.1021/nl404044d

[130] Lin, H., Allen, M.C., Wu, J., deGlee, B.M., Shin, D., Cai, Y., Sandhage, K.H., Deheyn, D.D., Meredith, J.C., Bio-Enabled, Core/Shell Microparticles with Tailored Multimodal Adhesion and Optical Reflectivity. *Chemistry of Materials*, 27 (21) (2015), 7321-7330. https://doi.org/10.1021/acs.chemmater.5b02782

[131] Su, B., Gong, S., Ma, Z., Yap, L. W, Cheng, W., Mimosa-inspired design of a flexible pressure sensor with touch sensitivity. *Small*, 11 (16) (2015), 1886-1891. https://doi.org/10.1002/smll.201403036

[132] Li, T., Luo, H., Qin, L., Wang, X., Xiong, Z., Ding, H., Gu, Y., Liu, Z., Zhang, T. Flexible Capacitive Tactile Sensor Based on Micropatterned Dielectric Layer. *Small*, 12 (36) (2016), 5042–5048. https://doi.org/10.1002/smll.201600760

[133] Zhu, J.Y., Zhuang, X.S., Conceptual net energy output for biofuel production from lignocellulosic biomass through biorefining. *Progress in Energy and Combustion Science*, 38 (2012), 360-1285. https://doi.org/10.1016/j.pecs.2012.03.007

[134] de Souza Lima, M.M., Borsali, R. Rodlike cellulose microcrystals: structure, properties, and applications. *Macromolecular Rapid Communications*, 25 (7) (2004), 771–787. https://doi.org/10.1002/marc.200300268

[135] Cheng, H., Du, Y., Wang, B., Mao, Z., Xu, H., Zhang, L., Zhong, Y., Jiang, W., Wang, L., Sui, X., Flexible cellulose-based thermoelectric sponge towards wearable pressure sensor and energy harvesting. *Chemical Engineering Journal*, 338 (2018), 1-7. https://doi.org/10.1016/j.cej.2017.12.134

[136] Isogai, A. Wood nanocelluloses: fundamentals and applications as new bio-based nanomaterials. *Journal of Wood Science*, 59 (2013), 449–459. https://doi.org/10.1007/s10086-013-1365-z

[137] Fukuzumi, H., Saito, T., Iwata, T., Kumamoto, Y., Isogai, A, Transparent and high gas barrier films of cellulose nanofibers prepared by TEMPO-mediated oxidation. *Biomacromolecules*, 10 (1) (2009), 162-5. https://doi.org/10.1021/bm801065u

[138] Isogai, A., Saito, T., Fukuzumi, H., TEMPO-Oxidized cellulose nanofibers. *Nanoscale*, 3 (2011), 71-85. http://dx.doi.org/10.1039/C0NR00583E

[139] Saito, T., Uematsu, T., Kimura, S., Enomae, T., Isogai, A., Self-aligned integration of native cellulose nanofibrils towards producing diverse bulk materials. *Soft Matter*, 7 (2011), 8804-8809. https://doi.org/10.1039/C1SM06050C

[140] Fang, Z., Zhu, H., Preston, C., Hu, L., Development, application and commercialization of transparent paper. *Translational Materials Research*, 1 (1) (2014), 015004. http://iopscience.iop.org/2053-1613/1/1/015004

[141] Jung, Y., Chang, T. H., Zhang, H., Yao, C., Zheng, Q., Yang, V.W., Mi, H., Kim, M., Cho, S.J., Park, D.W., Jiang, H., Lee, J., Qiu, Y., Zhou, W., Cai, Z., Gong, S., Ma, Z., High-performance green flexible electronics based on biodegradable cellulose nanofibril paper. *Nature Communications*, 6 (2015), 7170. https://doi.org/10.1038/ncomms8170

[142] Song, J., Chen, C., Wang, C., Kuang, Y., Li, Y., Jiang, F., Li, Y., Hitz, E., Zhang, Y., Liu, B., Gong, A., Bian, H., Zhu, J.Y., Zhang, J., Li, J., Hu, L., Superflexible Wood. *ACS Applied Materials & Interfaces*, 9 (28) (2017), 23520-23527. https://doi.org/10.1021/acsami.7b06529

[143] Wang, L., Jackman, J.A., Ng, W.B., Cho, N.J., Flexible, graphene-coated biocomposite for highly sensitive, real-time molecular detection. *Advanced Functional Materials*, 26 (2016a), 8623. https://doi.org/10.1002/adfm.201603550

[144] Wang, L., Ng, W., Jackman, J.A., Cho, N.J., A flexible, ultra-sensitive chemical sensor with 3D biomimetic templating for diabetes-related acetone detection. *Advanced Functional Materials*, 26 (2016b), 2097. https://doi.org/10.1039/C7TB00787F

[145] Zang, L., Bu, Z., Sun, L., Zhang, Y., Hollow carbon fiber sponges from crude catkins: an ultralow cost absorbent for oils and organic solvents. *RSC Advances*, 6 (2016), 48715-48719. https://doi.org/10.1039/C6RA08183E

[146] Li, L., Tao, H., Sun, H., Zhang, J., Wang, A., Pressure-sensitive and conductive carbon aerogels from poplars catkins for selective oil absorption and oil/water separation. *ACS Applied Materials & Interfaces*, 9 (21) (2017), 18001–18007. https://doi.org/10.1021/acsami.7b04687

[147] Si, Y., Wang, X., Yan, C., Yang, L., Yu, J., Ding, B., Ultralight Biomass-Derived Carbonaceous Nanofibrous Aerogels with Superelasticity and High Pressure-Sensitivity. *Advanced Materials*, 28 (43) (2016), 9512-9518. https://doi.org/10.1002/adma.201603143

[148] Kokkonen, H., Niiranen, H., Schols, H.A., Morra, M., Stenback, F., Tuukkanen, J., Pectin-coated titanium implants are well-tolerated in vivo. *Journal of Biomedical Materials Research Part A*, 93 (4) (2010), 1404–1409. https://doi.org/10.1002/jbm.a.32649

[149] Mohammadinejad, R., Maleki, H., Larraneta, E., Fajardo, A.R., Nik, A.B., Shavand A., Sheikhi, A., Ghorbanpour, M., Farokhi, M., Govindh, P., Cabane, E., Azizi, S., Aref, A.R., Mozafari, M., Mehrali, M., Thomas, S., Mano, J.F., Mishra, Y.K., Thakur, V.K., Status and future scope of plant-based green hydrogels in biomedical engineering. *Applied Materials Today*, 16 (2019), 213–246. https://doi.org/10.1016/j.apmt.2019.04.010

[150] Ngoenkam, J., Faikrua, A., Yasothornsrikul, S., Viyoch, J., Potential of an injectable chitosan/starch/β-glycerol phosphate hydrogel for sustaining normal chondrocyte function. *International Journal of Pharmaceutics*, 391(1-2) (2010), 115–24. https://doi.org/10.1016/j.ijpharm.2010.02.028

[151] Ciolacu, D.E., Nicu, R., Ciolacu, F. Cellulose-based hydrogels as sustained drug-delivery systems. *Materials*, 13 (22) (2020), 5270. https://doi.org/10.3390/ma13225270

[152] Sakurai, M.H., Matsumoto, T., Kiyohara, H., Yamada, H. B-cell proliferation activity of pectic polysaccharide from a medicinal herb, the roots of Bupleurum falcatum L. and its structural requirement. *Immunology*, 97 (3) (1999), 540–547. https://doi.org/10.1046/j.1365-2567.1999.00774.x

[153] Silindile, S.I., Phikelelani, P.S., Serumula, M.R., Musabayane, C., Transdermal delivery of insulin by amidated pectin hydrogel matrix patch in streptozotocin-induced diabetic rats: effects on some selected metabolic parameters. *PLoSONE*, 9 (7) (2014), e101461. https://doi.org/10.1371/journal.pone.0101461

[154] Modulevsky, D.J., Lefebvre, C., Haase, K., Al-Rekabi, Z., Pelling AE apple derived cellulose scaffolds for 3d mammalian cell culture. *PLoSONE*, 9 (5) (2014), e97835. https://doi.org/10.1371/journal.pone.0097835

[155] Zadegan, S., Hosainalipour, M., Rezaie, H., Ghassai, H., Shokrgozar, M.A., Synthesis and biocompatibility evaluation of cellulose/hydroxyapatitenano composite scaffold in 1-n-allyl-3-methylimidazolium chloride. *Materials Science and Engineering: C*, 31 (2011), 954–961. https://doi.org/10.1016/j.msec.2011.02.021

[156] Plant-Based Biomaterials: Engineering the Future. The Biochemist Blog, 2018. https://thebiochemistblog.com/2018/03/07/plant-based-biomaterials-engineering-the-future/

[157] Dolcimascolo, A., Calabrese, G., Conoci, S., Parenti, R., Biomaterial-supported tissue reconstruction or regeneration. In: Innovative biomaterials for tissue engineering, from the edited volume. InTechOpen: Rijeka, Croatia, 2019. https://doi.org/10.5772/intechopen.83839

[158] Oughlis, S., Lessim, S., Changotade, S., Bollotte, F., Poirier, F., Helary, G., Lataillade, J.J., Migonney, V., Lutomski, D., Development of proteomic tools to study protein adsorption on a biomaterial titanium grafted with poly (sodium styrene sulfonate). *Journal of Chromatography B*, 879 (31) (2011), 3681–3687. https://doi.org/10.1016/j.jchromb.2011.10.006

[159] Gilabert-Chirivella, E., Perez-Feito, R., Ribeiro, C., Ribeiro, S., Correia, D.M., González-Martín, M.L., Manero, J.M., Lanceros-Méndez, S., Ferrer, G.G., Gómez-Ribelles, J.L., Chitosan patterning on titanium implants. *Progress in Organic Coatings*, 111 (2017), 23-28. https://doi.org/10.1016/j.porgcoat.2017.04.027

[160] Wu, C., Zhou, Y., Xu, M., Han, P., Chen, L., Chang, J., Coppercontaining mesoporous bioactive glass scaffolds with multifunctional properties of angiogenesis capacity, osteostimulation and antibacterial activity. *Biomaterials*, 34 (2) (2013), 422–433. https://doi.org/10.1016/j.biomaterials.2012.09.066